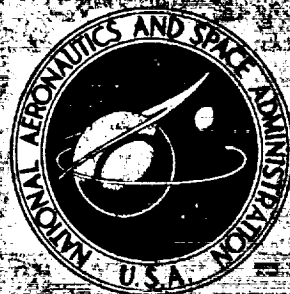


**NASA TECHNICAL
MEMORANDUM**



NASA TM X-3014

NASA TM X-3014

**CASE
COPY FILE**

**HYDES - A GENERALIZED HYBRID
COMPUTER PROGRAM FOR STUDYING
TURBOJET OR TURBOFAN ENGINE DYNAMICS**

by John R. Szuch

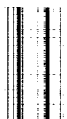
Lewis Research Center

Cleveland, Ohio 44135



1. Report No. NASA TM X-3014	2. Government Accession No.	3. Recipient's Catalog No.	
4. Title and Subtitle HYDES - A GENERALIZED HYBRID COMPUTER PROGRAM FOR STUDYING TURBOJET OR TURBOFAN ENGINE DYNAMICS		5. Report Date APRIL 1974	
		6. Performing Organization Code	
7. Author(s) John R. Szuch		8. Performing Organization Report No. E-7316	
		10. Work Unit No. 501-24	
9. Performing Organization Name and Address Lewis Research Center National Aeronautics and Space Administration Cleveland, Ohio 44135		11. Contract or Grant No.	
		13. Type of Report and Period Covered Technical Memorandum	
12. Sponsoring Agency Name and Address National Aeronautics and Space Administration Washington, D. C. 20546		14. Sponsoring Agency Code	
		15. Supplementary Notes	
16. Abstract <p>This report describes HYDES, a hybrid computer program capable of simulating one-spool turbojet, two-spool turbojet, or two-spool turbofan engine dynamics. HYDES is also capable of simulating two- or three-stream turbofans with or without mixing of the exhaust streams. The program is intended to reduce the time required for implementing dynamic engine simulations. HYDES was developed for running on the Lewis Research Center's Electronic Associates (EAI) 690 Hybrid Computing System and satisfies the 16 384-word core-size and hybrid-interface limits of that machine. The program could be modified for running on other computing systems. The use of HYDES to simulate a single-spool turbojet and a two-spool, two-stream turbofan engine is demonstrated. The form of the required input data is shown and samples of output listings (teletype) and transient plots (x-y plotter) are provided. HYDES is shown to be capable of performing both steady-state design and off-design analyses and transient analyses.</p>			
17. Key Words (Suggested by Author(s)) Hybrid computer; Simulation; Engine; Fan Propulsion; Turbojet; Dynamics; Analog; Turbofan; Transient; Digital; Generalized; Control; Integration; Performance		18. Distribution Statement Unclassified - unlimited CAT.28	
19. Security Classif. (of this report) Unclassified	20. Security Classif. (of this page) Unclassified	21. No. of Pages 134	22. Price* \$4.75

* For sale by the National Technical Information Service, Springfield, Virginia 22151



CONTENTS

	Page
SUMMARY	1
INTRODUCTION	2
ENGINE CONFIGURATIONS	3
MATHEMATICAL MODEL	10
Intercomponent Volumes.	10
Fans and Compressors	11
Turbines	14
Rotor Dynamics	16
Nozzles	16
Combustor and Ducts	18
HYBRID COMPUTER PROGRAM	19
Hybrid Computing System	19
Scaling	19
Engine Definition	22
Digital Program	23
Data input program	23
Main program	23
Subroutines	24
Analog Program	28
Input Data Preparation	29
Digital coefficients and DAC initial conditions	31
Component performance data	32
Analog coefficients	40
EXAMPLES	40
Single-Spool Turbojet (Configuration G)	40
Turbofan (Configuration E)	50
CONCLUDING REMARKS	59
APPENDIXES	
A - UNSCALED-VARIABLE SYMBOLS	61
B - SUMMARY OF UNSCALED EQUATIONS	68
C - SCALED-VARIABLE SYMBOLS	83
D - DEFINITIONS OF DIGITAL AND ANALOG COEFFICIENTS	88

	Page
E - COMPUTER LISTINGS OF DATA INPUT PROGRAM, MAIN PROGRAM, AND SUBROUTINES	106
F - SUMMARY OF SCALED EQUATIONS SOLVED ON ANALOG COMPUTER . .	120
G - COMPUTER LISTING OF TURBINE DATA CONVERSION PROGRAM.	124
H - TURBOFAN FUEL CONTROL SIMULATION	127
REFERENCES	131

HYDES - A GENERALIZED HYBRID COMPUTER PROGRAM FOR STUDYING TURBOJET OR TURBOFAN ENGINE DYNAMICS

by John R. Szuch
Lewis Research Center

SUMMARY

The selection of an efficient airframe-engine combination depends on the ability to analyze a broad range of engine types and sizes operating at both design and off-design conditions. Computer programs having the necessary steady-state calculation capabilities have previously been developed.

In addition to their use in steady-state studies, analyses of engine dynamics and control are also important in the selection of a suitable propulsion system. This report describes HYDES, a hybrid (analog-digital) computer program capable of simulating one-spool turbojet, two-spool turbojet, or two-spool turbofan engine dynamics. The program is also capable of simulating two- or three-stream turbofans with or without mixing of the exhaust streams. HYDES is intended to reduce the time required to implement dynamic engine simulations.

HYDES was developed for running on the Lewis Research Center's Electronic Associates (EAI) 690 Hybrid Computing System and satisfies the core-size (16 384 words) and hybrid-interface limits of that machine. The documentation of the program should allow the user to implement the program on another machine. The techniques employed and the resultant set of equations should be applicable in other generalized or specific engine simulations (analog, digital, or hybrid).

For the existing program, procedures are described for generating the required input data, specifying the engine configuration of interest, and operating the program. The use of HYDES to simulate selected turbojet and turbofan engines is demonstrated. The form of the required input data for these engines together with samples of output listings (teletype) and transient plots (x-y plotter) for each example are provided. HYDES does not provide for engine control but does accept, as user-supplied inputs, fuel flow rates and nozzle areas. The simulation of simplified fuel control systems on the analog computer is discussed, and their use with the hybrid program is demonstrated.

INTRODUCTION

The selection of an efficient airframe-engine combination depends on the ability to analyze a broad range of engine types and sizes operating at both design and off-design conditions. Computer programs having the necessary steady-state calculation capabilities have previously been developed. The SMOTE code, discussed in references 1 and 2, provides steady-state design and off-design calculation capability for both existing and theoretical turbofan engines. Theoretical engines are simulated by scaling component performance from existing engines to the design conditions of the theoretical engine. GENENG (ref. 3) extends the same techniques to handle turbojet engines as well as turbofans. GENENG II (ref. 4) was derived from GENENG and adds the capability of studying two- or three-spool turbofan engines having as many as three nozzles (airstreams).

In addition to their use in steady-state design- and off-design-point studies, analyses of engine dynamics and control are also important in the selection of a suitable propulsion system. For example, the use of turbofan engines as lift units for V/STOL aircraft (ref. 5) poses a number of engine control problems. At low flight speeds, the lift system must provide the fast thrust response needed for aircraft attitude control. The propulsion system must also be capable of correcting for upsetting moments caused by the loss of a lift engine. The required rapid engine accelerations must be accomplished without exceeding turbine-temperature, rotor-speed, and compressor-stall limits.

This report describes HYDES, a hybrid (analog-digital) computer program capable of simulating one-spool turbojet, two-spool turbojet, or two-spool turbofan engine dynamics. The program can easily be modified to handle the one-spool turbofan case. HYDES is capable of simulating two- or three-stream turbofans with or without mixing of the exhaust streams. The program is structured so as to allow the simulation of a wide range of engine sizes (as well as types) without changing the basic program. The hybrid computer was used because it combines the precision and logic capabilities of the digital computer with the integration and output capabilities of the analog computer. Steady-state design-point data (pressures, temperatures, etc.), generated by a program such as GENENG II, and the associated component performance maps are required to generate the necessary input data for the hybrid program. After the simulation has "settled-out" at the design point, a change in one of the input variables (such as fuel flow) will result in a transient excursion to a new steady-state operating point. Thus, the program is capable of steady-state design- and off-design-point operation, as well as possessing the desired transient capability.

HYDES does not provide for the simulation of control system dynamics. The digital portion of the program accepts values for fuel flow rates and nozzle area (or areas)

from the analog portion of the program. In general, the function generation and arithmetic operations required in simulating an engine control system could be performed on either an analog or digital computer. But hybrid interface limitations dictated that control system dynamics (when required) be simulated on the analog computer. To demonstrate the transient operation of the program for a selected engine, a fuel control system was assumed. The implementation of the fuel control and its relationship to the basic HYDES program are illustrated in this report.

HYDES was developed for running on the Lewis Research Center's Electronic Associates (EAI) 690 Hybrid Computing System. The structure of the program is very much influenced by the digital core size (16 384 words) and the hybrid-interface capability (24 analog-to digital converters and 24 digital-to-analog converters) of that machine. The documentation of the program, together with the associated digital computer software (available from the author upon request), should allow the direct use of the program on another EAI 690 computer. The simulation techniques and resultant equations, presented in this report, should also serve as a guide in the development of both generalized and specific turbojet and turbofan engine simulations for use with different computing systems.

ENGINE CONFIGURATIONS

HYDES can be used to simulate a number of different engine configurations. These configurations are referred to as configurations A to H. A discussion of each follows.

A schematic representation of configuration A is shown in figure 1. Configuration A represents an unmixed, two-spool, three-stream turbofan engine with separate performance maps for the fan-hub (low-pressure compressor) and fan-tip sections. All other configurations can be considered as variations of this configuration. The fan is driven by a separate low-pressure turbine. The fan-hub flow \dot{w}_{f1} discharges into a high-pressure-compressor-inlet volume $V_{2.1}$ which supplies (1) bleed flow for control purposes \dot{w}_{blc} , (2) flow to the second stream \dot{w}_{v2} , (3) bleed flow to the third stream \dot{w}_{bls} , and (4) flow to the core compressor \dot{w}_c . All unscaled-variable symbols are defined in appendix A. The core (high-pressure) compressor, which is driven by the high-pressure turbine, discharges into a combustor-inlet volume V_3 which supplies (1) overboard bleed flow \dot{w}_{ovb} , (2) cooling flow for the high-pressure turbine \dot{w}_{bl1} , (3) cooling flow for the low-pressure turbine \dot{w}_{bl2} , and (4) airflow to the combustor \dot{w}_b . The combustor airflow reacts in high-pressure-turbine-inlet volume V_4 with the injected fuel flow \dot{w}_F . The high-pressure-turbine flow \dot{w}_{t1} discharges into low-pressure-turbine-inlet volume V_5 , where it is diluted by the high-pressure-turbine cooling flow \dot{w}_{bl1} . Similarly, the low-pressure-turbine flow \dot{w}_{t2} discharges into

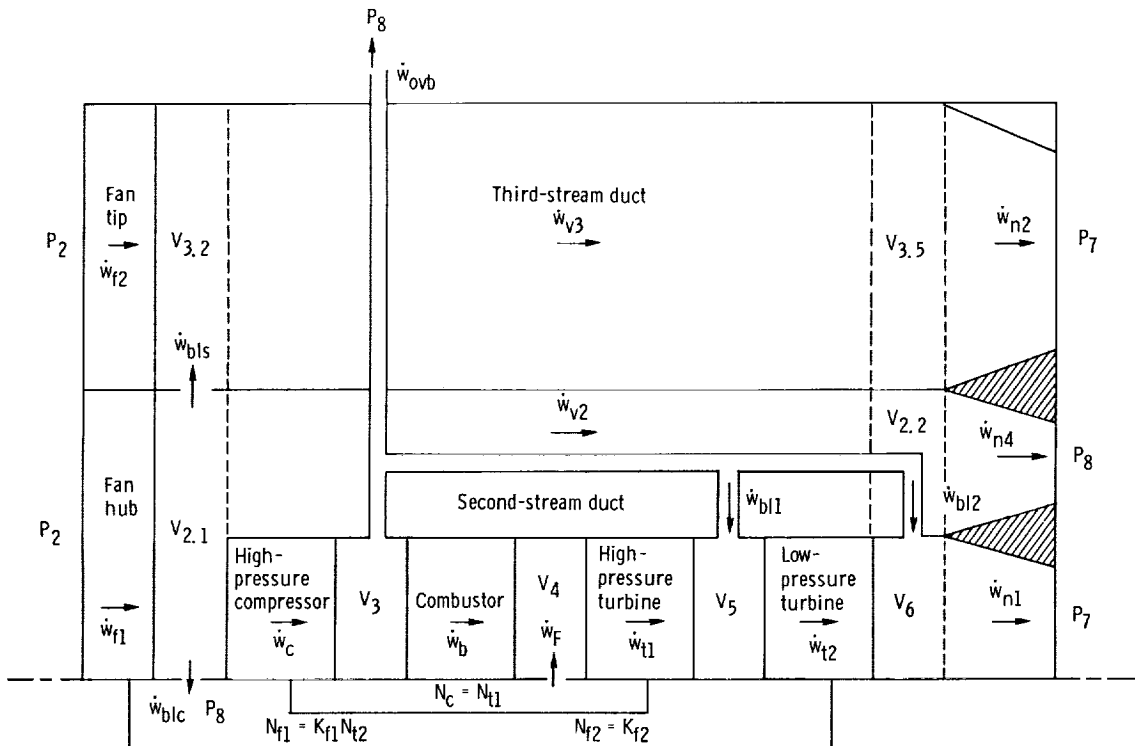


Figure 1. - Schematic representation of configuration A.

core-duct volume V_6 where it is diluted by the low-pressure-turbine cooling flow \dot{w}_{bl2} . All turbine cooling bleeds are assumed to enter downstream of the rotor (or rotors), thus contributing no work. Volume V_6 supplies flow to the core nozzle \dot{w}_{n1} . The second-stream flow \dot{w}_{v2} discharges into the second-stream-duct volume $V_{2.2}$ which, in turn, supplies flow to the second-stream nozzle \dot{w}_{n4} . The fan-tip flow \dot{w}_{f2} discharges into the bypass-fan-discharge volume $V_{3.2}$, where it is mixed with the interstream bleed flow \dot{w}_{bls} . Volume $V_{3.2}$ supplies flow to the third stream \dot{w}_{v3} . This flow discharges into the bypass-fan-duct volume $V_{3.5}$ which, in turn, supplies flow to the third-stream nozzle \dot{w}_{n2} . Constants K_{f1} and K_{f2} may be set to nonunity values to represent a gear-driven low-pressure compressor and fan, respectively. If the low-pressure compressor represents the fan hub, K_{f1} and K_{f2} are equal.

A schematic representation of configuration B is shown in figure 2. This configuration is identical to configuration A except for the mixing of the core and third-stream flows in the mixing volume V_7 . This volume then supplies flow to the mixed-flow nozzle \dot{w}_{n3} . The second-stream nozzle flow \dot{w}_{n4} discharges to the atmosphere at station 8.

A schematic representation of configuration C is shown in figure 3. Configuration C represents a two-spool, two-stream turbofan engine with the entire fan represented by one set of performance maps. Thrust is generated by the separate exhaust flows \dot{w}_{n1}

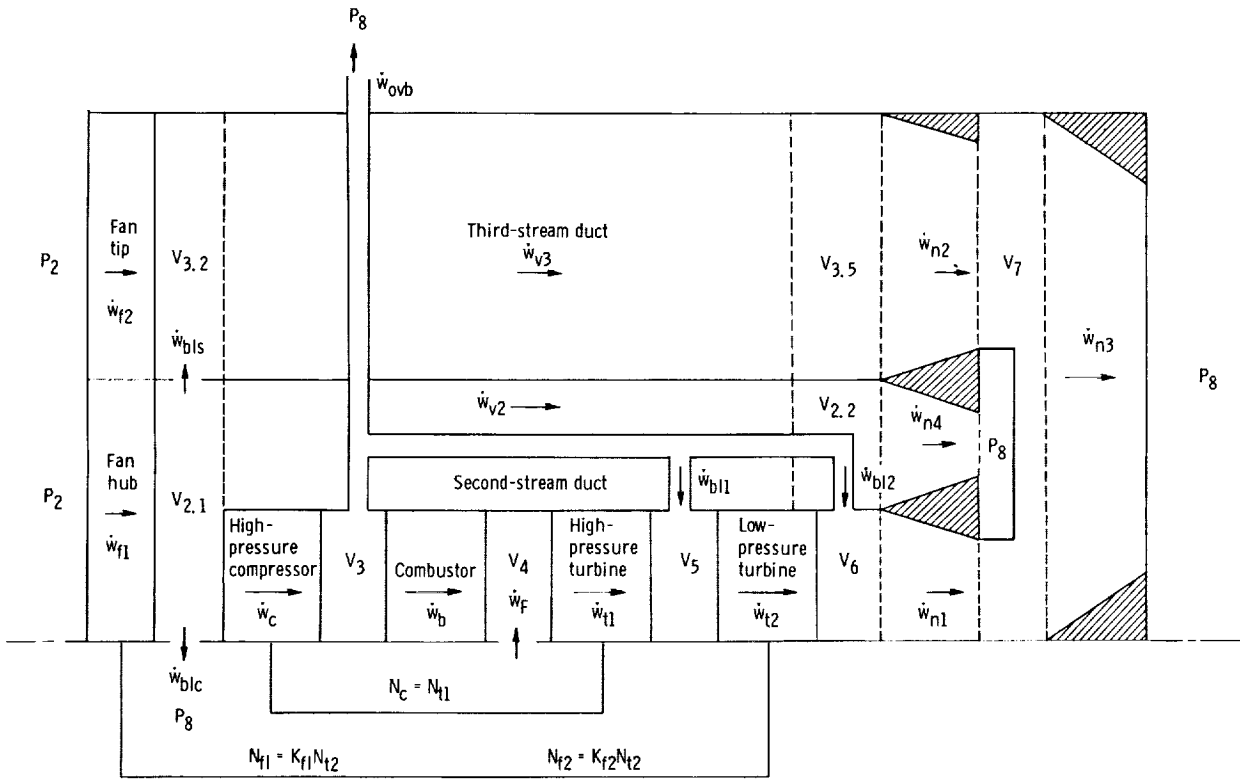


Figure 2. - Schematic representation of configuration B.

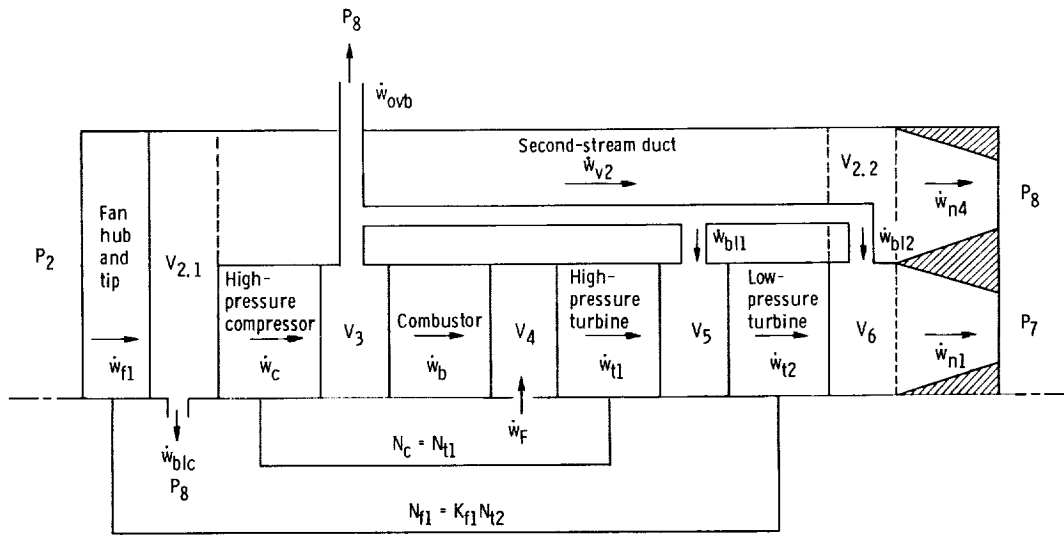


Figure 3. - Schematic representation of configuration C.

and \dot{w}_{n4} . This configuration is obtained by eliminating the fan-tip and third-stream calculations from configuration A (fig. 1). The mixed version of the two-spool, two-stream turbofan engine is shown, schematically, in figure 4 and is referred to as configuration D.

A schematic representation of configuration E is shown in figure 5. Configuration E represents a two-spool, two-stream turbofan engine with separate performance maps for the fan hub and tip sections. This configuration is formed by eliminating the second-stream calculations from configuration A. The mixed version of configuration E is

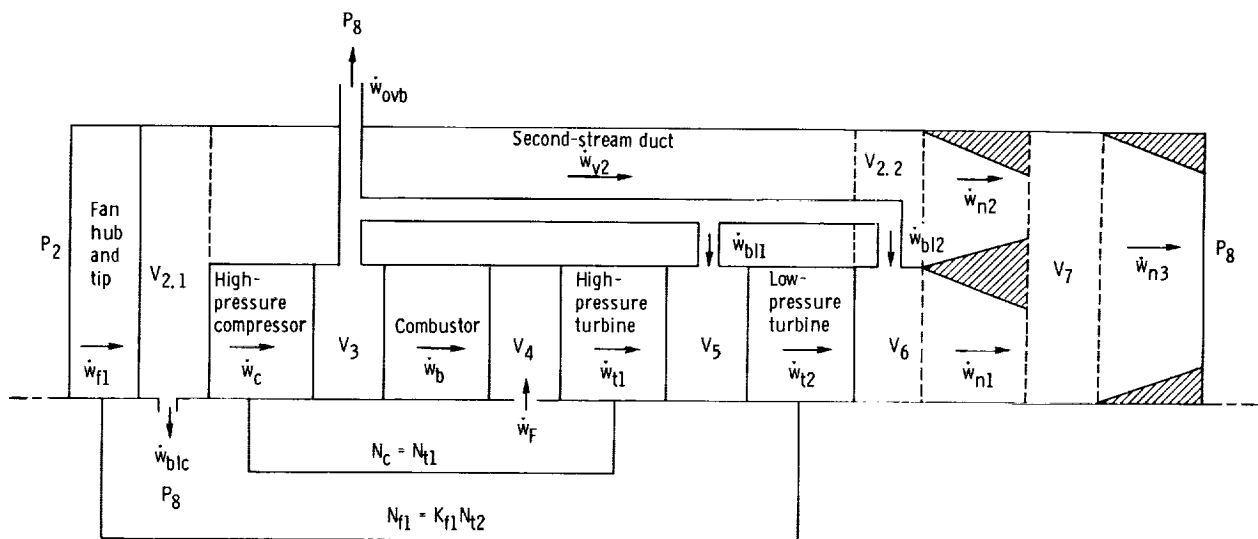


Figure 4. - Schematic representation of configuration D.

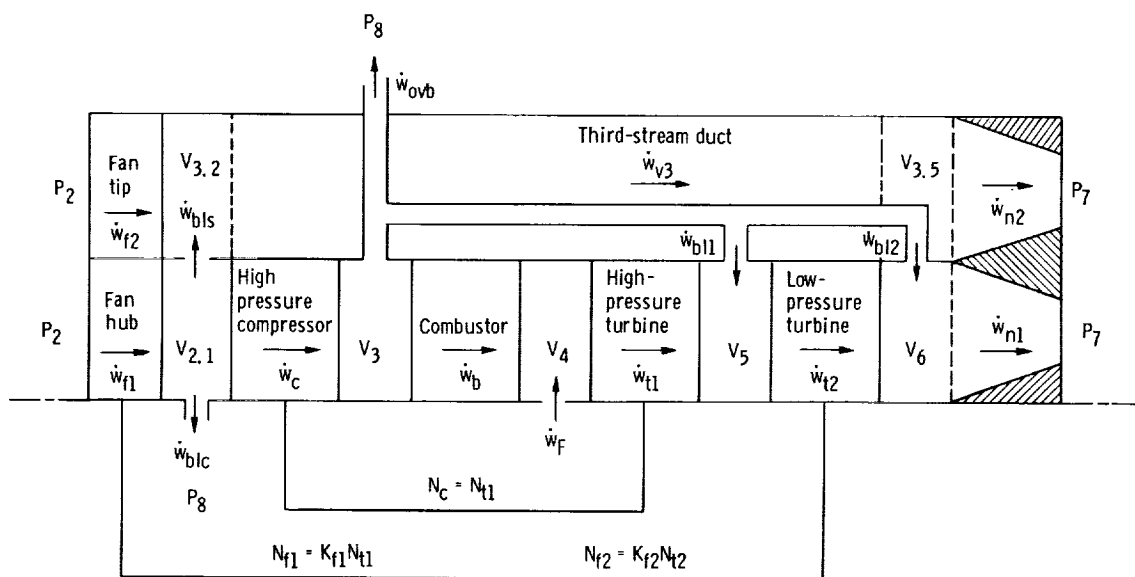


Figure 5. - Schematic representation of configuration E.

referred to as configuration F and is shown, schematically, in figure 6.

A conventional one-spool turbojet engine is referred to as configuration G and is shown, schematically, in figure 7. The one-spool turbojet configuration is formed from configuration C (fig. 3) (1) by eliminating the fan and second-stream calculations, (2) by equating the conditions in volume $V_{2.1}$ with the inlet conditions at station 2, (3) by eliminating the low-pressure-turbine calculations, and (4) by equating the conditions in volumes V_5 and V_6 .

A two-spool turbojet is referred to as configuration H and is shown, schematically, in figure 8. This configuration is formed from configuration E (fig. 5) by eliminating the fan-tip and third-stream calculations.

For configurations E and F, an option (-2) is provided in the HYDES program to allow the simulation of the fan tip without simulation of the fan hub. An example of this type of engine would be an aft-fan engine with a single core (high-pressure) compressor. For this option, the program does provide for supercharging of the high-pressure compressor (if required). A supercharger pressure ratio is computed as a linear function of the fan corrected speed. The supercharger torque is computed by using the high-pressure compressor flow (volume $V_{2.1}$ is assumed to be negligible). If supercharging is not required, the appropriate coefficients are set to give a supercharger pressure ratio of 1.0. When a gear-driven aft-fan is being simulated, the constant

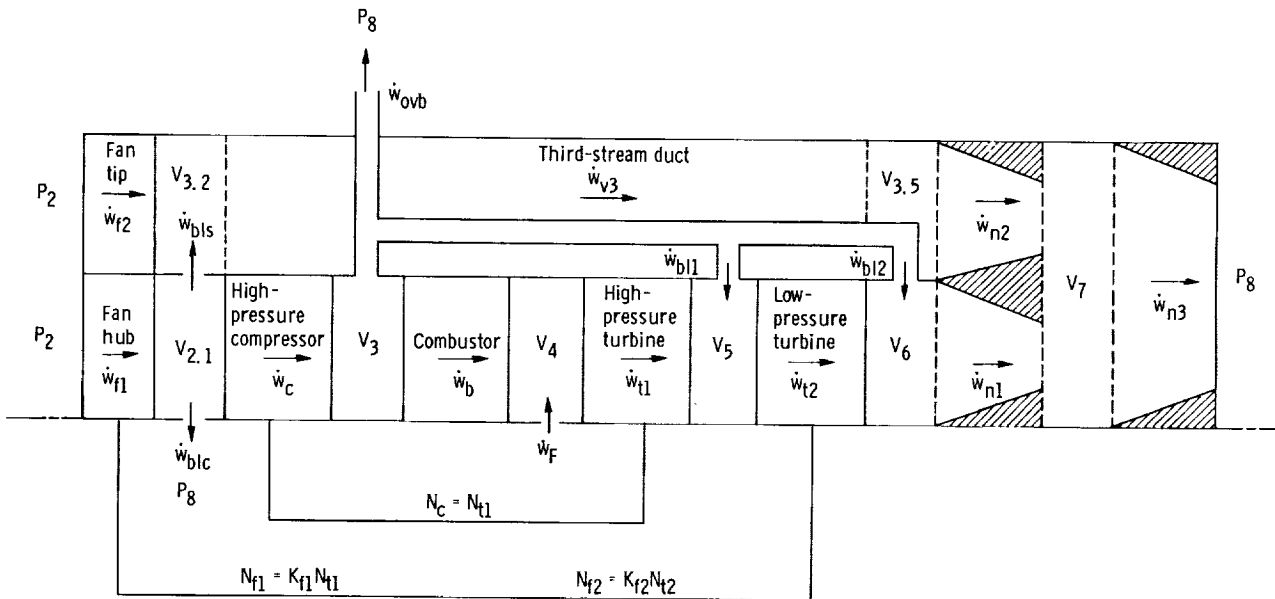


Figure 6. - Schematic representation of configuration F.

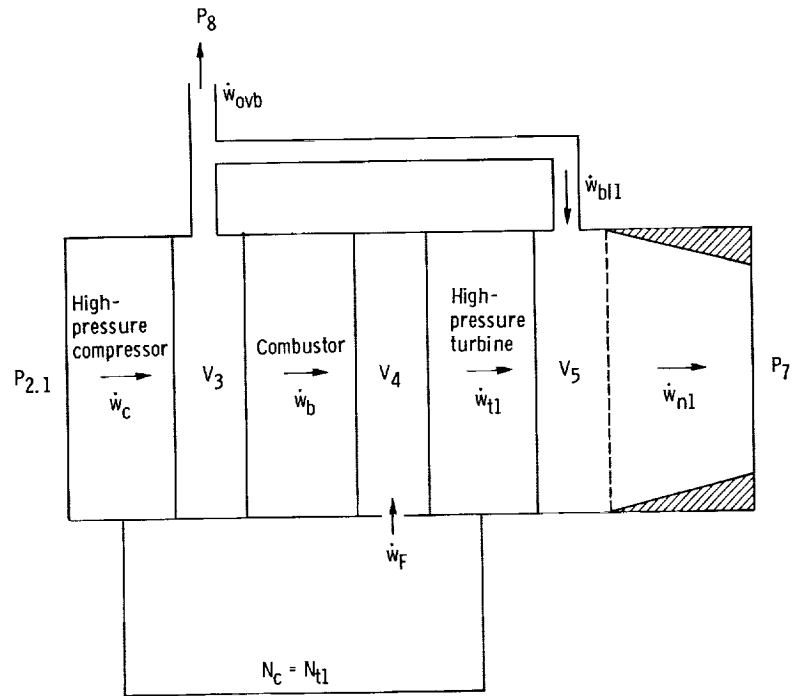


Figure 7. - Schematic representation of configuration G.

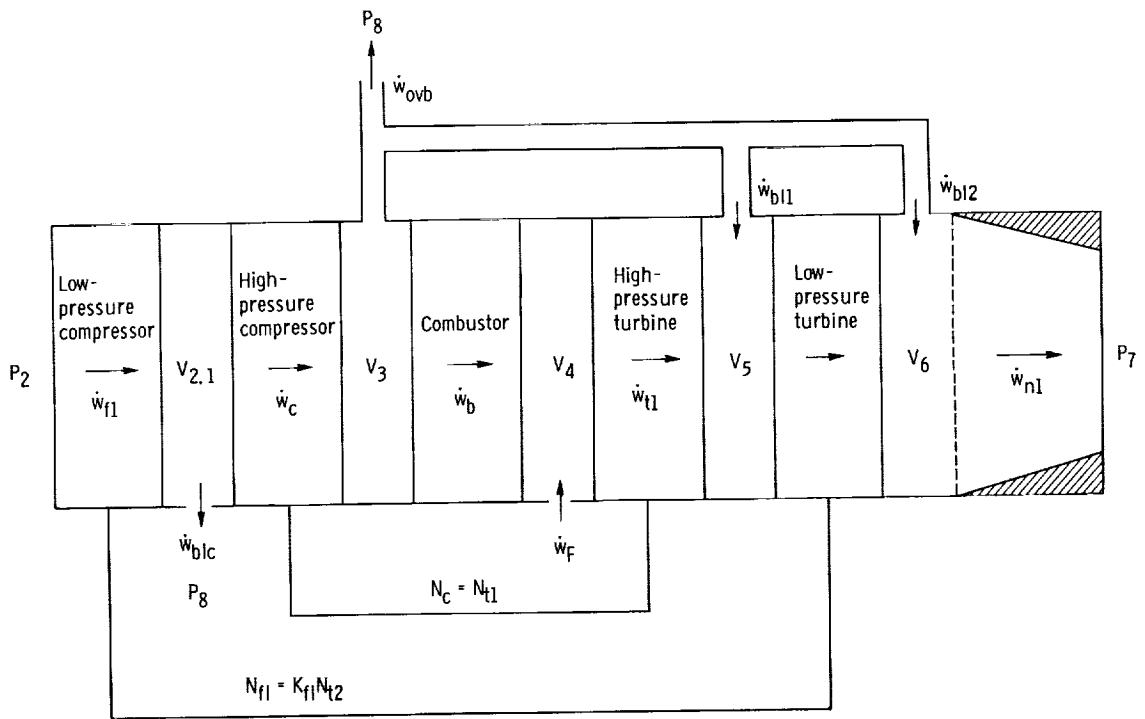


Figure 8. - Schematic representation of configuration H.

K_{f2} is set equal to the gear ratio.

Another option (-1) is provided for those configurations requiring separate performance maps for the fan hub and tip sections (A, B, E, and F). For these configurations, the fan-tip performance data may be in terms of either the total fan flow ($\dot{w}_{f1} + \dot{w}_{f2}$) or the fan-tip flow \dot{w}_{f2} . Table I summarizes the configurations and options available with the HYDES program. The simultaneous use of the -1 and -2 options is referred to as the -3 option.

TABLE I. - ENGINE CONFIGURATIONS AND OPTIONS FOR HYDES PROGRAM

Configuration	Description
A	Two-spool, three-stream, unmixed turbofan; separate maps for fan hub and tip sections
A-1	Same as configuration A with fan-tip performance in terms of total fan flow
B	Two-spool, three-stream, mixed turbofan; mixing of first and third streams; separate maps for fan hub and tip sections
B-1	Same as configuration B with fan-tip performance in terms of total fan flow
C	Two-spool, two-stream, unmixed turbofan; entire fan described by same map
D	Two-spool, two-stream, mixed turbofan; entire fan described by the same map
E	Two-spool, two-stream, unmixed turbofan; separate maps for fan hub and tip sections
E-1	Same as configuration E with fan-tip performance in terms of total fan flow
E-2	Same as configuration E with fan hub performance simplified for supercharger or aft-fan
E-3	Same as configuration E with fan-tip performance simplified for supercharger or aft-fan
F	Two-spool, two-stream, mixed turbofan; separate maps for fan hub and tip sections
F-1	Same as configuration F with fan-tip performance in terms of total fan flow
F-2	Same as configuration F with fan-hub performance simplified for supercharger or aft-fan
F-3	Same as configuration F with fan-tip performance simplified for supercharger or aft-fan
G	One-spool turbojet
H	Two-spool turbojet

MATHEMATICAL MODEL

The first step in developing any simulation is the formulation of a mathematical model. This model, in equation form, represents the functional relations that exist between system variables. In the case of turbojet and turbofan engine systems, these variables are pressures, temperatures, flow rates, rotor speeds, and so forth.

Intercomponent Volumes

Pressures and temperatures are computed in each of the intercomponent volumes shown in figures 1 to 8. In these volumes, storage of mass and energy occurs (ref. 6). Modified forms of the continuity and energy equations written for each volume are

$$W = \int_0^t \left[\sum_1^{NN} \dot{w}_{in,j} - \sum_1^{MM} \dot{w}_{out,k} \right] dt + W_i \quad (1)$$

$$T = \int_0^t \frac{1}{W} \left[\frac{\sum_1^{NN} \dot{w}_{in,j} h_{in,j} - h \sum_1^{MM} \dot{w}_{out,k}}{c_v} - T \left(\sum_1^{NN} \dot{w}_{in,j} - \sum_1^{MM} \dot{w}_{out,k} \right) \right] dt + T_i \quad (2)$$

A summary of all equations written for specific components is given in appendix B. With the results from equations (1) and (2), the pressure in the volume can be computed from the ideal-gas law:

$$P = \frac{R}{V} WT \quad (3)$$

The thermodynamic properties of air and fuel-air mixtures (c_p , c_v , γ , h) are calculated by considering variable specific heats and no dissociation. The air and fuel-air property tables of reference 7 were curve-fit by the authors of references 1

and 2. Those curve-fits were further simplified and used in the HYDES program. For each intercomponent volume in a particular engine configuration, the following gas properties are calculated:

$$c_p = f_1 (T, f/a) \quad (4)$$

$$R = f_2 (f/a) \quad (5)$$

$$c_v = c_p - \frac{R}{J} \quad (6)$$

$$\gamma = \frac{c_p}{c_v} \quad (7)$$

$$h = f_3 (T, f/a) \quad (8)$$

where f/a is the local fuel-air ratio.

While the gas constant R is, in general, a variable when mixtures of gases are considered, it was determined that the sensitivity of R to the fuel-air ratios expected in this type of simulation could be neglected. Therefore, the gas constant of air R_A is used in equation (3). The use of a constant value of R also prevents the occurrence of algebraic loops, which require iterative solutions.

Fans and Compressors

Fans and compressors can be modeled by a number of known techniques. One method is to represent multistage compressors with individual stage models (i. e., compute pressure and temperature rises across each stage). This technique is referred to as stage-stacking (ref. 8), but it requires a large computing facility when used in a total engine simulation. For the HYDES program, fans and compressors are represented by overall performance maps. This technique does not consider interstage gas dynamics. The effects of interstage bleeds or variable geometry, if they exist, must be reflected in the overall performance data. Figure 9 shows the form of the fan and compressor maps used in this program. Figure 9(a) shows a corrected flow parameter $fpfc$ plotted as a function of two variables - a pressure ratio pr and a corrected speed parameter $fcnp$. When performance data are not available for a particular fan or compressor (as in the case of theoretical engines), it is necessary to scale available data to the design point of the theoretical component. Scale factor (WACF, ETACF, PRCF)

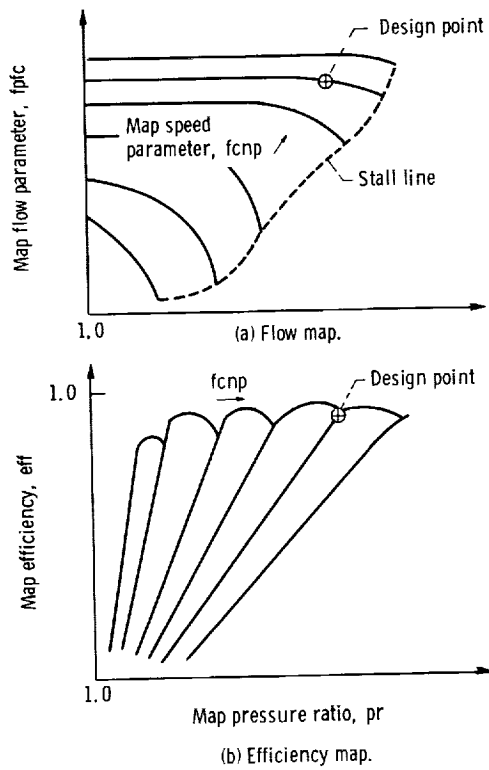


Figure 9. - Form of fan and compressor performance maps used in hybrid simulation.

are used to accomplish the performance scaling within the HYDES program. The validity of the scaled data decreases as the scale factors deviate from unity. Figure 9(b) shows fan or compressor efficiency eff plotted as a function of the same two independent variables. The following equations are used to compute fan or compressor flow, discharge enthalpy, and torque from specified inlet conditions, rotor speed, and back-pressure:

$$pr = \frac{\frac{P_{out}}{P_{in}} - 1}{PRCF} + 1 \quad (9)$$

$$fcnp = \frac{\frac{N}{N_{des}}}{\sqrt{\frac{T_{in}}{T_{in, des}}}} \quad (10)$$

$$fpfc = f_4(pr, fcnp) \quad (11)$$

$$\dot{w} = \frac{(WACF)(fpfc) \frac{P_{in}}{P_{sl}}}{\sqrt{\frac{T_{in}}{T_{std}}}} \quad (12)$$

$$eff = f_5(pr, fcnp) \quad (13)$$

$$\eta = (ETACF)(eff) \quad (14)$$

$$tr = \left(\frac{P_{out}}{P_{in}} \right)^{\frac{\bar{\gamma}-1}{\bar{\gamma}}} - 1 \quad (15)$$

$$T'_{out} = \left(\frac{tr}{\eta} + 1 \right) T_{in} \quad (16)$$

$$L = \frac{30J(h'_{out} - h'_{in})\dot{w}}{\pi N} \quad (17)$$

The fan or compressor discharge temperature T'_{out} and the corresponding enthalpy h'_{out} represent the inlet conditions to the downstream volume (eq. (2)). If the fan or compressor is the only component feeding the volume, the discharge conditions T'_{out} and h'_{out} will equal (in steady state) the temperature and enthalpy, respectively, in the downstream volume.

The solution of equation (15) requires a knowledge of the "average" thermodynamic properties in the fan or compressor. Since these properties are functions of temperature, they vary throughout the component. For this reason, a temperature interpolation constant β is adjusted for each fan or compressor to match available steady-state cycle data for the engine being simulated. That is,

$$\bar{T} = \beta T_{in} + (1 - \beta) T_{out} \quad (18)$$

$$\bar{c}_p = f_1(\bar{T}, f/a) \quad (19)$$

$$\bar{R} = f_2(f/a) \quad (20)$$

$$\bar{c}_v = \bar{c}_p - \frac{\bar{R}}{J} \quad (21)$$

$$\bar{\gamma} = \frac{\bar{c}_p}{\bar{c}_v} \quad (22)$$

The calculated value for $\bar{\gamma}$ should agree with the specific-heat ratio used to define the fan or compressor efficiency η . The temperature in the discharge volume T_{out} is used in calculating \bar{T} to avoid the occurrence of algebraic loops associated with the use of T'_{out} .

Turbines

As in the case of fans and compressors, the most direct approach to modeling multistage turbines would be to apply stage-stacking techniques. However, individual stage performance data are usually not available. It is therefore necessary to represent turbines by overall performance maps. Figure 10 shows the form of the turbine maps used in the HYDES program. Figure 10(a) shows a turbine flow parameter f_{pt} plotted as a function of pressure ratio pr and a turbine speed parameter tnp . Figure 10(b) shows a turbine enthalpy drop (work) parameter h_{pt} plotted as a function of the same two independent variables. As in the case of fans and compressors, scale factors (CNCF, DHCF, TFCF) are used to scale available performance data to the design point of theoretical turbines. The following equations are used to compute the turbine flow, discharge enthalpy, and torque from specified inlet conditions, rotor speed, and back-pressure:

$$pr = \frac{P_{out}}{P_{in}} \quad (23)$$

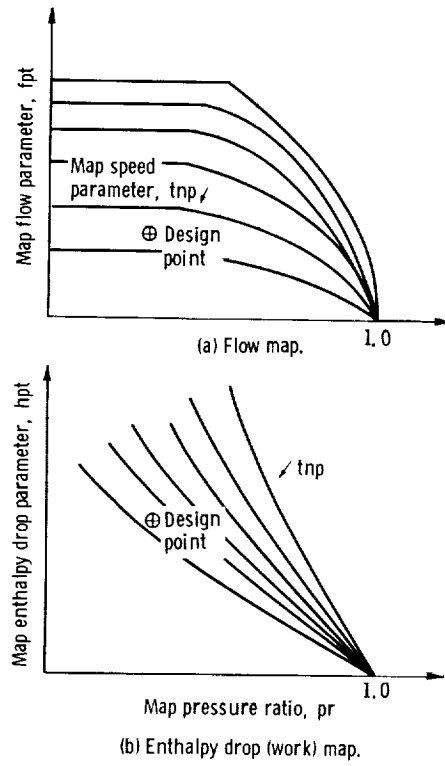


Figure 10. - Form of turbine performance maps used in hybrid simulation.

$$tnp = \frac{(CNCF)(N)}{\sqrt{T_{in}}} \quad (24)$$

$$fpt = f_6(pr, tnp) \quad (25)$$

$$hpt = f_7(pr, tnp) \quad (26)$$

$$\dot{w} = \frac{(CNCF)(fpt)(P_{in})(N)}{(TF CF)(T_{in})} \quad (27)$$

$$\Delta h = \frac{(DHCF)(hpt)(N) \sqrt{T_{in}} (CNCF)}{1000} \quad (28)$$

$$h'_{out} = h_{in} - \Delta h \quad (29)$$

$$L = \frac{30J(\Delta h)(\dot{w})}{\pi N} \quad (30)$$

It should be noted that a factor of 1000 has been included in the definition of the enthalpy parameter hpt.

In general, the discharge enthalpy for the turbine h'_{out} does not equal (in steady-state) the enthalpy in the downstream volume h_{out} because of the mixing of the turbine flow with the turbine cooling bleed.

Rotor Dynamics

After the fan, compressor, and turbine torques are computed, the rotor speed (or speeds) is computed by using the conservation of angular momentum. That is,

$$N = \frac{30}{\pi I} \int_0^t \Delta L \, dt + N_i \quad (31)$$

where ΔL denotes the difference between the driving turbine torque and the load torque (fans or compressors) and I represents the polar moment of inertia for the spool.

Nozzles

For all the engine configurations being considered (figs. 1 to 8), flows must be computed for each nozzle. All nozzles are assumed to be the convergent type, and the flow processes are assumed to be isentropic. For a specified inlet pressure, there exists, for each nozzle, a critical back-pressure (ref. 6) given by

$$P_{cr} = \left(\frac{2}{\gamma + 1} \right)^{\frac{\gamma}{\gamma - 1}} P_{in} \quad (32)$$

If the back-pressure is higher than the critical pressure, the flow is subsonic at the nozzle throat and may be expressed as

$$\dot{w} = P_{in} \sqrt{\frac{g_c}{RT_{in}}} A \left(\frac{P_{out}}{P_{in}}\right)^{\frac{1}{\gamma}} \sqrt{\frac{2\gamma}{(\gamma-1)} \left[1 - \left(\frac{P_{out}}{P_{in}}\right)^{\frac{\gamma-1}{\gamma}}\right]} \quad (33)$$

If the back-pressure is lower than the critical pressure, the flow is sonic or "choked" at the nozzle throat. For this case, the flow is given by

$$\dot{w} = P_{in} \sqrt{\frac{g_c}{RT_{in}}} A \sqrt{\gamma \left(\frac{2}{\gamma+1}\right)^{\frac{\gamma+1}{\gamma-1}}} \quad (34)$$

For those nozzles where thrust calculations are required, the following equations are used:

$$F = C_v \dot{w} \sqrt{\frac{2J}{g_c}} \sqrt{c_p T_{in} \left[1 - \left(\frac{P_{out}}{P_{in}}\right)^{\frac{\gamma-1}{\gamma}}\right]} \quad (35)$$

for subsonic flow, and

$$F = C_v \dot{w} \sqrt{\frac{2J}{g_c}} \sqrt{c_p T_{in} \left[1 - \left(\frac{P_{cr}}{P_{in}}\right)^{\frac{\gamma-1}{\gamma}}\right]} + A(P_{cr} - P_{out}) \quad (36)$$

for sonic flow.

To minimize the digital computation time, the effects of varying γ and R in the nozzle flow and thrust calculations have been neglected in the HYDES program. A constant value of γ , 1.35, and the gas constant of air are used for all nozzle calculations.

The turbine cooling, control, and overboard bleed flows are treated in the same manner as the nozzle flows. However, the high pressure ratios between the compressor discharge volume V_3 and the turbine discharge volumes V_5 and V_6 and the ambient pressure allow the turbine cooling and overboard bleed flows to be computed by using equation (34) without testing the pressure ratio.

Combustor and Ducts

For all engine configurations, total pressure losses are assumed in the combustor and in each of the bypass ducts (for turbofans). Mach numbers in the combustor and ducts are assumed to be low enough to allow the assumption of incompressible flow. Flows are computed from

$$\dot{w} = \sqrt{\frac{P_{in} - P_{out}}{\mathcal{R}}} \quad (37)$$

where \mathcal{R} is the flow resistance as determined from steady-state design-point data.

The inlet and discharge pressures for the combustor and bypass ducts are computed by using equations (1) to (3). For the bypass ducts, no heat addition to the ducts is assumed. Therefore, the input enthalpy for the duct-discharge temperature calculation is the enthalpy in the duct inlet volume. For the combustor, heat addition due to the burning of the injected fuel is assumed to take place in the combustor discharge volume V_4 . In the calculation of the combustor discharge temperature T_4 , the input energy to the volume V_4 is given by

$$\sum_1^{NN} \dot{w}_{in,j} h_{in,j} = \dot{w}_b \bar{h}_b + \eta_b \dot{w}_F HVF \quad (38)$$

where \bar{h}_b denotes the enthalpy of the combustor air. For this program, a constant combustor efficiency η_b is assumed. An interpolation constant β_b is adjusted to satisfy steady-state cycle data. That is,

$$\bar{T}_b = \beta_b T_3 + (1 - \beta_b) T_4 \quad (39)$$

$$\bar{h}_b = f_3 \left[\bar{T}_b, (f/a)_4 \right] \quad (40)$$

$$(f/a)_4 = \frac{\dot{w}_F}{\dot{w}_b} \quad (41)$$

HYBRID COMPUTER PROGRAM

Hybrid Computing System

The HYDES program was developed for running on the Lewis Research Center's Electronic Associates (EAI) Model 690 Hybrid Computing System. The 690 System (ref. 9) consists of an EAI 640 Digital Computer, an EAI 693 Hybrid Interface Unit, and an EAI 680 Analog Computer.

The basic digital computer has 16 384 words of core storage. Floating-point (real) numbers are represented by two 16-bit words. Scaled-fractions (numbers less than 1.0) are represented by a single 16-bit word. Arithmetic operations can be performed by the digital computer for both floating-point and scaled-fraction numbers. For digital input and output, the hybrid computer uses a teletypewriter, a high-speed paper-tape reader, and a high-speed paper-tape punch.

The interface unit provides the necessary communication between the analog and digital computers. Twenty-four analog-to-digital converters (ADC's) are used to transmit analog signals to the digital. Twenty-four digital-to-analog converters (DAC's) are used to transmit digital signals to the analog. The interface system also contains 16 control lines and eight sense lines. The logical states of the control lines are set by the digital program and may be sensed on the analog. Similarly, the logical states of the sense lines are set by the analog and sensed by the digital. Eight sense switches can be positioned at the digital control console and tested by the digital program.

The analog computer performs all the operations characteristic of analog machines (i. e., summing, integration with respect to time, limiting, attenuation, multiplication, function generation, etc.). The analog computer contains a total of 156 amplifiers, 124 potentiometers, and 24 quarter-square multipliers. In addition, the analog contains 16 comparators and 16 function relays which can be positioned by either the digital or analog computers. The use of peripheral equipment such as x-y plotters and strip-chart recorders allows continuous monitoring by the user of computed variables.

Scaling

To reduce the core requirements and computation time of the digital portion of the HYDES program, it was decided to use scaled fractions throughout the digital program. Therefore, all digital variables are scaled so as not to exceed unity during the program execution. For each variable x , a scale factor SF_X is chosen so as to limit the scaled variable $X = x/SF_X$ to the range $-1 < X < +1$. Similarly, all analog variables are scaled so that no analog signal exceeds 1.0 computer unit (10 volts on the EAI 680 computer).

While the choice of most scale factors is left to the user, certain variables have been prescaled to minimize core storage requirements. For example, all fuel-air ratios are scaled for a maximum of 0.05. In addition, certain variables are assumed to have the same scale factors as other variables. Table II contains a list of prescaled variables, their respective scale factors, and the implied relations between scale factors.

In addition to the previously described amplitude scaling, it is often necessary to time-scale the analog portion of a dynamic simulation. To allow the treatment of digital outputs as continuous input signals to the analog, a sufficient number of cycles through the digital loop must occur for each cycle of the analog frequencies. In some cases, computational stability can only be achieved by decreasing the analog frequencies. A time-scale factor SF_t , is selected such that the computer time t' equals $SF_t t$. For

TABLE II. - PRESCALED VARIABLES FOR
HYDES PROGRAM

Variable, x	Scale factor ^a , SF_X
$T_2, T_{2.1}, T_{2.1}', T_{3.2}, T_{3.2}', T_{2.2}, T_{3.5}, \bar{T}_{f1}, \bar{T}_{f2}$	555.55 K (1000° R)
T_3', T_3, \bar{T}_c	1111.1 K (2000° R)
T_4, \bar{T}_b	2777.8 K (5000° R)
T_5', T_5	2222.2 K (4000° R)
T_6', T_6, T_7	1388.9 K (2500° R)
h_i	$SF_{TI} SF_{CPI}$
c_p, c_v	2092.2 J/kg-K (0.5 Btu/lbm-°R)
γ	2.0
F_1	1.0
F_2	1.0
tr	1.25
f/a	0.05

^aThe following relations between scale factors are assumed:

$$\begin{aligned}
 SF_{TRQT1} &= SF_{TRQC} \\
 SF_{WDF1} &= SF_{WDC} = SF_{WDB} = SF_{WDT1} = SF_{WDT2} = SF_{WDN1} \\
 SF_{WDF2} &= SF_{WDV3} = SF_{WDN2} \\
 SF_{WDV2} &= SF_{WDN4} \\
 SF_{P3} &= SF_{P4} \\
 SF_{P32} &= SF_{P35} \\
 SF_{PS} &= SF_{PIN} \text{ for nozzles}
 \end{aligned}$$

this definition of $SF_{t'}$, a value exceeding 1.0 corresponds to a "slowing down" of the analog problem.

The selection of a suitable time-scale factor requires the user to estimate the real-time frequencies associated with the engine dynamics. Analog frequencies can be estimated for each intercomponent volume by assuming a "resistive" termination downstream. For this simplified first-order model, the time constant associated with each volume is given by

$$\tau = \frac{W}{\dot{w}} = \frac{PV}{RT\dot{w}} = \frac{1}{\omega_a} \quad (42)$$

where W is the stored mass in the volume, \dot{w} is the total flow through the volume, and ω_a is the real-time analog frequency. The ratio of digital frequency to the scaled cutoff frequency associated with the volume is given by

$$\frac{\omega_d}{\omega_a} = \frac{2\pi(SF_{t'})\tau}{t_d} \quad (43)$$

where t_d is the cycle time for the digital program. The cycle time for the existing digital program varies depending on the engine configuration but is between 23 and 44 milliseconds. Experience has shown that a minimum frequency ratio of 50:1 at the design point results in computational stability. A smaller ratio might prove satisfactory for a particular engine simulation, however. The achievement of this minimum ratio usually requires a combination of time scaling ($SF_{t'}$) and increasing of the smaller intercomponent volumes V . When increasing the volume above the actual value, care should be taken to keep the decreased cutoff frequency above the range of frequencies of interest.

For solution on the analog or digital computer, the equations given in appendix B must be rewritten in terms of scaled variables. Appendix C contains the definitions of the scaled (computer) variables. For the scaled equations solved on the digital computer, the scale factors and engine parameters are combined to form digital coefficients $SC(i)$. Similarly, the scale factors and engine parameters appearing in the analog-solved equations are combined to form analog coefficients $C(i)$. Appendix D contains the definitions of the digital and analog coefficients.

Engine Definition

The use of the HYDES program to simulate any of the configurations described in table I requires the user to supply to the computer information which defines the engine to be studied. The engine configuration is specified by a set of logical variables. These variables are either "TRUE" or "FALSE." The means of setting these variables is discussed in the section Input Data Preparation. Table III lists the combinations of these variables which define the 16 configurations (with options) previously discussed. Combinations of the variables which do not appear in table III may lead to fallacious results and should be avoided.

The logical variable HBPR="TRUE" denotes a fan requiring separate performance maps for the fan hub and tip sections (configurations A, B, E, and F). The variable MIX="TRUE" denotes mixed turbofans (configurations B, D, and F). The variable STRM3="TRUE" denotes three-stream turbofans (configurations A and B). TURBJ1="TRUE" and TURBJ2="TRUE" denote one-spool and two-spool turbojets, respectively (configurations G and H). For the HBPR="TRUE" configurations, SPLIT="TRUE" denotes the fan-tip performance data expressed in terms of total fan flow (-1 option). For the case when HBPR="TRUE" and STRM3="FALSE", SUPER="TRUE" denotes the simplified fan-hub performance map previously discussed (-2

TABLE III. - LOGICAL VARIABLES DENOTING ENGINE CONFIGURATIONS
AND OPTIONS FOR HYDES PROGRAM^a

Configuration	Logical variable						
	HBPR	MIX	STRM3	TURBJ1	TURBJ2	SUPER	SPLIT
A	T	F	T	F	F	F	F
A-1	↓	F	↓	↓	↓	↓	T
B	↓	T	↓	↓	↓	↓	F
B-1	↓	T	↓	↓	↓	↓	T
C	F	F	F	↓	↓	↓	F
D	F	T	↓	↓	↓	↓	F
E	T	F	↓	↓	↓	↓	F
E-1	↓	↓	↓	↓	↓	↓	T
E-2	↓	↓	↓	↓	↓	T	F
E-3	↓	↓	↓	↓	↓	T	T
F	↓	T	↓	↓	↓	F	F
F-1	↓	↓	↓	↓	↓	F	T
F-2	↓	↓	↓	↓	↓	T	F
F-3	↓	↓	↓	↓	↓	T	T
G	F	F	↓	T	↓	F	F
H	F	F	↓	F	↓	F	F

^aT denotes "TRUE" and F denotes "FALSE."

option).

To simulate a particular engine, the user must supply the values for the analog and digital coefficients defined in appendix D. The means of inputting these coefficients to the computer is discussed in the section Input Data Preparation. The digital coefficients are assumed to be scale fractions (less than unity). If a calculated value exceeds unity for the selected scale factors and/or engine parameters, the coefficient must be redefined and the corresponding equation (or equations) modified accordingly. Similarly, the analog coefficients defined in appendix D represent potentiometer settings which should be less than 1.0. Redefinition of an analog coefficient requires a corresponding change in an amplifier gain on the analog computer. The definitions of the analog and digital coefficients listed in appendix D have been chosen so as to minimize the changes required to simulate a wide range of engine types and sizes.

Digital Program

The digital portion of the HYDES program is used, primarily, to compute the time derivatives associated with the engine system's dynamics. The bracketed terms in equations (1) and (2) and the torque differentials associated with equation (31) are computed on the digital and transmitted to the analog by means of the DAC's. The analog computer is then used to compute the pressures, temperatures, and rotor speeds which are required as input to the digital program and are input through the ADC's.

Because of the large size of the simulation, the digital program was divided into two parts - a data input program and the main program.

Data input program. - The data input program reads and stores (1) digital coefficients $SC(i)$, (2) initial conditions for the DAC's $AI(i)$, (3) scale factors for the component map data, and (4) unscaled component performance data. The program proceeds to scale the component map data and stores the $SC(i)$'s, $AI(i)$'s, and scaled map data in COMMON blocks shared by the main program and associated subprograms. The program then tests the position of user-set sense switches to determine the states of the logical variables HBPR, MIX, etc. (see table III). Based on the specified configuration, the scaled component map data are stored in the proper storage locations.

The data input program (and associated library routines) requires 7367 words of core storage. Included in this total are 2214 words of storage used for the COMMON data. Appendix E contains a FORTRAN listing of the data input program as written for the Lewis Research Center's hybrid system. (The reading-in of the scaled-fraction $SC(i)$ and $AI(i)$ data requires the use of a special S format (ref. 10) in statement 5 of the listing.)

Main program. - The main digital program is used to perform all the algebraic

computation and function generation required to compute the temperature, stored-mass, and rotor-speed derivatives. The main program also tests sense switches to determine the engine configuration and proper branching within the program.

To reduce the core storage requirements, the main program utilizes subroutines to perform repeated operations. For example, a subroutine FNCMP is used to solve the scaled versions of equations (9) to (17) for each of the fans and/or compressors. The following section describes each of the subroutines utilized by the main program. The main digital program (and associated subroutines and library routines) requires 11 304 words of core storage. Included in this total are the 2214 words of storage used for COMMON data.

The main program accepts current values of pressures, temperatures, rotor speeds, nozzle areas, and fuel flow as input from the analog computer. Updated values for temperature derivatives, stored-mass derivatives, torque differentials, compressor map variables, and thrust are output to the analog through the DAC's. The user, by depressing a sense switch, can direct the program to output current values of selected engine variables on the teletype. The program also tests for scaled-fraction overflows and will output an appropriate message at the teletype if an overflow occurs. Appendix E contains a FORTRAN listing of the main program as written for the Lewis hybrid system. (The use of scaled fractions in the main program requires the suffix S on fractional constants and a special routine SSQRT to perform the square root operation (ref. 10)).

Subroutines. - The various subroutines called by the main digital program are listed here and the function of each is described. FORTRAN listings of the subroutines are included in appendix E.

PROCOM: Subroutine PROCOM calculates thermodynamic gas properties either for air or for a JP4-air mixture using curve-fits of the tables of reference 7. Inputs to the subroutine are the scaled-fraction temperature (rescaled for a maximum of 277.8 K (5000° R) prior to being input) and the scaled-fraction fuel-air ratio (scaled for a maximum of 0.05). The outputs of the subroutine are the scaled-fraction specific heats (scaled for a maximum of 0.5), the specific-heat ratio (scaled for a maximum of 2.0), and enthalpy (scaled for a maximum of 3.487×10^6 J/kg (1500 Btu/lbm)). A FORTRAN listing of subroutine PROCOM is given in appendix E.

TRAT: Subroutine TRAT calculates the isentropic temperature rise parameter $(\Delta T/T_{in})_{id}$ for a fan or compressor. The subroutine is called by the main program when SUPER="TRUE" and by FNCMP. The inputs to TRAT are the scaled-fraction pressure ratio (rescaled for a maximum of 15.0 prior to being input) and the average specific-heat ratio (scaled for a maximum of 2.0). The output of the subroutine is the scaled-fraction temperature rise parameter (scaled for a maximum of 1.25). Subroutine TRAT makes use of calls to subroutines NMXTR and CLCTR to perform the necessary

calculations. A FORTRAN listing of subroutine TRAT is given in appendix E.

NOZZL: Subroutine NOZZL computes those terms, sensitive to pressure ratio and specific-heat ratio, required in the calculation of flow and thrust for a convergent nozzle. The inputs to the subroutine are the scaled-fraction inlet and exit pressures and the ratio of the exit and inlet pressure scale factors. The outputs of the subroutine are the functions

$$\left(\frac{P_{out}}{P_{in}}\right)^{\frac{1}{\gamma}} \sqrt{\frac{2\gamma}{(\gamma-1)} \left[1 - \left(\frac{P_{out}}{P_{in}}\right)^{\frac{\gamma-1}{\gamma}}\right]}$$

and

$$\sqrt{1 - \left(\frac{P_{out}}{P_{in}}\right)^{\frac{\gamma-1}{\gamma}}}$$

(both scaled for a maximum of 1.0) and the static pressure at the nozzle throat P_s (scaled the same as P_{in}). The specific-heat ratio γ is assumed to be 1.35 for these calculations. Subroutine NOZZL makes use of calls to subroutines NRMPN, CLCFN, and CLCWN to perform the necessary calculations. A FORTRAN listing of subroutine NOZZL is given in appendix E.

FNCMP: Subroutine FNCMP calculates the flow, discharge enthalpy, and torque for a fan or compressor. The inputs to the subroutine are a component index N (N=1 for the fan hub or low-pressure compressor, N=2 for the high-pressure compressor, N=3 for the fan tip) and the scaled-fraction inlet pressure, inlet temperature, inlet enthalpy, exit pressure, exit volume temperature, and fraction of design rotor speed (the latter scaled for a maximum of 2.0). The outputs of the subroutine are the scaled-fraction flow, discharge enthalpy, torque, map pressure ratio, and map flow parameter. Subroutine FNCMP makes use of calls to subroutine MAPFUN to perform the radial interpolation of the map data stored in COMMON arrays. A FORTRAN listing of subroutine FNCMP is given in appendix E.

TURB: Subroutine TURB calculates the flow, discharge enthalpy, and torque for turbines. Subroutine TURB is similar to subroutine FNCMP in operation. The inputs to TURB are a component index N (N=1 for the high-pressure turbine, N=2 for the low-pressure turbine) and the scaled-fraction inlet pressure, inlet temperature, inlet enthalpy, exit pressure, and fraction of design rotor speed (scaled for a maximum of

2.0). The outputs of the subroutine are the scaled-fraction flow, discharge enthalpy, and torque. The FORTRAN listing of subroutine TURB is given in appendix E.

NRMPN: Subroutine NRMPN converts a scaled-fraction pressure ratio to a format suitable for use with the library-supplied function generation routines. Subroutine NRMPN is called by subroutine NOZZL and contains the pressure-ratio breakpoints used in the computation of the nozzle flow and thrust functions. The input to the subroutine is the scaled-fraction pressure ratio (scaled for a maximum of 1.0). The outputs of the subroutine are the normalized pressure ratio and an integer ERRFLG used to signal an out-of-range input. A FORTRAN listing of NRMPN is given in appendix E.

CLCFN: Subroutine CLCFN generates the function

$$\sqrt{1 - \left(\frac{P_{out}}{P_{in}}\right)^{\frac{\gamma-1}{\gamma}}}$$

required for convergent nozzle thrust calculations. Subroutine CLCFN is called by subroutine NOZZL and contains the function values (scaled for a maximum of 1.0) corresponding to the breakpoints contained in NRMPN with γ equal to 1.35. The input to the subroutine is the normalized pressure ratio. The output of the subroutine is the scaled-fraction thrust function. A FORTRAN listing of CLCFN is given in appendix E.

CLCWN: Subroutine CLCWN generates the function

$$\left(\frac{P_{out}}{P_{in}}\right)^{\frac{1}{\gamma}} \sqrt{\frac{2\gamma}{(\gamma-1)} \left[1 - \left(\frac{P_{out}}{P_{in}}\right)^{\frac{\gamma-1}{\gamma}}\right]}$$

required for convergent nozzle flow calculations. CLCWN is called by subroutine NOZZL and contains the function values (scaled for a maximum of 1.0) corresponding to the breakpoints contained in NRMPN with γ equal to 1.35. While the input to the subroutine is the normalized pressure ratio, it need not be included as an argument in the call statement when following a similar call to CLCFN. The output of the subroutine is the scaled-fraction flow function. A FORTRAN listing of CLCWN is given in appendix E.

NMXTR: Subroutine NMXTR converts a scaled-fraction pressure ratio to a format suitable for use with the library-supplied function generation routines. NMXTR is called by subroutine TRAT and contains the pressure ratio breakpoints (scaled for a maximum of 15.0) used in the computation of the isentropic temperature rise parameter for fans and compressors. The input to the subroutine is the rescaled pressure ratio.

The outputs of the subroutine are the normalized pressure ratio and an integer ERRFLG used to signal an out-of-range input. A FORTRAN listing of NMXTR is given in appendix E.

CLCTR: Subroutine CLCTR generates the isentropic temperature rise parameter $(\Delta T/T_{in})_{id}$ for a fan or compressor. CLCTR is called by subroutine TRAT and contains the parameter values (scaled for a maximum of 1.25) corresponding to the breakpoints contained in NMXTR with γ equal to 1.35. The input to the subroutine is the normalized pressure ratio from NMXTR. The output of the subroutine is the scaled-fraction temperature rise parameter. A FORTRAN listing of CLCTR is given in appendix E.

MAPFUN: Subroutine MAPFUN generates functions of two variables by radial interpolation. MAPFUN is called by subroutines FNCMP and TURB to calculate performance map outputs for specified pressure ratios and rotor speeds. The inputs to MAPFUN are a map index MN, the scaled-fraction pressure ratio, and the scaled-fraction corrected speed parameter. The map index is defined as follows: MN=1 for a fan-hub flow map, MN=2 for a fan-hub efficiency map, MN=3 for a high-pressure-compressor flow map, MN=4 for a high-pressure-compressor efficiency map, MN=5 for a high-pressure-turbine flow map, MN=6 for a high-pressure-turbine enthalpy drop map, MN=7 for a low-pressure-turbine flow map, MN=8 for a low-pressure-turbine enthalpy drop map, MN=9 for a fan-tip flow map, and MN=10 for a fan-tip efficiency map. The output of the subroutine is the appropriate scaled map variable. The scaled map data and search indices are shared by MAPFUN through the use of COMMON arrays. A FORTRAN listing of MAPFUN is given in appendix E.

MOOR: Subroutine MOOR signals the occurrence of out-of-range inputs to maps generated by MAPFUN. Termination of input data for fans and compressors at the stall line results in MOOR signaling fan or compressor stall. Subroutine MOOR may be written to suit the needs of the user. A FORTRAN listing of the existing version of MOOR is given in appendix E.

In addition to the subroutines previously described, the digital program makes use of a number of library-supplied routines. Subroutines VBNS, FNGN1, FNLK1, and CBNS are part of the library function generation system (ref. 11) and are used to generate functions of one variable. These routines are called by subroutines CLCFN, CLCWN, and CLCTR. For other computing systems, similar function generation routines are usually available. Library routines are also required for performing scaled-fraction arithmetic, integer and logical operations, input-output control, and hybrid linkage.

Analog Program

The analog portion of the HYDES program is used, primarily, to perform the integration with respect to time associated with the engine dynamics. Appendix F is a summary of the scaled equations, solved on the analog computer. For each intercomponent volume, the scaled-fraction stored mass, temperature, and pressure are computed by using the scaled versions of equations (1) to (3). Figure 11 illustrates the analog calculation of pressure P_3 and temperature T_3 . Other pressures and temperatures are calculated in the same way.

The analog coefficients $C(i)$ are calculated by the user from the definitions contained in appendix D. Scaled-fraction rotor speeds are computed by using the scaled version of equation (31).

Inputs to the analog (through the DAC's) are the scaled stored-mass derivatives $DW_{_}$, the scaled temperature derivative terms $T_{_}DN$, and the scaled torque differentials $DTQT1$ and $DTQT2$. Derivatives for volumes or spools not being used are set to zero by the digital program (see main program listing). Control lines are also set to allow the user to hold the appropriate analog integrators in the initial condition (IC) if drift becomes a problem. Also input to the analog (for display purposes) are the high-pressure-compressor map pressure ratio PRC and flow parameter FPC , total engine thrust $TAUT$, and either the fan-hub flow $WDF1$ for $HBPR="FALSE"$ or the fan-tip flow

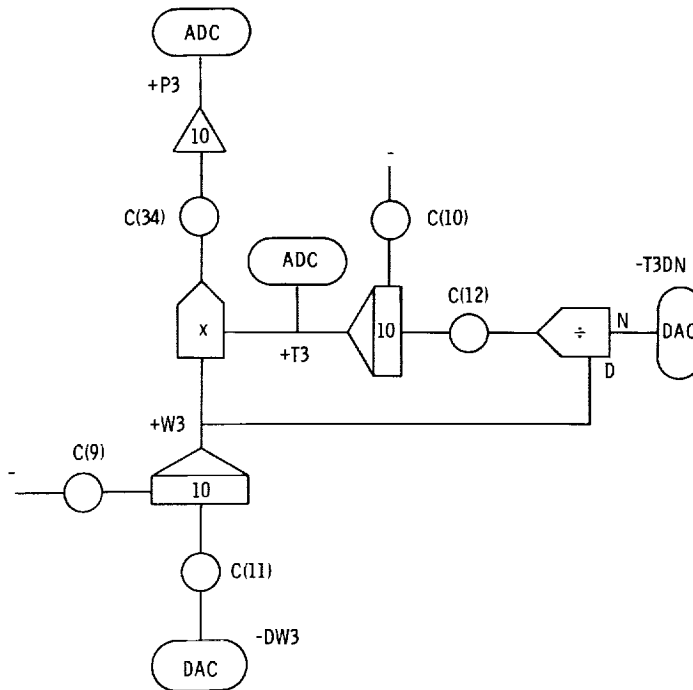


Figure 11. - Analog computation of high-compressor discharge conditions in combustor inlet volume.

WDF2 for HBPR="TRUE." The choice of variables to be transmitted to the analog for display was dictated by the shortage of available DAC channels and might be changed by the user for a particular problem. The outputs from the analog (through the DAC's) are the scaled pressures $P_{_}$, temperatures $T_{_}$, and the fraction of design rotor speeds PCNT1 and PCNT2. Also supplied to the digital by the analog are the scaled nozzle areas AN1 and AN2, the scaled inlet pressure P2, and fuel flow WDF. Again, the choice of these variables was dictated by the shortage of available ADC channels.

The basic HYDES program does not provide for the simulation of control system dynamics. The shortage of hybrid interface channels does, however, dictate that the simulation of controls take place on the analog computer. The simulation of a selected engine and fuel control is described in a following section. That example illustrates the relation between an analog-simulated fuel control and the basic hybrid engine simulation and demonstrates the transient operation of the program. The analog portion of the simulation (without controls) requires 16 summers, 20 integrators, 18 quarter-square multipliers, and 57 attenuators.

Input Data Preparation

The use of the HYDES program requires that the user provide input data appropriate to the engine system being simulated. These data include (1) values for the logical variables HBPR, MIX, STRM3, TURBJ1, TURBJ2, SUPER, and SPLIT which define the engine configuration; (2) values for the digital coefficients SC(i); (3) initial conditions AI(i) for the DAC variables; (4) unscaled performance data for the fans, compressors, and turbines; (5) scale factors to be used in scaling the component performance data; and (6) values for the analog coefficients C(i). The following sections describe the preparation of this input data and the steps required to input the data to the computer.

Configuration specification. - The execution of the data input program and the main digital program (appendix E) requires that the user specify the engine configuration to be simulated. For the existing programs, the configuration specification is accomplished by depressing sense switches at the control console. Table IV summarizes the configuration specification procedure.

Prior to executing the data input program, the user must position sense switches 2, 5, 6, and 7 as dictated by table IV. For the one-spool turbojet case (configuration G), depressing sense switch 5 results in the logical variable TURBJ1 being set "TRUE" in the data input program. By sensing this value of TURBJ1, the data input program accepts performance data for only one compressor and turbine and stores the resultant scaled component data in the proper locations. For configurations A, B, E, and F, sense switch 2 is depressed by the user, resulting in the logical variable HBPR being

TABLE IV. - CONFIGURATION SPECIFICATION PROCEDURE FOR THE EXISTING HYDES PROGRAM^a

Configuration	Procedure prior to executing data input program				Procedure prior to executing main program							
	Logical variable											
	HBPR Depress SSW ^b 1?	TURBJ1 Depress SSW 5?	TURBJ2 Depress SSW 6?	SUPER Depress SSW 7?	HBPR Depress SSW 2?	MIX Depress SSW 3?	STRM3 Depress SSW 4?	TURBJ1 Depress SSW 5?	TURBJ2 Depress SSW 6?	SUPER Depress SSW 7?	SPLIT Depress SSW 8?	
A	Y	N	N	N	Y	Y	N	N	N	N	N	
A-1	Y	N	N	N	Y	Y	N	N	N	N	N	
B	N	N	N	N	Y	Y	N	N	N	N	N	
B-1	N	N	N	N	Y	Y	N	N	N	N	N	
C	N	N	N	N	Y	Y	N	N	N	N	N	
D	N	N	N	N	Y	Y	N	N	N	N	N	
E	Y	N	N	N	Y	Y	N	N	N	N	N	
E-1	Y	N	N	N	Y	Y	N	N	N	N	N	
E-2	Y	N	N	N	Y	Y	N	N	N	N	N	
E-3	Y	N	N	N	Y	Y	N	N	N	N	N	
F	Y	N	N	N	Y	Y	N	N	N	N	N	
F-1	Y	N	N	N	Y	Y	N	N	N	N	N	
F-2	Y	N	N	N	Y	Y	N	N	N	N	N	
F-3	Y	N	N	N	Y	Y	N	N	N	N	N	
G	N	N	N	N	Y	Y	N	N	N	N	N	
H	N	N	N	N	Y	Y	N	N	N	N	N	

^aY denotes "yes" and N denotes "no."

^bSSW denotes sense switch.

set "TRUE" in the data input program. This provides for the input and storage of performance data for a fan or compressor in the bypass stream (fig. 5). For either configuration E or F, the user may depress sense switch 7, resulting in the variable SUPER being set "TRUE" in the data input program. This option (-2) bypasses the data input and storage required for mapping the fan hub (low-pressure compressor). A linear relation between the "supercharger" pressure ratio and corrected speed is used in the main program in place of the usual performance map.

The execution of the data input program results in the required component performance data, digital coefficients, and DAC initial conditions being stored in the proper storage locations for the selected configuration. However, further configuration definition is required prior to executing the main program (table IV). If mixing of streams is desired (configurations B, D, or F), sense switch 3 is depressed, resulting in a logical variable MIX being set "TRUE" in the main program. This variable is tested in the program to accomplish the necessary branching and computation associated with volume V_7 and the mixed nozzle. For the three-stream configurations (configurations A or B), sense switch 4 is depressed, resulting in the logical variable STRM3 being set "TRUE." This option provides for the branching and computation associated with volume $V_{2.2}$ and the fourth nozzle (fig. 1). For configurations A, B, E, and F, depressing sense switch 8 results in the variable SPLIT being set "TRUE" in the main program. The program then interprets the fan-tip data as being in terms of the total fan flow (-1 option). For this case, the flow output of the N=3 call to subroutine FNCMP (fan tip) is assumed to be the total fan flow. The bypass flow is then calculated by subtracting the fan-hub flow from the total fan flow. Since the torque output of the N=3 call to FNCMP is computed by using the total fan flow, it must be multiplied by the ratio of bypass flow to total fan flow.

Digital coefficients and DAC initial conditions. - The solution of the scaled equations in the main program (appendix E) requires that the digital coefficients SC(i) be stored in a COMMON array by using the data input program. The data input program is set up to accept NSC values of SC(i), where $NSC \leq 125$. The existing program uses 103 values of SC(i). The addition of a limited number of new equations and coefficients to the main program may be accomplished without modifying the data input program. The values of the SC(i)'s are calculated by the user from the definitions given in appendix D. The ordering of calculations in the program was chosen to allow the SC(i)'s to be represented as scaled fractions. If a calculated SC(i) equals or exceeds unity, the coefficient must be redefined or scale factors changed to correct the situation.

In addition to the NSC values of the digital coefficients, the user must also specify initial conditions to be transmitted to the analog through the 24 DAC's. Since, for the existing program, the DAC's are used only for transmitting derivatives and display variables, the initial conditions may be set to zero.

In the Lewis hybrid computing system, digital input is accomplished by using paper tape and a high-speed paper-tape reader. Table V illustrates the format used for the input of the digital coefficients and DAC initial condition data. The first line (starting in column 1) contains the integer value of NSC (I4 format). The next lines contain the scaled-fraction values of the digital coefficients (5S8 format). The last five lines contain the scaled-fraction values of the DAC initial conditions (5S8 format).

For certain engine configurations, a particular digital coefficient may not be needed. A value of unity (0.99999) should be inserted in the data.

Component performance data. - The data input program is used to input, scale, and store performance data for the fans, compressors, and turbines associated with the engine being simulated. Fan and compressor data, in the form shown in figure 9, are required. Turbine data must be in the form shown in figure 10.

Fan and compressor performance data are usually found in the form shown in figure 12. The conversion of this data to the desired form merely involves reversing the pressure ratio and corrected flow axes for the flow map and the reading of efficiency values along constant speed lines at selected values of pressure ratio for the efficiency map.

TABLE V. - DIGITAL COEFFICIENT AND DAC INITIAL
CONDITION INPUT DATA (CONFIGURATION E)

103					Integer value of NSC
.51867	.00000	.00000	.99999	.99999	} Scaled-fraction values of digital coefficients
.45731	.59066	.66125	.40000	.99999	
.31877	.40000	.06667	.03333	.80000	
.38623	.80000	.43427	.16491	.26667	
.00000	.00000	.00000	.10000	.99999	
.00000	.07500	.00000	.00000	.00000	
.00000	.00000	.00000	.00000	.00000	
.00000	.13906	.20000	.06667	.03333	
.02000	.99158	.14615	.02000	.03333	
.02667	.99999	.00000	.00000	.20000	
.99999	.99999	.20000	.25000	.40472	
.39203	.23858	.37063	.00000	.00000	
.12752	.17090	.10000	.12500	.29280	
.40436	.76349	.49547	.63501	.96400	
.79212	.96400	.62554	.82422	.75317	
.99999	.54454	.99999	.16667	.66667	
.08333	.04122	.28516	.01532	.00000	
.00000	.00000	.22443	.00000	.00000	
.00000	.10539	.00045	.00801	.25409	
.24941	.25028	.50000	.28284	.00500	
.06667	.00000	.73500			
.00000	.00000	.00000	.00000	.00000	} Scaled-fraction values of initial conditions
.00000	.00000	.00000	.00000	.00000	
.00000	.00000	.00000	.00000	.00000	
.00000	.00000	.00000	.00000	.00000	
.00000	.00000	.00000	.00000	.00000	

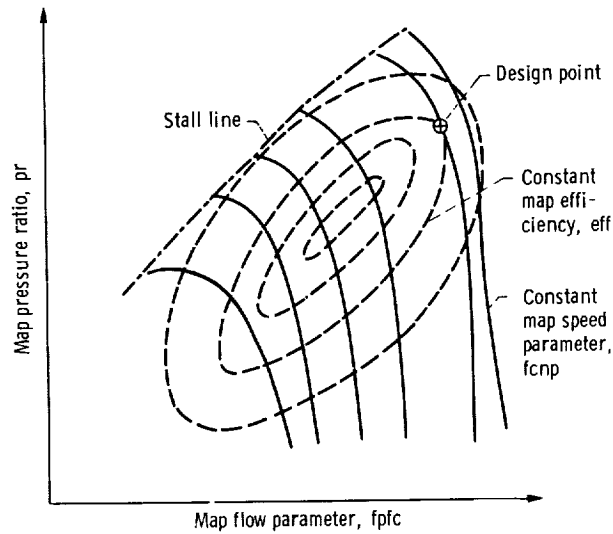


Figure 12. - Typical fan or compressor performance data.

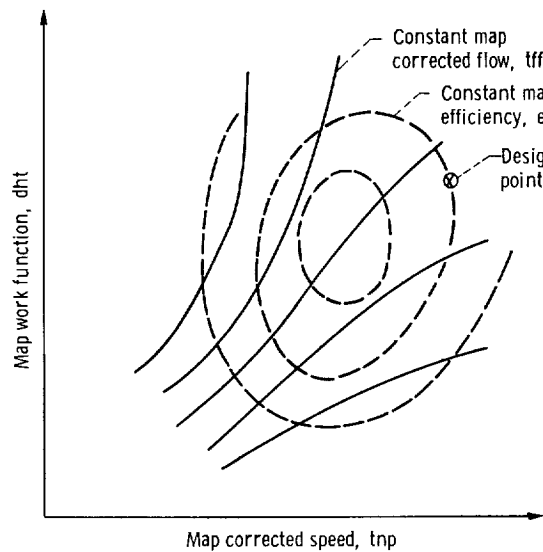


Figure 13. - Typical turbine performance data.

Turbine performance data are usually found in the form shown in figure 13. A turbine work function $dht = \Delta h/T_{in}$ is plotted against the turbine corrected speed for constant values of the turbine corrected flow function $tff = \dot{w} \sqrt{T_{in}/P_{in}}$ and efficiency. Since the hybrid program uses pressure ratio as an independent variable in turbine calculations, the performance data shown in figure 13 must be converted to a more suitable form.

A digital program, written in FORTRAN for running on the IBM 7094 computer, has been developed by the authors of reference 8 to accomplish the turbine map conversion. Appendix G contains a listing of that program. For each selected speed parameter (in

ascending order), values of the flow function and efficiency are read from figure 13 for selected values of the work function. These values, together with the desired pressure ratio breakpoints, are read into the conversion program. The conversion program proceeds (1) to compute the pressure ratio at each specified point on the map; (2) to interpolate, for each speed parameter, the input data to determine values of the work function and flow function at the specified pressure-ratio breakpoints; (3) to convert the work function and flow function values to the desired flow and enthalpy drop parameters (i. e., $hpt = dht/tnp$ and $fpt = tff/tnp$). Since the available turbine map data might have to be scaled to the design point of a theoretical engine, the map scaling coefficients DHCF and ETTCF must be used in the calculation of actual pressure ratios in the conversion program. Also required as input to the conversion program are the specific-heat ratio GAM and the specific heat CP for the turbine. The values corresponding to the design-point discharge temperature and turbine fuel-air ratio are used. The output data from the conversion program are plotted in the form shown in figure 10 to facilitate the removal of any irregularities that may exist in the computed data.

The configuration specification outlined in table IV enables the user to input only the data for components actually required in the simulation. The order of input of map data is (1) fan-hub flow map (if required), (2) fan-hub efficiency map (if required), (3) high-pressure-compressor flow map, (4) high-pressure-compressor efficiency map, (5) high-pressure-turbine flow map, (6) high-pressure-turbine enthalpy drop map, (7) low-pressure-turbine flow map (if required), (8) low-pressure-turbine enthalpy drop map (if required), (9) fan-tip flow map (if required) (in terms of total fan flow for SPLIT="TRUE" option), and (10) fan-tip efficiency map (if required).

For the existing data input program, the number of curves per map NCV and the number of points per curve NPT have been set to eight. These values may be changed by the user, provided the limits of MAPFUN ($NPT \leq 10$, $NCV \leq 8$) are not exceeded.

Table VI illustrates the format used for the input of the component performance data. For convenience, all data are placed on one data tape. For each map, the first line of data (starting in column 1) contains the map scale factors XSC, YSC, and ZSC (3F9.4 format). These scale factors are real numbers and are used to scale the map pressure ratio, speed parameter, and map output, respectively. For example, if the maximum pressure ratio on the map is 10.0, a scale factor of XSC=20 might be chosen. The second line of data contains the eight values of the unscaled speed parameter for the map in ascending order (8F9.3 format). The next 16 lines contain the unscaled-pressure-ratio map output pairs for each specified speed parameter. The data are arranged (four pairs to a line) in order of ascending pressure ratio, starting with the data for the lowest speed parameter. An 8F9.4 format is used. (The scale factor on the speed parameter for fans and compressors must be 2.0, and the scale factor on turbine

TABLE VI. - COMPONENT MAP SCALE FACTORS AND DATA (CONFIGURATION E)

(a) Fan hub (including booster)

5.00	2.00	226.80	.800	.900	.950	1.000	1.050	1.120
.350	.600	.800	.900	.950	1.000	1.050	1.120	1.120
1.0000	68.0385	1.0500	60.1007	1.0810	53.8865	1.0930	50.4392	50.4392
1.1020	47.6270	1.1100	44.2250	1.1140	41.2627	1.1160	37.8294	37.8294
1.0000	100.9238	1.1000	100.2434	1.2110	98.0662	1.2970	92.9859	92.9859
1.3300	88.9036	1.3450	85.5017	1.3700	79.3782	1.3900	70.0796	70.0796
1.0000	129.9535	1.3900	129.9535	1.5600	129.1824	1.6450	127.3227	127.3227
1.6950	124.7372	1.7500	116.7994	1.7650	112.4903	1.7700	102.5113	102.5113
1.0000	148.3239	1.5400	148.3239	1.8550	147.8703	1.9380	146.2828	146.2828
2.0070	142.4273	2.0350	137.8914	2.0500	134.9430	2.0720	125.4176	125.4176
1.0000	155.1278	1.6100	155.1278	2.0120	153.1278	2.1140	153.9031	153.9031
2.1700	151.4083	2.2100	147.9610	2.2300	143.0169	2.2450	137.5284	137.5284
1.0000	160.5255	2.1010	160.5255	2.1400	160.4348	2.2000	160.2533	160.2533
2.3160	159.2101	2.3750	156.9421	2.4110	154.5835	2.4500	149.7754	149.7754
1.0000	163.7006	1.8820	163.7006	2.2650	163.8821	2.3990	162.6120	162.6120
2.4280	162.0677	2.4800	160.7976	2.5300	159.2101	2.5700	157.6225	157.6225
1.0000	167.6015	1.9400	167.6015	2.0000	167.6015	2.1000	167.6015	167.6015
2.3000	167.7829	2.5000	167.6015	2.6250	167.4645	2.6790	166.4675	166.4675

Unscaled pressure-ratio-map output pairs
(Output data are in kg/sec.)

5.00	2.00	1.00	.800	.900	.950	1.000	1.050	1.120
.350	.600	.800	.900	.950	1.000	1.050	1.120	1.120
1.0000	.5000	1.0810	.7500	1.0930	.7690	1.1020	.7650	.7650
1.1100	.7630	1.1140	.7500	1.1160	.7000	1.1180	.5000	.5000
1.0000	.5000	1.2110	.7500	1.2380	.8200	1.2650	.8400	.8400
1.3300	.8480	1.3750	.8200	1.3800	.8000	1.4000	.5000	.5000
1.0000	.5000	1.3900	.6500	1.5600	.8000	1.6450	.8500	.8500
1.7200	.8670	1.7650	.8300	1.7700	.7500	1.7900	.5000	.5000
1.0000	.5000	1.5400	.6500	1.7970	.8000	1.9380	.8600	.8600
2.0070	.8700	2.0350	.8500	2.0720	.7500	2.0800	.5000	.5000
1.0000	.5000	1.6100	.6500	1.9100	.8000	2.0120	.8400	.8400
2.1450	.8630	2.1920	.8500	2.2300	.8000	2.2500	.5000	.5000
1.0000	.5000	1.6770	.8400	1.8900	.7500	2.1400	.8300	.8300
2.2000	.8400	2.3480	.8400	2.4360	.7500	2.4600	.5000	.5000
1.0000	.5000	1.7450	.6500	1.9820	.7500	2.2650	.8000	.8000
2.4280	.8200	2.4800	.8000	2.5700	.6750	2.6000	.5000	.5000
1.0000	.5000	1.9400	.6500	2.1000	.6600	2.3000	.6600	.6600
2.5000	.6600	2.6250	.6500	2.6790	.6000	2.7500	.5000	.5000

Unscaled pressure-ratio-map output pairs

TABLE VI. - Continued. COMPONENT MAP SCALE FACTORS AND DATA (CONFIGURATION E)

(b) High-pressure compressor

	20.00	2.00	34.02								Map scale factors XSC, YSC, ZSC (ZSC is in kg/sec.)
	.600	.800	.850	.900	.950	1.000	1.050	1.150			
1.0000	7.0760	1.2500	6.8492	1.5200	6.6678	1.000	2.2300	5.8967			
2.4700	5.4884	2.5200	5.3070	2.5300	4.5359	2.5400	4.0823	4.0823			
1.0000	14.0613	2.0000	13.8345	2.4100	13.7211	2.8500	2.8500	13.5170			
3.6000	13.0634	4.2700	12.5191	4.8200	11.9748	5.1400	5.1400	11.6119			
1.0000	17.9168	2.8000	17.5539	3.6200	17.3045	4.6500	4.6500	16.8962			
5.3000	16.4653	5.8000	16.0117	6.2000	15.5128	6.8000	6.8000	14.5602			
1.0000	21.5455	3.8000	21.3414	4.8500	21.2507	6.0500	6.0500	20.9785			
7.4800	20.1848	8.1500	19.5044	8.7700	18.2343	8.9200	8.9200	17.7580			
1.0000	24.9474	4.9000	24.1763	7.3500	23.9722	8.3500	8.3500	23.7001			
9.8500	22.7702	10.2300	22.3847	10.8400	21.3641	11.0800	11.0800	20.7971			
1.0000	26.5804	6.6000	26.5804	8.2800	26.4897	10.0500	10.0500	26.2629			
10.8500	26.0814	11.8000	25.6278	12.6400	24.9928	13.3200	13.3200	23.9949			
1.0000	27.9411	7.9000	27.9411	11.1600	27.4649	11.7800	11.7800	27.3888			
12.8500	26.9432	13.7400	26.4896	14.3500	25.9680	14.4900	14.4900	25.8320			
1.0000	28.3947	8.5000	28.3947	9.7500	28.3040	11.0000	11.0000	28.2586			
12.6500	28.0092	13.6000	27.6917	14.5300	27.2154	15.1000	15.1000	26.8072			

	20.00	2.00	1.00								Map scale factors XSC, YSC, ZSC (ZSC is in kg/sec.)
	.600	.800	.850	.900	.950	1.000	1.050	1.150			
1.0000	3.000	1.2500	1.5200	1.5200	1.5200	1.6000	2.2300	.6250			
2.4700	6.000	2.5200	5.670	2.7500	4.500	4.500	3.0000	.3000			
1.0000	3.000	2.0000	6.000	2.4100	7.000	2.8500	2.8500	.7500			
.6000	.8000	4.2700	.8100	4.8200	.8000	9.0000	9.0000	.3000			
1.0000	.3000	2.8000	6.000	3.2000	.7000	4.2500	4.2500	.8000			
5.3000	.8400	5.8000	.8440	6.8000	.8120	12.0000	12.0000	.3000			
1.0000	.3000	3.8000	6.000	4.3500	.7000	5.6500	5.6500	.8000			
7.4800	.8600	7.8500	.8630	8.7700	.8400	14.0000	14.0000	.3000			
1.0000	.3000	4.9000	6.000	5.5500	.7000	7.3500	7.3500	.8000			
9.2000	.8600	9.8500	.8640	10.9900	.8200	15.0000	15.0000	.3000			
1.0000	.3000	6.6000	6.000	7.3500	.7000	9.5800	9.5800	.8000			
10.8500	.8400	11.8000	.8510	12.6400	.8400	17.5000	17.5000	.3000			
1.0000	.3000	7.9000	6.000	8.8500	.7000	11.1600	11.1600	.8000			
12.6000	.8400	13.1100	.8400	13.7400	.8200	17.5000	17.5000	.3000			
1.0000	.3000	8.5000	6.000	9.7500	.7000	12.6500	12.6500	.5000			
13.6000	.8120	14.1000	.8000	15.1000	.6300	17.5000	17.5000	.3000			

Unscaled pressure-ratio-map output pairs
(Output data are in kg/sec.)

TABLE VI. - Continued. COMPONENT MAP SCALE FACTORS AND DATA (CONFIGURATION E)

(c) High-pressure turbine									
1.00	670.80	.0731	268.186	306.556	359.146	383.161	459.766		
153.211	191.580	229.950	.0476	.5000	.0476	.6000	.0471		
.0000	.0417	.2661	.0307	.9400	.0150	1.0000	.0000		
.7500	.0381	.8500	.0381	.5000	.0380	.6350	.0369		
.0000	.0319	.2661	.0241	.9200	.0124	1.0000	.0000		
.7500	.0318	.8300	.0318	.5000	.0317	.6550	.0301		
.0000	.0264	.2661	.0212	.9150	.0113	1.0000	.0000		
.7500	.0272	.8200	.0272	.5000	.0272	.6700	.0252		
.0000	.0229	.2661	.0197	.9120	.0106	1.0000	.0000		
.7500	.0238	.8150	.0238	.5000	.0238	.6820	.0217		
.0000	.0203	.2661	.0174	.9100	.0102	1.0000	.0000		
.7500	.0203	.8100	.0203	.5000	.0201	.6900	.0188		
.0000	.0181	.2661	.0166	.9060	.0097	1.0000	.0000		
.7500	.0190	.8070	.0190	.5000	.0190	.6950	.0179		
.0000	.0173	.2661	.0157	.9040	.0093	1.0000	.0000		
.7500	.0159	.8040	.0159	.5000	.0158	.7000	.0156		
.0000	.0155	.2661	.0155	.9000	.0088	1.0000	.0000		
.7500		.8000							
Unscaled pressure-ratio-map output pairs (Output data are in kg-K-cm ² /N-rpm-sec)									
1.00	670.80	3118.7	268.186	306.556	359.146	383.161	459.766		
153.211	191.580	229.950	1774.5	.2661	1528.2	3000	1422.1		
.0000	2806.8	.2000	760.9	.8000	371.1	1.0000	0.0		
.4500	1060.4	.6000	1603.0	.2661	1372.2	.3000	1272.4		
.0000	2495.0	.2000	642.4	.8000	296.3	1.0000	0.0		
.4500	920.0	.6000	1443.9	.2661	1231.9	.3000	1144.6		
.0000	2339.0	.2000	545.8	.8000	243.9	1.0000	0.0		
.4500	810.9	.6000	1263.1	.2661	1075.9	.3000	1013.6		
.0000	2027.2	.2000	470.9	.8000	205.2	1.0000	0.0		
.4500	717.3	.6000	1122.7	.2661	951.2	.3000	895.1		
.0000	1871.2	.2000	408.5	.8000	173.4	1.0000	0.0		
.4500	623.7	.6000	969.9	.2661	830.5	.3000	773.4		
.0000	1559.4	.2000	343.0	.8000	137.2	1.0000	0.0		
.4500	530.2	.6000	913.8	.2661	779.7	.3000	720.4		
.0000	1481.4	.2000	318.1	.8000	120.4	1.0000	0.0		
.4500	499.0	.6000	761.0	.2661	639.3	.3000	595.7		
.0000	1325.4	.2000	250.7	.8000	91.7	1.0000	0.0		
.4500	405.4	.6000							
Unscaled pressure-ratio-map output pairs (Output data are in J/kg-K ^{1/2} -rpm)									
1.00	670.80	3118.7	268.186	306.556	359.146	383.161	459.766		
153.211	191.580	229.950	1774.5	.2661	1528.2	3000	1422.1		
.0000	2806.8	.2000	760.9	.8000	371.1	1.0000	0.0		
.4500	1060.4	.6000	1603.0	.2661	1372.2	.3000	1272.4		
.0000	2495.0	.2000	642.4	.8000	296.3	1.0000	0.0		
.4500	920.0	.6000	1443.9	.2661	1231.9	.3000	1144.6		
.0000	2339.0	.2000	545.8	.8000	243.9	1.0000	0.0		
.4500	810.9	.6000	1263.1	.2661	1075.9	.3000	1013.6		
.0000	2027.2	.2000	470.9	.8000	205.2	1.0000	0.0		
.4500	717.3	.6000	1122.7	.2661	951.2	.3000	895.1		
.0000	1871.2	.2000	408.5	.8000	173.4	1.0000	0.0		
.4500	623.7	.6000	969.9	.2661	830.5	.3000	773.4		
.0000	1559.4	.2000	343.0	.8000	137.2	1.0000	0.0		
.4500	530.2	.6000	913.8	.2661	779.7	.3000	720.4		
.0000	1481.4	.2000	318.1	.8000	120.4	1.0000	0.0		
.4500	499.0	.6000	761.0	.2661	639.3	.3000	595.7		
.0000	1325.4	.2000	250.7	.8000	91.7	1.0000	0.0		
.4500	405.4	.6000							

TABLE VI. - Continued. COMPONENT MAP SCALE FACTORS AND DATA (CONFIGURATION E)

(d) Low-pressure turbine															
1.00		201.24		1.462		88.814		99.815		107.328		122.086		133.221	
55.542	.0000	66.543	.9868	77.679	.2000	88.814	.9623	99.815	.2294	107.328	.9594	122.086	.3000	133.221	.9305
.4000	.0000	.8834	.6000	.7342	.6000	.8015	.3000	.8050	.3000	.7949	.3000	.7696	.0000	.7696	.0000
.4000	.0000	.7244	.6000	.5922	.6000	.4112	.3000	.4112	.3000	.4112	.3000	.4112	.0000	.4112	.0000
.4000	.0000	.7218	.2000	.6820	.2000	.4943	.3000	.4943	.3000	.4943	.3000	.4943	.6510	.4943	.6510
.4000	.0000	.6213	.6000	.5886	.6000	.4186	.3000	.4186	.3000	.4186	.3000	.4186	.0000	.4186	.0000
.4000	.0000	.5191	.2000	.4882	.2000	.3611	.3000	.3611	.3000	.3611	.3000	.3611	.5596	.3611	.5596
.4000	.0000	.4499	.6000	.4186	.6000	.2924	.3000	.2924	.3000	.2924	.3000	.2924	.0000	.2924	.0000
.4000	.0000	.5025	.2000	.4748	.2000	.3334	.3000	.3334	.3000	.3334	.3000	.3334	.4845	.3334	.4845
.4000	.0000	.4477	.6000	.4057	.6000	.2832	.3000	.2832	.3000	.2832	.3000	.2832	.0000	.2832	.0000
.4000	.0000	.4020	.2000	.3662	.2000	.2650	.3000	.2650	.3000	.2650	.3000	.2650	.3421	.2650	.3421
.4000	.0000	.3187	.6000	.2832	.6000	.2294	.3000	.2294	.3000	.2294	.3000	.2294	.0000	.2294	.0000
1.00	.0000	201.24	.6237.4	77.679	.2000	88.814	.9623	99.815	.2294	107.328	.9594	122.086	.3000	133.221	.9305
.5000	.0000	4023.1	.2000	2862.9	.2000	1347.3	.2000	7000	.2000	2744.4	.2000	1.0000	.2000	2479.4	.2000
.5000	.0000	1727.8	.6000	1347.3	.6000	2791.2	.6000	7000	.6000	976.2	.6000	1.0000	.6000	0.0	.6000
.5000	.0000	3991.9	.2000	2791.2	.2000	1144.6	.2000	7000	.2000	2691.7	.2000	1.0000	.2000	2317.2	.2000
.5000	.0000	1497.0	.6000	1144.6	.6000	2607.2	.6000	7000	.6000	785.9	.6000	1.0000	.6000	0.0	.6000
.5000	.0000	3960.7	.2000	2607.2	.2000	960.6	.2000	7000	.2000	2479.4	.2000	1.0000	.2000	2126.9	.2000
.5000	.0000	1322.3	.6000	960.6	.6000	2404.5	.6000	7000	.6000	614.4	.6000	1.0000	.6000	0.0	.6000
.5000	.0000	3929.6	.2000	2404.5	.2000	760.9	.2000	7000	.2000	2229.9	.2000	1.0000	.2000	1911.8	.2000
.5000	.0000	1119.6	.6000	760.9	.6000	2186.2	.6000	7000	.6000	530.2	.6000	1.0000	.6000	0.0	.6000
.5000	.0000	3867.2	.2000	2186.2	.2000	567.6	.2000	7000	.2000	2042.7	.2000	1.0000	.2000	1690.3	.2000
.5000	.0000	945.0	.6000	567.6	.6000	2042.7	.6000	7000	.6000	343.0	.6000	1.0000	.6000	0.0	.6000
.5000	.0000	3461.8	.2000	2042.7	.2000	458.4	.2000	7000	.2000	1883.7	.2000	1.0000	.2000	1553.1	.2000
.5000	.0000	804.6	.6000	458.4	.6000	1749.6	.6000	7000	.6000	249.5	.6000	1.0000	.6000	0.0	.6000
.5000	.0000	3118.7	.2000	1749.6	.2000	374.2	.2000	7000	.2000	1590.5	.2000	1.0000	.2000	1294.3	.2000
.5000	.0000	614.4	.6000	374.2	.6000	1546.9	.6000	7000	.6000	218.3	.6000	1.0000	.6000	0.0	.6000
.5000	.0000	2900.4	.2000	1546.9	.2000	280.7	.2000	7000	.2000	1434.6	.2000	1.0000	.2000	1122.7	.2000
.5000	.0000	502.1	.6000	280.7	.6000	187.1	.6000	7000	.6000	187.1	.6000	1.0000	.6000	0.0	.6000

Map scale factors XSC, YSC, ZSC
(ZSC is in $\text{kg-K-cm}^2/\text{N-rpm-sec}$)

Unscaled pressure-ratio-map output pairs
(Output data are in $\text{kg-K-cm}^2/\text{N-rpm-sec}$)

Map scale factors XSC, YSC, ZSC
(ZSC is in $\text{J/kg-K}^{1/2}\text{-rpm}$)

Unscaled pressure-ratio-map output pairs
(Output data are in $\text{J/kg-K}^{1/2}\text{-rpm}$)

TABLE VI. - Concluded, COMPONENT MAP SCALE FACTORS AND DATA (CONFIGURATION E)

(e) Fan tip

		Map scale factors XSC, YSC, ZSC (ZSC is in kg/sec.)									
2.00	2.00	68,038	.700	.800	.900	1.000	1.100	1.150			
.500	.600										
1.0000	34.0192	1.0300	31.7513	1.0350	30.6173	1.0400	29.4833				
1.0450	27.2154	1.0500	26.0814	1.0550	24.9474	1.0600	22.6795				
1.0000	38.5552	1.0300	36.2872	1.0500	35.1532	1.0650	34.0192				
1.0750	31.7513	1.0850	29.4834	1.0900	27.2154	1.0910	24.9474				
1.0000	43.0910	1.0500	40.8231	1.0800	38.5552	1.0880	37.7840				
1.1040	35.2893	1.1150	32.7492	1.1220	30.2544	1.1240	28.9844				
1.0000	45.3590	1.1100	43.0910	1.1400	41.9571	1.1500	40.8231				
1.1600	39.6891	1.1650	38.5552	1.1700	36.2872	1.1800	33.7924				
1.0000	48.7609	1.1000	47.6270	1.1600	45.3590	1.1890	42.8189				
1.2040	40.3242	1.2080	39.0541	1.2130	37.7840	1.2140	36.5594				
1.0000	51.2557	1.1500	50.3485	1.2220	47.8991	1.2410	46.6790				
1.2540	45.3590	1.2610	44.0889	1.2650	42.8189	1.2680	41.5942				
1.0000	53.2968	1.1500	53.0700	1.2590	51.6639	1.2930	50.3938				
1.1360	49.1238	1.3280	47.8991	1.3319	46.6290	1.3320	45.3590				
1.0000	54.8844	1.1000	54.8344	1.1500	54.6576	1.2000	54.4308				
1.2500	53.7504	1.3000	52.6164	1.3600	49.8949	1.3850	48.0805				
2.00	2.00	1.00									
.500	.600	.700	.800	.900	1.000	1.100	1.150				
1.0000	.3000	1.0100	.6000	1.0200	.7500	1.0300	.8200				
1.0400	.8500	1.0500	.8750	1.0550	.8850	1.0600	.3000				
1.0000	.3000	1.0300	.6000	1.0500	.7500	1.0600	.8000				
1.0800	.8700	1.0850	.8750	1.0900	.8900	1.0830	.3000				
1.0000	.3000	1.0500	.6000	1.0850	.7500	1.0880	.7680				
1.1040	.8470	1.1150	.8780	1.1220	.8810	1.3548	.3000				
1.0000	.3000	1.0700	.6000	1.1100	.7500	1.1250	.8000				
1.1400	.8500	1.1500	.8750	1.1600	.8900	1.6140	.3000				
1.0000	.3000	1.0900	.6000	1.1600	.7950	1.1890	.8700				
1.2040	.8880	1.2080	.8860	1.2130	.8790	1.2660	.3000				
1.0000	.3000	1.1200	.6000	1.2220	.8350	1.2410	.8730				
1.2540	.8900	1.2610	.8920	1.2650	.8860	1.4250	.3000				
1.0000	.3000	1.1500	.6000	1.2590	.7950	1.2930	.8550				
1.3160	.8870	1.3280	.8950	1.3319	.8880	1.3360	.3000				
1.0000	.3000	1.2000	.6000	1.2900	.7500	1.3200	.8000				
1.3450	.8500	1.3500	.8750	1.3800	.8950	1.6780	.3000				
2.00	2.00	1.00									
.500	.600	.700	.800	.900	1.000	1.100	1.150				
1.0000	.3000	1.0100	.6000	1.0200	.7500	1.0300	.8200				
1.0400	.8500	1.0500	.8750	1.0550	.8850	1.0600	.3000				
1.0000	.3000	1.0300	.6000	1.0500	.7500	1.0600	.8000				
1.0800	.8700	1.0850	.8750	1.0900	.8900	1.4830	.3000				
1.0000	.3000	1.0500	.6000	1.0850	.7500	1.0880	.7680				
1.1040	.8470	1.1150	.8780	1.1220	.8810	1.3548	.3000				
1.0000	.3000	1.0700	.6000	1.1100	.7500	1.1250	.8000				
1.1400	.8500	1.1500	.8750	1.1600	.8900	1.6140	.3000				
1.0000	.3000	1.0900	.6000	1.1600	.7950	1.1890	.8700				
1.2040	.8880	1.2080	.8860	1.2130	.8790	1.2660	.3000				
1.0000	.3000	1.1200	.6000	1.2220	.8350	1.2410	.8730				
1.2540	.8900	1.2610	.8920	1.2650	.8860	1.4250	.3000				
1.0000	.3000	1.1500	.6000	1.2590	.7950	1.2930	.8550				
1.3160	.8870	1.3280	.8950	1.3319	.8880	1.3360	.3000				
1.0000	.3000	1.2000	.6000	1.2900	.7500	1.3200	.8000				
1.3450	.8500	1.3500	.8750	1.3800	.8950	1.6780	.3000				

Unscaled pressure-ratio-map output pairs
(Output data are in kg/sec.)

Unscaled pressure-ratio-map output pairs

pressure ratio must be 1.0.) The inclusion of scale factors as input data allows the user to input dimensioned map data in any desired system of units.

Analog coefficients. - Prior to the execution of the main program, the analog program should be set up to perform the calculations listed in appendix F. The amplifier gains and attenuator settings should be set to achieve the analog coefficients C(i) defined in appendix D. The existing program (without controls) uses 57 values of C(i).

If, for a particular engine configuration, a portion of the analog simulation is not used (e.g., calculation of W22, T22, and P22 for STRM3="FALSE" engines), the corresponding coefficients should be set by the user to values that will not result in analog component overloads. Since the initial condition on the stored mass is used as the denominator in the temperature calculation (fig. 11), it should not be set to zero.

EXAMPLES

To demonstrate the flexibility of the hybrid computer program, together with its steady-state and transient computing capabilities, two engine types are discussed as examples. The first - a single-spool, nonafterburning turbojet (configuration G) - represents the minimum requirement in terms of component performance mapping capability. The second - a high-bypass, two-spool, two-stream turbofan (configuration E) - requires the full performance mapping capability of the program.

Single-Spool Turbojet (Configuration G)

A single-spool turbojet, described in table VII, was operated at NASA's Lewis Research Center to determine the effect of inlet distortion on compressor stall limits. The HYDES program was used to support those studies, and results from the program will serve to demonstrate both the off-design and dynamic capabilities of the program.

Table VII lists the design-point and engine parameter data for the selected turbojet engine. The unity values for the component scaling coefficients (WACCF, DHHPCF, etc.) shown in table VII indicate that the performance data for the compressor and turbine were available and not a result of scaling of other component data. The compressor temperature interpolation constant β_c was adjusted to give $T_3' = T_3$ at the design point by using equations (B20) to (B23). Similarly, the temperature interpolation constant for the combustor β_b was adjusted to give

$$\bar{h}_b = \left[1 + (f/a)_4 \right] h_4 - (f/a)_4 \eta_b (HVF) \quad (44)$$

TABLE VII. - DESIGN-POINT AND ENGINE PARAMETER DATA FOR SELECTED ONE-SPOOL TURBOJET (CONFIGURATION G)

Fan inlet pressure, P_2 ; high-pressure-compressor inlet pressure, $P_{2,1}$; mixing volume pressure, P_7 , N/cm ² (psia)	10.132 (14.696)
Combustor inlet pressure, P_3 , N/cm ² (psia)	67.97 (98.58)
High-pressure-turbine inlet pressure, P_4 , N/cm ² (psia)	62.98 (91.22)
Low-pressure-turbine inlet pressure, P_5 ; core duct pressure, P_6 , N/cm ² (psia)	22.56 (32.72)
Fan inlet temperature, T_2 ; high-pressure-compressor inlet temperature, $T_{2,1}$; mixing volume temperature, T_7 , K (°R)	288.15 (518.67)
Combustor inlet temperature, T_3 , K (°R)	538.08 (968.56)
High-pressure-turbine inlet temperature, T_4 , K (°R)	1142.2 (2056.0)
Low-pressure-turbine inlet temperature, T_5 ; core duct temperature, T_6 , K (°R)	911.66 (1641.0)
High-pressure-compressor flow rate, \dot{w}_c , kg/sec (lbm/sec)	19.92 (43.91)
Combustor flow rate, \dot{w}_b , kg/sec (lbm/sec)	19.26 (42.46)
Fuel flow rate, \dot{w}_F , kg/sec (lbm/sec)	0.319 (0.703)
High-pressure-turbine flow rate, \dot{w}_{t1} , kg/sec (lbm/sec)	19.58 (43.16)
Core nozzle flow rate, \dot{w}_{n1} , kg/sec (lbm/sec)	20.23 (44.61)
Overboard bleed flow rate, \dot{w}_{ovb} , kg/sec (lbm/sec)	0
High-pressure-turbine cooling bleed flow rate, \dot{w}_{b11} , kg/sec (lbm/sec)	0.658 (1.45)
Total thrust, F_{tot} , N (lbf)	12 661 (2846.4)
High-pressure-turbine rotational speed, N_{t1} ; high-pressure-compressor rotational speed, N_c , rpm	16 500
Design high-pressure-turbine rotational speed, $N_{t1,des}$; design high-pressure-compressor rotational speed, $N_{c,des}$, rpm	16 500
Design high-pressure-compressor inlet temperature, $T_{2,1,des}$, K (°R)	288.15 (518.67)
High-pressure-compressor pressure-ratio scaling coefficient, PRCCF	1.0
High-pressure-compressor flow scaling coefficient, WACCF	1.0
High-pressure-compressor efficiency scaling coefficient, ETACCF	1.0
High-pressure-turbine speed scaling coefficient, CNHPCF	1.0
High-pressure-turbine flow scaling coefficient, TFHPCF	1.0
High-pressure-turbine enthalpy scaling coefficient, DHHPCF	1.0
Combustor inlet volume, V_3 , cm ³ (in. ³)	38 526 (2351)
High-pressure-turbine inlet volume, V_4 , cm ³ (in. ³)	26 596 (1623)
Low-pressure-turbine inlet volume, V_5 , cm ³ (in. ³)	61 451 (3750)
High-pressure-turbine polar moment of inertia, I_{t1} , N-cm-sec ² (in.-lbf-sec ²)	70.05 (6.20)
Core nozzle effective cross-sectional area, A_{n1} , cm ² (in. ²)	678.7 (105.2)
High-pressure-turbine cooling-bleed effective cross-sectional area, A_{b11} , cm ² (in. ²)	5.572 (0.8636)
Overboard bleed effective cross-sectional area, A_{ovb} , cm ² (in. ²)	0
Core nozzle velocity coefficient, $C_{v,n1}$	1.0
Combustor pressure loss coefficient, R_b , N-sec ² /kg ² -cm ² (lbf-sec ² /lbm ² -in. ²)	(0.01368 (4.082×10 ⁻³))
Combustor efficiency, η_b	0.9834
High-pressure-compressor temperature interpolation constant, β_c	0.32117
Combustor temperature interpolation constant, β_b	0.98028

TABLE VIII. - SCALE FACTORS FOR SELECTED ONE-SPOOL

TURBOJET (CONFIGURATION G)

[Computer time, t', 100 t.]

Unscaled variable, x	Scaled variable, X	Scale factor, SF _X
P _{2.1}	P21	13.790 N/cm ² (20 psia)
P ₃	P3	137.90 N/cm ² (200 psia)
P ₄	P4	137.90 N/cm ² (200 psia)
P ₅	P5	34.474 N/cm ² (50 psia)
P ₇	P7	13.790 N/cm ² (20 psia)
W ₃	W3	0.22680 kg (0.5 lbm)
W ₄	W4	0.09072 kg (0.2 lbm)
W ₅	W5	0.09072 kg (0.2 lbm)
w _c	WDC	45.359 kg/sec (100 lbm/sec)
w _b	WDB	
w _{t1}	WDT1	
w _{n1}	WDN1	
w _F	WDF	0.45359 kg/sec (1.0 lbm/sec)
w _{bl1}	WDBL1	0.90718 kg/sec (2.0 lbm/sec)
L _{t1} , L _c	TRQT1, TRQC	4.5194×10 ⁵ N-cm (4×10 ⁴ in.-lbf)
A _{n1}	AN1	1290.3 cm ² (200 in. ²)
F _{n1} , F _{tot}	TAUN1, TAUT	2.2241×10 ⁴ N (5000 lbf)
t _{1np}	T1NP	1341.6 rpm/K ^{1/2} (1000 rpm/ ^o R ^{1/2})
fpt1	FPT1	0.09137 $\frac{\text{N-K-cm}^2}{\text{sec-rpm-N}}$ $\left(0.25 \frac{\text{lbm-}^{\circ}\text{R-in.}^2}{\text{sec-rpm-lbf}}\right)$
Δh _{t1}	DHT1	2.1088×10 ⁵ J/kg (200 Btu/lbm)
hpt1	HPT1	3118.7 $\frac{\text{J}}{\text{kg-K}^{1/2}\text{-rpm}}$ $\left(1.0 \frac{\text{Btu}}{\text{lbm-}^{\circ}\text{R}^{1/2}\text{-rpm}}\right)$
prc	PRC	10
fpc	FPC	45.359 kg/sec (100 lbm/sec)
cnp	CNP	2.0
ceff	CEFF	1.0

at the design point by using equations (B27) to (B30) and equation (B39). The resulting values for β_c and β_b assure a steady-state balance ($dT_3/dt = 0$ and $dT_4/dt = 0$) of energy in volumes V_3 and V_4 when continuity of flow is satisfied.

Based on the design-point data, scale factors were selected for each variable and are summarized in table VIII. As noted previously, certain engine variables have fixed scale factors (table II). The specified engine parameters and selected amplitude scale factors were used to calculate the values of the 103 digital coefficients SC(i) by means of the definitions in appendix D. The previously discussed FORMAT was used to prepare the digital coefficient and DAC initial condition data tape. The contents of that tape are shown in table IX.

TABLE IX. - DIGITAL COEFFICIENT AND DAC INITIAL CONDITION

INPUT DATA (CONFIGURATION G)

103					Integer value of NSC
.51867	.00000	.00000	.00000	.00000	} Scaled-fraction values of digital coefficients
.74996	.00000	.00000	.00000	.00000	
.45180	.20000	.02000	.00000	.00000	
.64372	.00000	.00000	.00000	.40000	
.00000	.00000	.00000	.99999	.00000	
.00000	.00000	.00000	.00000	.00000	
.00000	.00000	.00000	.00000	.00000	
.00000	.20338	.50000	.02000	.00000	
.00000	.98028	.07277	.01000	.01000	
.00000	.00000	.00000	.00000	.00000	
.00000	.00000	.25000	.00000	.23334	
.00000	.31390	.00000	.00000	.00000	
.08571	.00000	.08000	.00000	.67570	
.00000	.00000	.99999	.00000	.00000	
.96400	.00000	.00000	.68046	.00000	
.00000	.32117	.00000	.00000	.66667	
.00000	.00000	.10012	.00000	.00000	
.00000	.00000	.00000	.00000	.00000	
.00000	.00000	.00000	.00000	.00000	
.25000	.00000	.00000	.00000	.00000	
.00000	.00000	.73500			
.00000	.00000	.00000	.00000	.00000	} Scaled-fraction value of initial conditions
.00000	.00000	.00000	.00000	.00000	
.00000	.00000	.00000	.00000	.00000	
.00000	.00000	.00000	.00000	.00000	
.00000	.00000	.00000	.00000	.00000	

The compressor and turbine performance data, in the form required by the hybrid program, are available in reference 8. Table X shows the contents of the prepared component performance data tape.

The volumes listed in table VII resulted in a minimum time constant (eq. (42)) of 2.6 milliseconds. A time scale factor SF_t' of 100 was selected to give a minimum ratio of digital to analog frequencies equal to 70.8. The amplitude and time-scale factors were used in the calculation of the analog coefficients C(i) as defined in appendix D. The resulting coefficients were implemented by using amplifiers and attenuators and are listed in table XI.

Prior to loading and executing the data input program, configuration G was specified as per table IV. Sense switch 5 was depressed for the single-spool turbojet case. The data input program (appendix E) prompts the user to load (in order) the digital coeffi-

TABLE X. -COMPONENT MAP SCALE FACTORS AND DATA (CONFIGURATION G)

(a) High-pressure compressor

		Map scale factors XSC, YSC, ZSC (ZSC is in kg/sec.)									
		Unscaled pressure-ratio-map output pairs (Output data are in kg/sec.)									
10.00	2.00	45.359									
	.712	.801	.850	.900	.950	.975	1.0000	1.080			
1.0000	11.8840	1.6000	11.8840	2.2000	2.2000	11.7026	2.5000	11.5665			
2.7500	11.4305	3.0000	11.1513	3.3500	3.3500	10.3418	3.3600	9.3893			
1.0000	14.0613	2.1500	13.9706	2.9000	2.9000	13.8793	3.4400	13.8708			
3.8000	13.7438	4.1500	13.4263	4.2500	4.2500	13.3355	4.2800	10.6140			
1.0000	15.4674	2.5500	15.4221	3.4000	3.4000	15.3994	4.0000	15.3313			
4.5000	15.1953	4.8000	14.8324	5.1000	5.1000	14.3334	5.1500	11.8387			
1.0000	17.2818	3.0500	17.2818	4.0000	4.0000	17.2818	4.7000	17.1003			
5.2500	16.7828	5.6000	16.4653	5.9000	5.9000	15.8756	5.9300	12.9727			
1.0000	18.8693	3.5000	18.8693	4.5000	4.5000	18.8693	5.3500	18.8240			
6.1000	18.6879	6.5000	18.3704	6.7500	6.7500	17.8714	6.7700	14.1520			
1.0000	19.6858	3.7000	19.6858	4.7500	4.7500	19.6858	5.7000	19.6858			
6.5000	19.5044	7.0000	19.2776	7.3000	7.3000	18.9601	7.3200	14.9685			
1.0000	19.9580	3.7500	19.9580	4.8500	4.8500	19.9580	5.8000	19.9580			
6.7500	19.9353	7.2500	19.8899	7.9000	7.9000	19.8672	7.9200	15.7849			
1.0000	20.5476	3.9000	20.5476	5.0000	5.0000	20.5476	6.0000	20.5476			
7.0000	20.5476	7.6000	20.5476	8.2500	8.2500	20.5476	8.3000	16.3292			
10.00	2.00	1.00									
	.712	.801	.850	.900	.950	.975	1.000	1.080			
1.000	.0000	1.3000	.3500	.3500	1.5500	.6400	2.2000	.8000			
3.0000	.8800	3.3500	.8600	4.5000	4.5000	.5500	6.5000	.0000			
1.0000	.0000	1.5000	.3500	1.9000	1.9000	.6450	2.8500	.8200			
3.8000	.9000	4.2000	.8700	5.3500	5.3500	.5500	7.2500	.0000			
1.0000	.0000	1.6500	.3500	2.2500	2.2500	.6500	3.3000	.8250			
4.5000	.8750	5.0000	.8500	6.1000	6.1000	.5500	7.9500	.0000			
1.0000	.0000	1.8500	.3500	2.8500	2.8500	.7500	4.0000	.8350			
5.2000	.8750	5.7000	.8500	6.7500	6.7500	.5500	8.6000	.0000			
1.0000	.0000	2.2500	.3500	3.5000	3.5000	.6750	5.5000	.8300			
6.2500	.8500	6.7500	.8300	8.6500	8.6500	.5500	9.9000	.3500			
1.0000	.0000	2.5000	.3500	4.0000	4.0000	.6900	5.7500	.8200			
7.0000	.8400	7.3000	.8200	9.3000	9.3000	.6000	8.9000	.5250			
1.0000	.0000	2.7000	.3500	4.2000	4.2000	.6700	5.9000	.8000			
7.1000	.8230	7.9000	.8100	9.5000	9.5000	.6850	9.9000	.6500			
1.0000	.0000	3.2500	.3500	4.5000	4.5000	.5500	6.0000	.7000			
7.1000	.7400	8.2500	.7300	9.5000	9.5000	.7000	9.9000	.6850			

Map scale factors XSC, YSC, ZSC

Unscaled pressure-ratio-map output pairs

TABLE X. - Concluded. COMPONENT MAP SCALE FACTORS AND DATA (CONFIGURATION G)

(b) High-pressure turbine

	1.00	1341.60	.09137		201.240	268.320	335.400	402.480	590.304	804.960
	.0000	.0822	.2000	.0822	.4000	.0815	.6000	.0786		
	.7500	.0672	.8500	.0497	.9500	.0201	1.0000	.0000		
	.0000	.0658	.2000	.0658	.4000	.0650	.5900	.0647		
	.7350	.0548	.8370	.0391	.9400	.0164	1.0000	.0000		
	.0000	.0548	.2000	.0544	.4000	.0537	.5800	.0519		
	.7250	.0446	.8300	.0322	.9300	.0146	1.0000	.0000		
	.0000	.0402	.2000	.0395	.4000	.0391	.5700	.0387		
	.7100	.0329	.8150	.0227	.9200	.0110	1.0000	.0000		
	.0000	.0318	.2000	.0317	.4000	.0311	.5600	.0303		
	.7000	.0256	.8100	.0172	.9100	.0084	1.0000	.0000		
	.0000	.0263	.2000	.0263	.4000	.0263	.5600	.0245		
	.7000	.0212	.8100	.0146	.9100	.0077	1.0000	.0000		
	.0000	.0179	.2000	.0179	.4000	.0175	.5500	.0164		
	.6900	.0135	.8000	.0099	.9000	.0051	1.0000	.0000		
	.0000	.0146	.2000	.0146	.4000	.0139	.5500	.0128		
	.6850	.0110	.8000	.0080	.9000	.0044	1.0000	.0000		

Map scale factors XSC, YSC, ZSC
(ZSC is in $\text{kg-K-cm}^2/\text{N-rpm-sec}$)

Unscaled pressure-ratio-map output pairs
(Output data are in $\text{kg-K-cm}^2/\text{N-rpm-sec}$)

	1.00	1341.60	3118.7		201.240	268.320	335.400	402.480	590.304	804.960
	.0000	826.4	.2000	826.4	.4850	826.4	.6000	804.960		
	.7000	452.2	.8000	296.3	.9000	155.9	1.0000	608.1		
	.0000	795.3	.2000	795.3	.4150	795.3	.5700	561.4		
	.6880	405.4	.7950	265.1	.8900	140.3	1.0000	000.0		
	.0000	779.7	.2000	779.7	.3600	779.7	.5500	514.6		
	.6750	358.6	.7900	233.9	.8850	118.5	1.0000	000.0		
	.0000	686.1	.2000	686.1	.3050	686.1	.5150	452.2		
	.6600	311.9	.7800	196.5	.8800	109.2	1.0000	000.0		
	.0000	654.9	.2000	654.9	.2850	654.9	.4950	421.0		
	.6500	265.1	.7750	162.2	.8750	93.6	1.0000	000.0		
	.0000	623.7	.2000	623.7	.2750	623.7	.4800	389.8		
	.6400	233.9	.7700	140.3	.8650	62.4	1.0000	000.0		
	.0000	467.8	.2000	467.8	.2750	467.8	.4300	296.3		
	.6150	140.3	.7550	62.4	.8550	31.2	1.0000	000.0		
	.0000	374.2	.2000	374.2	.2750	374.2	.4000	249.5		
	.6000	93.6	.7500	31.2	.8500	15.6	1.0000	000.0		

Map scale factors XSC, YSC, ZSC
(ZSC is in $\text{J/kg-K}^{1/2}\text{-rpm}$)

Unscaled pressure-ratio-map output pairs
(Output data are in $\text{J/kg-K}^{1/2}\text{-rpm}$)

TABLE XI. - CALCULATED ANALOG
 COEFFICIENTS FOR SELECTED
 TURBOJET ENGINE (CONFIGURATION G)

i	Coefficient, C_i	i	Coefficient, C_i
1	0	30	0
2	.9999	31	.9999
3	0	32	0
4	.5187	33	0
5	.0000	34	.1362
6	.9999	35	.9999
7	0	36	.3542
8	0	37	.0187
9	.7472	38	.1969
10	.4843	39	.5000
11	.2000	40	0
12	.2000	41	.2732
13	.5636	42	0
14	.4112	43	0
15	.5000	44	0
16	.5000	45	0
17	.5851	46	0
18	.4102	47	0
19	.5000	48	0
20	.5000	49	.2075
21	.9999	50	0
22	0	51	0
23	0	52	0
24	0	53	0
25	0	54	0
26	.1417	55	.7350
27	.9999	56	.5260
28	0	57	.7030
29	0		

coefficients, DAC initial conditions, and component performance data tapes. After the user loads the data listed in tables IX and X, the data are stored in the appropriate COMMON blocks.

As indicated in table IV, no further steps are required to define the single-spool turbojet configuration prior to loading and executing the main digital program. Prior to reading ADC values and calculating derivatives, the main digital program outputs initial conditions for the derivatives (through the DAC's) and puts the analog console in the initial condition (IC) mode. The design-point values of pressure, temperature, nozzle

area, and fuel flow rate are computed by using the preset analog coefficients and are transmitted to the digital through the 24 ADC's. The stored digital coefficients result in the digital program computing near-zero derivatives for the temperatures and stored masses, which are transmitted to the analog through the 24 DAC's. This balanced condition results in minimal changes in the engine variables when the analog is manually placed in the "operate" mode and the integrations commence.

To allow transient variations in the simulated turbojet's operating point, a simplified fuel control model was added to the analog portion of the simulation. A proportional-plus-integral speed controller was assumed. The unscaled equation, describing the controller, is

$$\Delta \dot{w}_F = K_1(N_{t1, dem} - N_{t1}) + K_2 \int_0^t (N_{t1, dem} - N_{t1}) dt \quad (45)$$

Gain values of $K_1 = 2.211 \times 10^{-4}$ kg/sec-rpm (9.306×10^{-4} lbm/sec-rpm) and $K_2 = 5.620 \times 10^{-4}$ kg/sec²-rpm (1.239×10^{-3} lbm/sec²-rpm) were selected to give satisfactory response characteristics. The scaled version of equation (45) was implemented on the analog to provide the scaled fuel flow WDF to the digital program through an ADC.

With the fuel controller maintaining the compressor speed at the design-point value, a steady-state listing of selected engine variables (scaled) was obtained at the teletype by depressing sense switch 1 (appendix E). The resulting listing is shown in table XII, together with the corresponding values of the unscaled variables. A comparison of tables XII and VII indicates the following maximum differences between the computed and specified design points: pressures, 0.27 percent; temperatures, 0.30 percent; flow rates, 0.56 percent; thrust, 0.44 percent.

For the Lewis turbojet tests, a baseline stall limit was to be established, experimentally, by reducing the core nozzle area A_{n1} at selected rotor speeds until stall was observed. Difficulties arose, however, at high speeds because turbine temperature limits were reached before stall occurred. The possibility of decreasing the stall margin by decreasing the turbine nozzle area was investigated by using the hybrid simulation. The experimental tests were to be conducted with a compressor inlet pressure of 6.895 N/cm^2 (10 psia). The hybrid-simulated inlet pressure was reduced by decreasing the analog coefficient C(26) (appendix D) and thus causing a shift in the 100-percent-speed operating point. Table XIII shows the steady-state computer listing for the reduced inlet pressure.

Stall data were obtained for both the nominal turbine area and an area equal to 85.7 percent of the nominal area. The decreasing of the turbine nozzle area was simulated by increasing the digital coefficient SC(57) (appendix D). The fuel controller was used to maintain the rotor speed at desired values, ranging from 100 percent to 87 percent of

TABLE XII. - STEADY-STATE DATA FOR SELECTED TURBOJET ENGINE

(CONFIGURATION G) AT HIGH-PRESSURE-COMPRESSOR INLET

PRESSURE OF 10.133 N/cm² (14.696 psia)

[Percent of design speed, 100.]

(a) Scaled teletype output

WDF1	WDC	WDB	WDT1	WDT2
.00009	.43911	.42703	.43124	.44580
WDN1	WDN2	WDN3	WDN4	WDF2
.44580	.00000	.00000	.00000	.00000
P2	P21	P35	P3	P4
.73498	.73437	-.00036	.49206	.45483
P5	P6	P7	P22	P32
.65283	.67283	.73474	.00024	.00000
T35	T3	T4	T5	T6
.00000	.48376	.41027	.40905	.65447
T7	T2	T21	TAUN1	TAUN2
.20727	.51867	.51818	.56680	.00000
TAUN3	WDF	PCNT1	PCNT2	PCNF1
.00000	.69836	.49938	.00000	.00000
PCNF2	PCNC	AN1	AN2	AN3
.00000	.49938	.52600	.00000	.00000
AN4	ABLC	ABLS	TAUN4	TAUT
.00000	.00000	.00000	.00000	.56677

(b) Unscaled data

High-pressure-compressor flow rate, \dot{w}_c , kg/sec (lbm/sec)	19.92 (43.91)
Combustor flow rate, \dot{w}_b , kg/sec (lbm/sec)	19.37 (42.70)
High-pressure-turbine flow rate, \dot{w}_{t1} , kg/sec (lbm/sec)	19.56 (43.12)
Core nozzle flow rate, \dot{w}_{n1} , kg/sec (lbm/sec)	20.22 (44.58)
High-pressure-compressor inlet pressure, $P_{2.1}$, N/cm ² (psia)	10.12 (14.68)
Combustor inlet pressure, P_3 , N/cm ² (psia).	67.85 (98.41)
High-pressure-turbine inlet pressure, P_4 , N/cm ² (psia)	62.72 (90.97)
Low-pressure-turbine inlet pressure, P_5 , N/cm ² (psia)	22.50 (32.64)
High-pressure-compressor inlet temperature, $T_{2.1}$, K (^o R)	287.9 (518.2)
Combustor inlet temperature, T_3 , K (^o R)	537.5 (967.5)
High-pressure-turbine inlet temperature, T_4 , K (^o R).	1139 (2051)
Low-pressure-turbine inlet temperature, T_5 , K (^o R).	908.9 (1636)
Fuel flow rate, \dot{w}_F , kg/sec (lbm/sec)	0.3168 (0.6984)
Ratio of high-pressure-turbine rotational speed to design, $N_{t1}/N_{t1,des}$	0.9988
Total thrust, F_{tot} , N (lbf)	12 606 (2834)

TABLE XIII. - STEADY-STATE DATA FOR SELECTED TURBOJET ENGINE

(CONFIGURATION G) AT HIGH-PRESSURE-COMPRESSOR INLET

PRESSURE OF 6.895 N/cm^2 (10 psia)

[Percent of design speed, 100.]

(a) Scaled teletype output

WDF1 .00009	WDC .29873	WDB .28720	WDT1 .29428	WDT2 .30361
WDN1 .30361	WDN2 .00000	WDN3 .00000	WDN4 .00000	WDF2 .00000
P2 .73498	P21 .49938	P35 .00024	P3 .33068	P4 .31384
P5 .46362	P6 .46362	P7 .73425	P22 .00000	P32 -.00024
T35 .00000	T3 .48291	T4 .41918	T5 .42114	T6 .67382
T7 .20727	T2 .51867	T21 .51855	TAUN1 .30416	TAUN2 .00000
TAUN3 .00000	WDF .49951	PCNT1 .50012	PCNT2 .00012	PCNF1 .00000
PCNF2 .00000	PCNC .50012	AN1 .52612	AN2 .00000	AN3 .00000
AN4 .00000	ABLC .00000	ABLS .00000	TAUN4 .00000	TAUT .30413

(b) Unscaled data

High-pressure-compressor flow rate, \dot{w}_c , kg/sec (lbm/sec).	13.55 (29.87)
Combustor flow rate, \dot{w}_b , kg/sec (lbm/sec).	13.03 (28.72)
High-pressure-turbine flow rate, \dot{w}_{t1} , kg/sec (lbm/sec).	13.35 (29.43)
Core nozzle flow rate, \dot{w}_{n1} , kg/sec (lbm/sec).	13.77 (30.36)
High-pressure-compressor inlet pressure, $P_{2.1}$, N/cm^2 (psia).	6.886 (9.988)
Combustor inlet pressure, P_3 , N/cm^2 (psia).	45.60 (66.14)
High-pressure-turbine inlet pressure, P_4 , N/cm^2 (psia).	43.28 (62.77)
Low-pressure-turbine inlet pressure, P_5 , N/cm^2 (psia).	15.98 (23.18)
High-pressure-compressor inlet temperature, $T_{2.1}$, K ($^{\circ}\text{R}$).	288.1 (518.6)
Combustor inlet temperature, T_3 , K ($^{\circ}\text{R}$).	536.6 (965.8)
High-pressure-turbine inlet temperature, T_4 , K ($^{\circ}\text{R}$).	1164 (2096)
Low-pressure-turbine inlet temperature, T_5 , K ($^{\circ}\text{R}$).	935.5 (1684)
Fuel flow rate, \dot{w}_F , kg/sec (lbm/sec).	0.2266 (0.4995)
Ratio of high-pressure-compressor rotational speed to design, $N_c/N_{c,des}$.	1.000
Total thrust, F_{tot} , N (lbf).	6765.7 (1521)

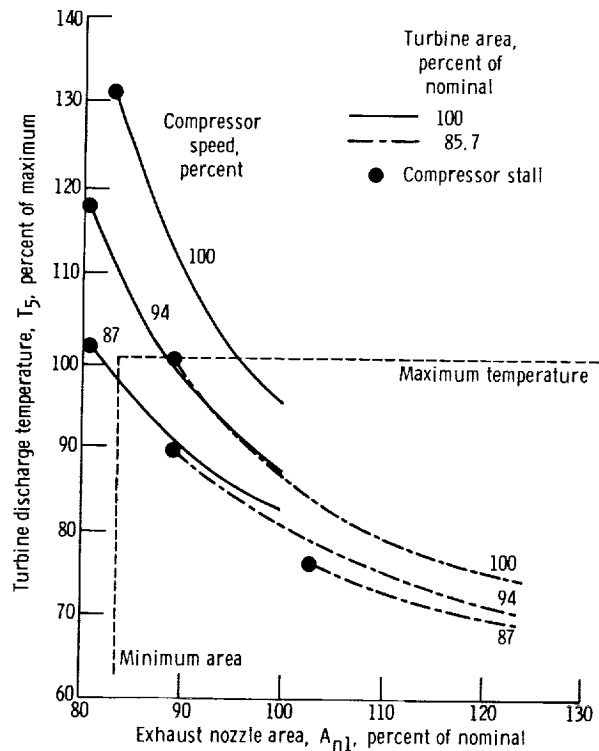


Figure 14. - Effect of turbine nozzle area on compressor stall margin for turbojet engine (configuration G).

the design speed. At each selected speed, the core nozzle area was reduced by decreasing the coefficient $C(56)$ on the analog. Compressor stall was detected by monitoring the compressor flow map variables PRC and FPC on an x-y plotter. These variables are transmitted to the analog through the DAC's. Oscillations along constant-speed lines were observed when stall was initiated. Figure 14 shows the results of that study. With the nominal turbine area, stall could not be initiated without exceeding the maximum T_5 or minimum A_{n1} limits. For the 100-, 94-, and 87-percent rotor speeds, however, the reduced turbine area allowed the compressor to stall with temperatures below the T_5 limit and nozzle areas above the minimum A_{n1} . With this information, the required turbine modifications were made and the experimental program continued.

Turbofan (Configuration E)

To further demonstrate the capabilities of the HYDES program, a two-spool, two-stream turbofan (configuration E) was selected for simulation. Configuration E was selected because of its extensive function generation requirements. A total of 10 functions of two variables were required to describe the low-pressure compressor (boosted fan hub), high-pressure compressor, high-pressure turbine, low-pressure turbine, and

bypass fan (fan tip). Table XIV lists the steady-state characteristics of the selected turbofan engine at 50 percent of its design thrust. The nonunity values of the component scaling coefficients indicate that the performance data being used were scaled from other engine components. As in the case of the turbojet, temperature interpolation constants β_{f1} , β_{f2} , β_c , and β_b were adjusted to give steady-state energy balances in volumes $V_{2.1}$, $V_{3.2}$, V_3 , and V_4 , respectively.

Scale factors were selected for each variable and are summarized in table XV. The specified engine parameters and selected amplitude scale factors were used to calculate the 103 digital coefficients SC(i). The contents of the digital coefficient and DAC initial condition tape are shown in table V.

The fan, compressor, and turbine performance data for the selected engine were available in the forms shown in figures 12 and 13. The turbine data conversion program (appendix G) was used to convert the data for each turbine to the required form. Table VI shows the contents of the component performance data tape for the selected turbofan.

The volumes listed in table XIV resulted in a minimum time constant of 4.75 milliseconds. A time scale factor SF_t of 100 was selected to give a minimum ratio of digital to analog frequencies equal to 68.3. The amplitude and time scale factors were used to calculate the analog coefficients C(i). The resulting coefficients are listed in table XVI.

Before the data input program was loaded and executed, configuration E was specified as per table IV. Sense switch 2 was depressed to denote the HBPR="TRUE" case. Sense switch 7 was not depressed since the fan hub or low-pressure-compressor had to be represented by a full set of data (SUPER="FALSE"). After the digital coefficient, DAC initial condition, and component performance data were loaded, no further steps were required to define the engine. The main program was then loaded.

To allow transient variations in the simulated turbofan's operating point, a portion of a proposed fuel control system was implemented on the analog computer. The features of the fuel control system and its implementation are described in appendix H. Basically, the control provides for closed-loop control of fan speed under quasi-steady-state conditions.

With the fuel control maintaining the fan speed at the initial value (73.2 percent of design), a steady-state listing of selected engine variables was obtained at the teletype by depressing sense switch 1. The resulting listing is shown in table XVII together with the corresponding unscaled values.

A transient was initiated by ramping the demanded low rotor speed $N_{t2, dem}$ from the 73.2 percent value to 100 percent of the design-point value in 50 milliseconds (5 sec of computer time). Figure 15 shows the resultant responses of thrust and turbine inlet temperature T_4 , respectively. These plots were obtained by monitoring the outputs of the corresponding analog amplifiers with an x-y plotter. An integrator was used to time the transient. With the nominal acceleration schedule of fuel flow (eq. (H12)), 63 percent of the desired thrust change was achieved in about 1.1 seconds. However, the

TABLE XIV. - Concluded. STEADY-STATE AND ENGINE PARAMETER DATA FOR SELECTED TURBOFAN ENGINE

(CONFIGURATION E) AT 50-PERCENT-THRUST CONDITION

Low-pressure-compressor pressure-ratio scaling coefficient, PR1CF	1.0091
Fan pressure ratio scaling coefficient, PRFCF	0.98424
High-pressure-compressor flow scaling coefficient, WACCF	0.27579
Low-pressure-compressor flow scaling coefficient, WAICF	1.0690
Fan flow scaling coefficient, WAFCF	14.800
High-pressure-compressor efficiency scaling coefficient, ETACCF	1.0024
Low-pressure-compressor efficiency scaling coefficient, ETAICF	0.98389
Fan efficiency scaling coefficient, ETAFCF	0.98888
High-pressure-turbine speed scaling coefficient, CNHPCF	1.0021
Low-pressure-turbine speed scaling coefficient, CNLPCF	0.89926
High-pressure-turbine flow scaling coefficient, TFHPCF	0.91126
Low-pressure-turbine flow scaling coefficient, TFLPCF	1.8993
High-pressure-turbine enthalpy scaling coefficient, DHHPCF	0.96882
Low-pressure-turbine enthalpy scaling coefficient, DHLPCF	1.6191
High-pressure-compressor inlet volume, $V_{2.1}$, cm^3 (in. ³)	3.861×10^5 (23 562)
Compressor inlet volume, V_3 , cm^3 (in. ³)	50 193 (3063)
High-pressure-turbine inlet volume, V_4 , cm^3 (in. ³)	78 133 (4768)
Low-pressure-turbine inlet volume, V_5 , (in. ³)	1.164×10^5 (7105)
Bypass fan discharge volume, $V_{3.2}$; bypass fan duct volume, $V_{3.5}$, cm^3 (in. ³)	2.392×10^7 (1.46×10^6)
High-pressure-turbine polar moment of inertia, I_{t1} , N-cm-sec (in.-lbf-sec ²)	1807.7 (160)
Low-pressure-turbine polar moment of inertia, I_{t2} , N-cm-sec (in.-lbf-sec ²)	4688.7 (415)
Core nozzle effective cross-sectional area, A_{n1} , cm^2 (in. ²)	4747.1 (735.8)
Third-stream nozzle effective cross-sectional area, A_{n2} , cm^2 (in. ²)	32 342 (5013)
High-pressure-turbine cooling bleed effective cross-sectional area, A_{bl1} , cm^2 (in. ²)	6.7948 (1.0532)
Low-pressure-turbine cooling bleed effective cross-sectional area, A_{bl2} , cm^2 (in. ²)	4.3881 (0.68016)
Overboard bleed effective cross-sectional area, A_{ovb} , cm^2 (in. ²)	2.9471 (0.45680)
Interstream bleed effective cross-sectional area, A_{blc} , cm^2 (in. ²)	0
Core nozzle velocity coefficient, $C_{v,n1}$; third-stream nozzle velocity coefficient, $C_{v,n2}$	0.975
Compressor pressure loss coefficient, R_b , N-sec ² /kg ² -cm ² (lbf-sec ² /lbm ² -in. ²)	7.567×10^{-3} (2.258×10^{-3})
Third-stream valve or duct pressure loss coefficient, R_{v3} , N-sec ² /kg ² -cm ² (lbf-sec ² /lbm-in. ²)	1.055×10^{-6} (3.148×10^{-7})
Compressor efficiency, η_b	0.9875
Low-pressure-compressor temperature interpolation constant, β_{f1} ; fan temperature interpolation constant, β_{f2}	1.0
High-pressure-compressor temperature interpolation constant, β_c	0.54454
Compressor temperature interpolation constant, β_b	0.99158
Design fan inlet temperature, $T_{2,des}$, K (°R)	288.15 (518.67)
Design high-pressure-compressor inlet temperature, $T_{2.1,des}$, K (°R)	350.67 (631.22)
Ratio of low-pressure-compressor to low-pressure-turbine speed, K_{f1} ; ratio of fan to low-pressure-turbine speed, K_{f2}	1.0

TABLE XIV. - STEADY-STATE AND ENGINE PARAMETER DATA FOR SELECTED TURBOFAN ENGINE
(CONFIGURATION E) AT 50-PERCENT-THRUST CONDITION

Fan inlet pressure, P_2 , N/cm ² (psia)	9.981 (14.476)
High-pressure-compressor inlet pressure, $P_{2,1}$, N/cm ² (psia)	13.86 (20.10)
Combustor inlet pressure, P_3 , N/cm ² (psia)	125.0 (181.3)
High-pressure-turbine inlet pressure, P_4 , N/cm ² (psia)	119.6 (173.5)
Low-pressure-turbine pressure, P_5 , N/cm ² (psia)	10.60 (15.37)
Core duct pressure, P_6 , N/cm ² (psia)	32.77 (47.53)
Mixing volume pressure, P_7 ; nozzle discharge pressure, P_8 , N/cm ² (psia)	10.132 (14.696)
Bypass fan discharge pressure, $P_{3,2}$, N/cm ² (psia)	11.31 (16.41)
Bypass fan duct pressure, $P_{3,5}$, N/cm ² (psia)	11.08 (16.07)
Fan inlet temperature, T_2 ; mixing volume temperature, T_7 , K (°R)	288.15 (518.67)
High-pressure-compressor inlet temperature, $T_{2,1}$, K (°R)	322.0 (579.6)
Combustor inlet temperature, T_3 , K (°R)	640.2 (1152.3)
High-pressure-turbine temperature, T_4 , K (°R)	1234.9 (2222.9)
Low-pressure-turbine inlet temperature, T_5 , K (°R)	925.8 (1666.5)
Core duct temperature, T_6 , K (°R)	717.5 (1291.5)
Bypass fan discharge temperature, $T_{3,2}$; bypass fan duct temperature, K (°R)	299.2 (538.6)
Low-pressure-compressor flow rate, \dot{w}_{f1} , kg/sec (lbm/sec)	29.57 (65.20)
High-pressure-compressor flow rate, \dot{w}_c , kg/sec (lbm/sec)	26.68 (58.82)
Combustor flow rate, \dot{w}_b , kg/sec (lbm/sec)	27.26 (60.11)
High-pressure-turbine flow rate, \dot{w}_{t1} , kg/sec (lbm/sec)	28.60 (63.05)
Low-pressure-turbine flow rate, \dot{w}_{t2} , kg/sec (lbm/sec)	29.98 (66.09)
Core nozzle flow rate, \dot{w}_{n1} , kg/sec (lbm/sec)	475.7 (1048.8)
Fan flow rate, \dot{w}_{f2} ; second-stream duct flow rate, \dot{w}_{n2} , kg/sec (lbm/sec)	0
Interstream bleed flow rate, \dot{w}_{bls} ; control bleed flow rate, \dot{w}_{blc} , kg/sec (lbm/sec)	0.1814 (0.40)
Overboard bleed flow rate, \dot{w}_{ovb} , kg/sec (lbm/sec)	1.33 (2.94)
High-pressure-turbine cooling bleed flow rate, \dot{w}_{bl1} , kg/sec (lbm/sec)	1.38 (3.04)
Low-pressure-turbine cooling bleed flow rate, \dot{w}_{bl2} , kg/sec (lbm/sec)	3719.6 (836.2)
Core nozzle thrust, F_{n1} , N (lbf)	53 868 (12 110)
Third-stream nozzle thrust, F_{n2} , N (lbf)	57 586 (12 946)
Total thrust, F_{tot} , N (lbf)	12 683
High-pressure-turbine rotational speed, N_{t1} , rpm	3026.2
Low-pressure-turbine rotational speed, N_{t2} , rpm	14 279
Design high-pressure-turbine rotational speed, $N_{t1,des}$, rpm	4135.8
Design low-pressure-turbine rotational speed, $N_{t2,des}$, rpm	4135.8
Design low-pressure-compressor rotational speed, $N_{f1,des}$, rpm	4135.8
Design fan rotational speed, $N_{f2,des}$, rpm	14 279
Design high-pressure-compressor rotational speed, $N_{c,des}$, rpm	14 279
High-pressure-compressor pressure-ratio scaling coefficient, PRCCF	0.65489

TABLE XV. - SCALE FACTORS FOR SELECTED TURBOFAN (CONFIGURATION E)
 [Computer time, t', 100t.]

Unscaled variable, x	Scaled variable, X	Scale factor, SF _X	Unscaled variable, x	Scaled variable, X	Scale factor, SF _X
P ₂	P ₂	13.790 N/cm ² (20 psia)	L _{t1} , L _c	TRQT1, TRQC	2.2596×10 ⁶ N-cm (2×10 ⁵ in.-lbf)
P _{2.1}	P ₂₁	34.474 N/cm ² (50 psia)	L _{f1}	TRQF1	1.1298×10 ⁶ N-cm (1×10 ⁵ in.-lbf)
P ₃	P ₃	344.74 N/cm ² (500 psia)	L _{f2}	TRQF2	5.6490×10 ⁶ N-cm (5×10 ⁵ in.-lbf)
P ₄	P ₄	344.74 N/cm ² (500 psia)	L _{t2}	TRQT2	5.6490×10 ⁶ N-cm (5×10 ⁵ in.-lbf)
P ₅	P ₅	68.948 N/cm ² (100 psia)	A _{n1}	AN1	6451.6 cm ² (1000 in. ²)
P ₆	P ₆	17.237 N/cm ² (25 psia)	A _{n2}	AN2	48 387 cm ² (7500 in. ²)
P ₇	P ₇	13.790 N/cm ² (20 psia)	F _{n1}	TAUN1	22 224 cm ² (5000 lbf)
P ₈	P ₈	13.790 N/cm ² (20 psia)	F _{n2}	TAUN2	2.2224×10 ⁵ N (50 000 lbf)
P _{3.2}	P ₃₂	17.237 N/cm ² (25 psia)	P _{tot}	TAUT	2.2224×10 ⁵ N (50 000 lbf)
P _{3.5}	P ₃₅	17.237 N/cm ² (25 psia)	t _{1np}	TINP	670.80 rpm/K ^{1/2} (500 rpm/°R ^{1/2})
W _{2.1}	W ₂₁	0.90718 kg (2 lbm)	f _{pt1}	FPT1	0.07310 $\frac{\text{kg-K-cm}^2}{\text{sec-rpm-N}}$ $\left(0.2 \frac{\text{lbm-}^{\circ}\text{R-in.}^2}{\text{sec-rpm-lbf}}\right)$
W ₃	W ₃	0.90718 kg (2 lbm)	Δh _{t1}	DHT1	2.636×10 ⁵ J/kg (250 Btu/lbm)
W ₄	W ₄	0.68038 kg (1.5 lbm)	h _{pt1}	HPT1	3118.7 $\frac{\text{kg-K}^{1/2}\text{-rpm}}{\text{J}}$ $\left(1 \frac{\text{Btu}}{\text{lbm-}^{\circ}\text{R}^{1/2}\text{-rpm}}\right)$
W ₅	W ₅	0.22680 kg (0.5 lbm)	t _{2np}	T2NP	201.24 rpm/K ^{1/2} (150 rpm/°R ^{1/2})
W ₆	W ₆	0.45359 kg (1.0 lbm)	f _{pt2}	FPT2	1.4619 $\frac{\text{kg-K-cm}^2}{\text{sec-rpm-N}}$ $\left(4 \frac{\text{lbm-}^{\circ}\text{R-in.}^2}{\text{sec-rpm-lbf}}\right)$
W _{3.2}	W ₃₂	45.359 kg (100 lbm)	Δh _{t2}	DHT2	2.636×10 ⁵ J/kg (250 Btu/lbm)
W _{3.5}	W ₃₅	45.359 kg (100 lbm)	h _{pt2}	HPT2	6237.4 $\frac{\text{kg-K}^{1/2}\text{-rpm}}{\text{J}}$ $\left(2 \frac{\text{Btu}}{\text{lbm-}^{\circ}\text{R}^{1/2}\text{-rpm}}\right)$
ψ _{f1}	WDF1	68.038 kg/sec (150 lbm/sec)	prf1	PRF1	5
ψ _c	WDC		f _{1np}	F1NP	2
ψ _b	WDB		f _{pf1}	FPF1	266.79 kg/sec (500 lbm/sec)
ψ _{t1}	WDT1		f _{1eff}	F1EFF	1
ψ _{t2}	WDT2		prc	PRC	20
ψ _{n1}	WDN1		cnp	CNP	2
ψ _{f2}	WDF2	907.18 kg/sec (2000 lbm/sec)	fpc	FPC	34.019 kg/sec (75 lbm/sec)
ψ _{y3}	WDV3	907.18 kg/sec (2000 lbm/sec)	ceff	CEFF	1
ψ _{n2}	WDN2	907.18 kg/sec (2000 lbm/sec)	prf2	PRF2	2
ψ _F	WDF	1.3608 kg/sec (3 lbm/sec)	f _{2np}	F2NP	2
ψ _{bl1}	WDBL1	4.5359 kg/sec (10 lbm/sec)	f _{pf2}	FPF2	68.039 kg/sec (150 lbm/sec)
ψ _{bl2}	WDBL2	2.2689 kg/sec (5 lbm/sec)	f _{2eff}	F2EFF	1
ψ _{ovb}	WDOVB	1.3608 kg/sec (3 lbm/sec)			

TABLE XVI. - CALCULATED ANALOG
 COEFFICIENTS FOR SELECTED
 TURBOFAN ENGINE
 (CONFIGURATION E)

i	Coefficient, C_i	i	Coefficient, C_i
1	0.7500	30	0
2	.6390	31	.6954
3	.7500	32	.1754
4	.5800	33	0
5	0	34	.1672
6	.9999	35	.9999
7	0	36	.3542
8	0	37	.0042
9	.3752	38	.2014
10	.5758	39	.4438
11	.0750	40	.0139
12	.0750	41	.1802
13	.3849	42	.3660
14	.4446	43	.1319
15	.1000	44	.2000
16	.1000	45	.5387
17	.6284	46	.2000
18	.4195	47	.5392
19	.3000	48	0
20	.3000	49	.2075
21	.8940	50	0
22	.5206	51	0
23	.1500	52	0
24	.1500	53	0
25	.2000	54	.6684
26	.1087	55	.7238
27	.6810	56	.7358
28	.1754	57	.3358
29	.2000		

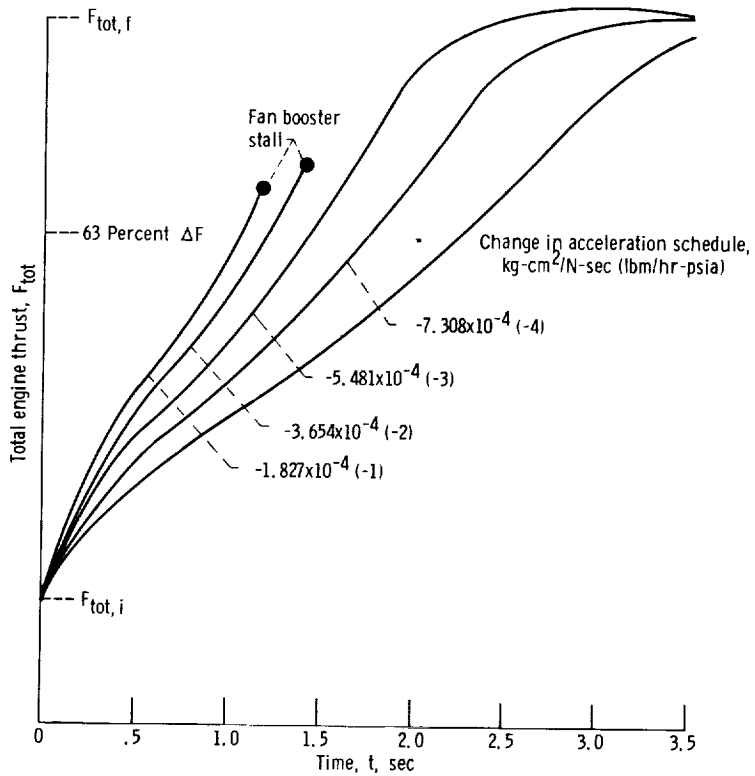
TABLE XVII. - STEADY-STATE DATA FOR SELECTED TURBOFAN ENGINE
(CONFIGURATION E) AT 73.2 PERCENT OF DESIGN SPEED

(a) Scaled teletype output

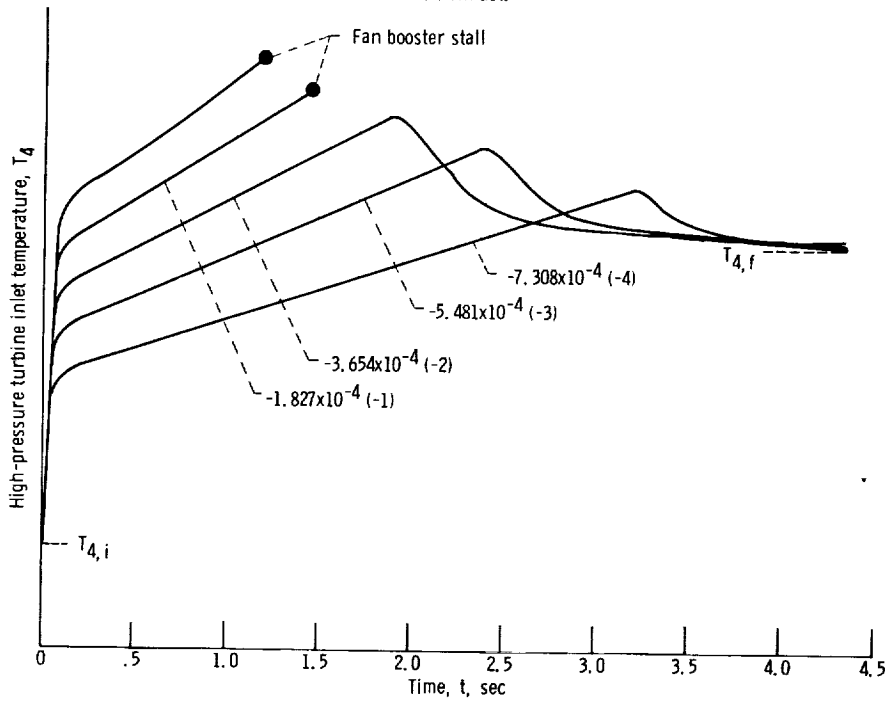
WDF1 .43469	WDC .43475	WDB .39212	WDT1 .40072	WDT2 .42034
WDN1 .44061	WDN2 .52441	WDN3 .00000	WDN4 .00000	WDF2 .52346
P2 .72378	P21 .40197	P35 .64294	P3 .36254	P4 .34692
P5 .47534	P6 .61486	P7 .73474	P22 -.00048	P32 .65649
T35 .53857	T3 .57617	T4 .44458	T5 .41662	T6 .51660
T7 .20727	T2 .51867	T21 .57958	TAUN1 .16723	TAUN2 .24221
TAUN3 .00000	WDF .33044	PCNT1 .44409	PCNT2 .36584	PCNF1 .36581
PCNF2 .36581	PCNC .44409	AN1 .73547	AN2 .66809	AN3 .00000
AN4 .00000	ABLC .00000	ABLS .00000	TAUN4 .00000	TAUT .25891

(b) Unscaled data

Low-pressure-compressor flow rate, \dot{w}_{f1} , kg/sec (lbm/sec)	29.57 (65.20)
High-pressure-compressor flow rate, \dot{w}_c , kg/sec (lbm/sec)	29.57 (65.20)
Combustor flow rate, \dot{w}_b , kg/sec (lbm/sec)	26.68 (58.82)
High-pressure-turbine flow rate, \dot{w}_{t1} , kg/sec (lbm/sec)	27.26 (60.10)
Low-pressure-turbine flow rate, \dot{w}_{t2} , kg/sec (lbm/sec)	28.59 (63.04)
Core nozzle flow rate, \dot{w}_{n1} , kg/sec (lbm/sec)	29.98 (66.09)
Fan flow rate, \dot{w}_{f2} ; third-stream nozzle flow rate, \dot{w}_{n2} , kg/sec (lbm/sec)	475.8 (1049)
Fan inlet pressure, P_2 , N/cm ² (psia)	9.984 (14.48)
High-pressure-compressor inlet pressure, $P_{2.1}$, N/cm ² (psia)	13.86 (20.10)
Combustor inlet pressure, P_3 , N/cm ² (psia)	124.9 (181.2)
High-pressure-turbine inlet pressure, P_4 , N/cm ²	119.56 (173.4)
Low-pressure-turbine inlet pressure, P_5 , N/cm ²	32.77 (47.53)
Core duct pressure, P_6 , N/cm ² (psia)	10.60 (15.37)
Bypass fan discharge pressure, $P_{3.2}$, N/cm ²	11.31 (16.41)
Bypass fan duct pressure, $P_{3.5}$, N/cm ² (psia)	11.08 (16.07)
Fan inlet temperature, T_2 , K (°R)	288.2 (518.7)
High-pressure-compressor inlet temperature, $T_{2.1}$, K (°R)	322.0 (579.6)
Combustor inlet temperature, T_3 , K (°R)	640.0 (1152)
High-pressure-turbine inlet temperature, T_4 , K (°R)	1235 (2223)
Low-pressure-turbine inlet temperature, T_5 , K (°R)	925.5 (1666)
Core duct temperature, T_6 , K (°R)	717.8 (1292)
Fuel flow rate, \dot{w}_F , kg/sec (lbm/sec)	0.4496 (0.9912)
Ratio of high-pressure-turbine rotational speed to design, $N_{t1}/N_{t1,des}$	0.8882
Ratio of low-pressure-turbine rotational speed to design, $N_{t2}/N_{t2,des}$	0.7316
Total thrust, F_{tot} , N (lbf)	57 582 (12 945)



(a) Thrust.



(b) Temperature.

Figure 15. - Response of selected turbofan engine to 50-millisecond ramp demand in low rotor speed. Initial speed demand, 73.2 percent of design; final speed demand, 100 percent of design. Analog-simulated fuel control. Variable coefficient K_{φ} in acceleration schedule.

TABLE XVIII. - STEADY-STATE DATA FOR SELECTED TURBOFAN ENGINE

(CONFIGURATION E) AT 100 PERCENT OF DESIGN SPEED

(a) Scaled teletype output

WDF1	WDC	WDB	WDT1	WDT2
.63925	.63973	.57156	.58990	.62103
WDN1	WDN2	WDN3	WDN4	WDF2
.64282	.72888	.00000	.00000	.72671
P2	P21	P35	P3	P4
.72378	.51513	.69653	.61328	.58007
P5	P6	P7	P22	P32
.77160	.64953	.73474	-.00036	.72326
T35	T3	T4	T5	T6
.55590	.68188	.57385	.54235	.62341
T7	T2	T21	TAUN1	TAUN2
.20727	.51867	.63146	.43151	.47259
TAUN3	WDF	PCNT1	PCNT2	PCNF1
.00000	.72692	.50024	.49951	.49948
PCNF2	PCNC	AN1	AN2	AN3
.49948	.50024	.73559	.66809	.00000
AN4	ABLC	ABLS	TAUN4	TAUT
.00000	.00000	.00000	.00000	.51571

(b) Unscaled data

Low-pressure-compressor flow rate, \dot{w}_{f1} , kg/sec (lbm/sec)	43.51 (95.92)
High-pressure-compressor flow rate, \dot{w}_c , kg/sec (lbm/sec)	43.51 (95.92)
Combustor flow rate, \dot{w}_b , kg/sec (lbm/sec)	38.89 (85.74)
High-pressure-turbine flow rate, \dot{w}_{t1} , kg/sec (lbm/sec)	40.13 (88.48)
Low-pressure-turbine flow rate, \dot{w}_{t2} , kg/sec (lbm/sec)	42.25 (93.15)
Core nozzle flow rate, \dot{w}_{n1} , kg/sec (lbm/sec)	43.74 (96.42)
Fan flow rate, \dot{w}_{f2} ; third-stream nozzle flow rate, \dot{w}_{n2} , kg/sec (lbm/sec)	660.4 (1456)
Fan inlet pressure, P_2 , N/cm ² (psia)	9.984 (14.48)
High-pressure-compressor inlet pressure, $P_{2.1}$, N/cm ² (psia)	17.76 (25.76)
Combustor inlet pressure, P_3 , N/cm ² (psia)	211.4 (306.6)
High-pressure-turbine inlet pressure, P_4 , N/cm ² (psia)	199.9 (290.0)
Low-pressure-turbine inlet pressure, P_5 , N/cm ² (psia)	53.20 (77.16)
Core duct pressure, P_6 , N/cm ² (psia)	11.20 (16.24)
Bypass fan discharge pressure, $P_{3.2}$, N/cm ² (psia)	12.46 (18.08)
Bypass fan duct pressure, $P_{3.5}$, N/cm ² (psia)	12.00 (17.41)
Fan inlet temperature, T_2 , K (^o R)	288.2 (518.7)
High-pressure-compressor inlet temperature, $T_{2.1}$, K (^o R)	350.8 (631.5)
Combustor inlet temperature, T_3 , K (^o R)	757.8 (1364)
High-pressure-turbine inlet temperature, T_4 , K (^o R)	1594 (2869)
Low-pressure-turbine inlet temperature, T_5 , K (^o R)	1205 (2170)
Core duct temperature, T_6 , K (^o R)	865.5 (1558)
Fuel flow rate, \dot{w}_F , kg/sec (lbm/sec)	0.9893 (2.181)
Ratio of high-pressure-turbine rotational speed to design, $N_{t1}/N_{t1,des}$	1.0000
Ratio of low-pressure-turbine rotational speed to design, $N_{t2}/N_{t2,des}$	0.9990
Total thrust, F_{tot} , N (lbf)	1.1507×10^5 (25.870)

transient was terminated automatically after 1.2 seconds when the boosted-fan-hub map inputs went out of range (booster stall). The stall condition was caused by the excessive turbine inlet temperature shown in figure 15(b).

To demonstrate the effects of reducing the acceleration schedule of fuel flow, the coefficient K_ϕ (eq. (H12)) was reduced in steps of 1.827×10^{-4} kg-cm²/sec-N (1.0 lbm/hr-psia). The engine was accelerated successfully with the acceleration schedule reduced by more than 3.654×10^{-4} kg-cm²/sec-N (2.0 lbm/hr-psia). Figure 15 shows the trade-off between reduced turbine inlet temperatures and fast thrust response.

At the end of one of the transients, a teletype listing of steady-state variables was obtained by depressing sense switch 1. The resulting listing is shown in table XVIII. A comparison of table XVIII with steady-state data generated with GENENG II (ref. 4) at this operating point indicates the following maximum differences between the two programs: pressures, 0.07 percent; temperatures, 0.42 percent; flows rates, 0.77 percent; thrust, 4.4 percent.

CONCLUDING REMARKS

This report has described HYDES, a hybrid computer program capable of simulating either one-spool turbojet, two-spool turbojet, or two-spool turbofan engine dynamics. The program is also capable of simulating two-or three- stream turbofans with or without mixing of the exhaust streams. HYDES was developed for running on the Lewis Research Center's Electronic Associates (EAI) 690 Hybrid Computing System. The hybrid computer combines the precision and logic capabilities of the digital computer with the integration and data output capabilities of the analog computer. The HYDES program is intended to eliminate the need for developing individual simulations for each new engine study.

In the HYDES program, the analog computer is used, primarily, for performing integration with respect to time. The use of the digital computer to perform all function generation and most of the algebraic calculations results in digital cycle times between 23 and 44 milliseconds. These long cycle times make real-time simulation impossible and require time scaling of the dynamics on the analog computer.

The documentation of the HYDES program, together with the digital computer software (available from the author upon request), should allow the user to quickly implement the program on a similar computer. It is expected that this report will also prove valuable in the development of both generalized and specific engine simulations on other computers. The scaling techniques, discussed in the report, are applicable to all

analog simulations. The branching techniques and program structure associated with the generalization of the HYDES program should be applicable to all digital simulations.

Lewis Research Center,
National Aeronautics and Space Administration,
Cleveland, Ohio, September 25, 1973,
501-24.

APPENDIX A

UNSCALED-VARIABLE SYMBOLS

A	effective cross-sectional area, cm^2 (in.^2)
a	supercharger map intercept
b	supercharger map slope
C_v	nozzle velocity coefficient
CNCF	general turbine speed scaling coefficient
CNHPCF	high-pressure-turbine speed scaling coefficient
CNLPCF	low-pressure-turbine speed scaling coefficient
c_p	specific heat at constant pressure, J/kg-K ($\text{Btu/lbm-}^\circ\text{R}$)
c_v	specific heat at constant volume, J/kg-K ($\text{Btu/lbm-}^\circ\text{R}$)
ceff	high-pressure-compressor map efficiency
cnp	high-pressure-compressor map speed parameter
ctr	high-pressure-compressor temperature rise parameter
DHCF	general turbine enthalpy scaling coefficient
DHHPCF	high-pressure-turbine enthalpy scaling coefficient
DHLPCF	low-pressure-turbine enthalpy scaling coefficient
dht	general turbine map work function, J/kg-K ($\text{Btu/lbm-}^\circ\text{R}$)
ETACCF	high-pressure-compressor efficiency scaling coefficient
ETACF	general fan or compressor efficiency scaling coefficient
ETAFCF	fan efficiency scaling coefficient
ETAICF	low-pressure-compressor efficiency scaling coefficient
ETTFCF	general turbine efficiency scaling coefficient
eff	general component map efficiency
F	thrust, N(lbf)
ΔF	thrust increment, N(lbf)
F_i	nozzle function, $i = 1$ for flow, $i = 2$ for thrust
f_i	functional relation

f/a	local fuel-air ratio
fcnp	general fan or compressor map speed parameter
f1eff	low-pressure-compressor map efficiency
f1np	low-pressure-compressor map speed parameter
f1tr	low-pressure-compressor ideal temperature rise parameter
fpc	high-pressure-compressor map flow parameter, kg/sec (lbm/sec)
fpfc	general fan or compressor map flow parameter, kg/sec (lbm/sec)
fpf1	low-pressure-compressor map flow parameter, kg/sec (lbm/sec)
fpf2	fan map flow parameter, kg/sec (lbm/sec)
fpt	general turbine map flow parameter, kg-K-cm ² /N-rpm-sec (lbm-°R-in. ² /lbf-rpm-sec)
fpt1	high-pressure-turbine map flow parameter, kg-K-cm ² /N-rpm-sec (lbm-°R-in. ² /lbf-rpm-sec)
fpt2	low-pressure-turbine map flow parameter, kg-K-cm ² /N-rpm-sec (lbm-°R-in. ² /lbf-rpm-sec)
f2eff	fan map efficiency
f2np	fan map speed parameter
f2tr	fan map ideal temperature rise parameter
g _c	gravitational conversion factor, 100 cm-kg/N-sec ² (386.3 lbm-in./lbf-sec ²)
HVF	heating value of fuel, 4.302×10 ⁷ J/kg (18 500 Btu/lbm)
h	enthalpy, J/kg, (Btu/lbm)
Δh	general turbine enthalpy drop, J/kg (Btu/lbm)
hpt	general turbine map enthalpy drop parameter, J/kg-K ^{1/2} -rpm (Btu/lbm-°R ^{1/2} -rpm)
hpt1	high-pressure-turbine map enthalpy drop parameter, J/kg-K ^{1/2} -rpm (Btu/lbm-°R ^{1/2} -rpm)
hpt2	low-pressure-turbine map enthalpy drop parameter, J/kg-K ^{1/2} -rpm (Btu/lbm-°R ^{1/2} -rpm)
I	polar moment of inertia, N-cm-sec ² (in.-lbf-sec ²)
J	mechanical equivalent of heat, 100 N-cm/J (9339.1 in.-lbf/Btu)

K_{f1}	low-pressure-compressor/low-pressure-turbine speed ratio
K_{f2}	fan/low-pressure-turbine speed ratio
K_i	controller gain
K_ϕ	acceleration schedule coefficient, $\text{kg-cm}^2/\text{sec-N}$ (lbf-in.-hr-psi)
L	torque, N-cm (in.-lbf)
ΔL	differential torque, N-cm (lbf-in.)
MM	number of streams fed by control volume
N	rotational speed, rpm
NN	number of streams feeding control volume
P	total pressure, N/cm^2 (lbf/in. ²)
P_s	static pressure, N/cm^2 (lbf/in. ²)
PRCCF	high-pressure-compressor pressure-ratio scaling coefficient
PRCF	general fan or compressor pressure-ratio scaling coefficient
PRFCF	fan pressure-ratio scaling coefficient
PRICF	low-pressure-compressor pressure-ratio scaling coefficient
pr	map pressure ratio
prc	high-pressure-compressor map pressure ratio
prf1	low-pressure-compressor map pressure ratio
prf2	fan map pressure ratio
prt1	high-pressure-turbine pressure ratio
prt2	low-pressure-turbine pressure ratio
R	gas constant, N-cm/kg-K (in.-lbf/lbm- ^o R)
R_A	gas constant of air, 44.83 N-cm/kg-K (640.1 in.-lbf/lbm- ^o R)
\mathcal{A}	pressure loss coefficient, $\text{N-sec}^2/\text{kg}^2\text{-cm}^2$
S	Laplacian operator, sec^{-1}
T	total temperature, $\text{K}(\text{oR})$
ΔT	fan or compressor temperature rise, $\text{K}(\text{oR})$

TFCF	general turbine flow scaling coefficient
TFHPCF	high-pressure-turbine flow scaling coefficient
TFLPCF	low-pressure-turbine flow scaling coefficient
t	time, sec
dt	differential time, sec
tff	general turbine map flow function, $\text{kg-K}^{1/2}\text{-cm}^2/\text{N-sec}$ ($\text{lbm-}^\circ\text{R}^{1/2}\text{-in.}^2/\text{lb-sec}$)
tnp	general turbine map speed parameter
tr	general fan or compressor temperature rise parameter
t1np	high-pressure-turbine map speed parameter, $\text{rpm}/\text{K}^{1/2}$ ($\text{rpm}/^\circ\text{R}^{1/2}$)
t2np	low-pressure-turbine map speed parameter, $\text{rpm}/\text{K}^{1/2}$ ($\text{rpm}/^\circ\text{R}^{1/2}$)
V	volume, cm^3 (in.^3)
W	stored mass, kg (lbm)
WACCF	high-pressure-compressor flow scaling coefficient
WACF	general fan or compressor flow scaling coefficient
WAFCF	fan flow scaling coefficient
WAICF	low-pressure-compressor flow scaling coefficient
\dot{w}	flow rate, kg/sec (lbm/sec)
$\Delta\dot{w}_f$	output of fuel controller, kg/sec (lbm/sec)
x	general unscaled variable
y	position signal
α	power lever angle
β	temperature interpolation constant
γ	specific-heat ratio
ϵ	control error signal
η	efficiency
τ	time constant, sec
φ	acceleration schedule output, $\text{kg-cm}^2/\text{sec-N}$ (lbm/hr-psia)

ω frequency, sec^{-1}

Subscripts:

a analog
accel acceleration
b combustor
blc control bleed
bls interstream bleed
bl1 high-pressure-turbine cooling bleed
bl2 low-pressure-turbine cooling bleed
c high-pressure compressor
cr critical
d digital
dem demanded value
des design value
F fuel
FB feedback
f final value
fm fan map
f1 low-pressure compressor
f2 fan
i initial value
id ideal
in input to control volume
j index on flows into control volume
k index on flows out of control volume
m measured
max maximum value

min	minimum value
nom	nominal value
n1	core nozzle
n2	third-stream nozzle
n3	mixing nozzle
n4	second-stream nozzle
out	out of control volume
ovb	overboard bleed
sc	supercharger
sl	sea level, 10.133 N/cm ² (14.696 psia)
std	standard day, 288.1 K (518.67 ^o R)
tot	total
t1	high-pressure turbine
t2	low-pressure turbine
v2	second-stream valve or duct
v3	third-stream valve or duct
2	fan inlet
2.1	high-pressure-compressor inlet
2.2	second-stream duct
3	combustor inlet
3.2	bypass fan discharge
3.5	bypass fan duct
4	high-pressure-turbine inlet
5	low-pressure-turbine inlet
6	core duct
7	mixing volume
8	nozzle discharge

Superscripts:

- ($\bar{\quad}$) average value
- (\prime) inlet to control volume
- ($\dot{\quad}$) time derivative

APPENDIX B

SUMMARY OF UNSCALED EQUATIONS

$$f_{1np} = \frac{\left(\frac{N_{f1}}{N_{f1, des}} \right)}{\sqrt{\frac{T_2}{T_{2, des}}}} \quad (B1)$$

$$prf1 = \frac{\left(\frac{P_{2.1}}{P_2} - 1 \right)}{PRICF} + 1 \quad (B2)$$

$$fpf1 = f_1(prf1, f_{1np}) \quad (B3)$$

$$\dot{w}_{f1} = \frac{(WAICF)(fpf1) \left(\frac{P_2}{P_{s1}} \right)}{\sqrt{\frac{T_2}{T_{std}}}} \quad (B4)$$

$$f_{1eff} = f_2(prf1, f_{1np}) \quad (B5)$$

$$\eta_{f1} = (ETAICF)(f_{1eff}) \quad (B6)$$

$$fltr = \left(\frac{P_{2.1}}{P_2} \right)^{\frac{\gamma_{f1}-1}{\gamma_{f1}}} - 1 \quad (B7)$$

$$\gamma_{f1} = f_3(\bar{T}_{f1}, 0) \quad (B8)$$

$$\bar{T}_{f1} = \beta_{f1} T_2 + (1 - \beta_{f1}) T_{2.1} \quad (B9)$$

$$T'_{2.1} = \left(\frac{f1tr}{\eta_{f1}} + 1 \right) T_2 \quad (B10)$$

$$h'_{2.1} = f_4(T'_{2.1}, 0) \quad (B11)$$

$$L_{f1} = \frac{30J(h'_{2.1} - h_2)\dot{w}_{f1}}{\pi N_{f1}} \quad (B12)$$

$$h_2 = f_4(T_2, 0) \quad (B13)$$

$$cnp = \frac{\frac{N_c}{N_{c,des}}}{\sqrt{\frac{T_{2.1}}{T_{2.1,des}}}} \quad (B14)$$

$$prc = \frac{\left(\frac{P_3}{P_{2.1}} - 1 \right)}{PRCCF} + 1 \quad (B15)$$

$$fpc = f_5(prc, cnp) \quad (B16)$$

$$\dot{w}_c = \frac{(WACCF)(fpc) \frac{P_{2.1}}{P_{sl}}}{\sqrt{\frac{T_{2.1}}{T_{std}}}} \quad (B17)$$

$$ceff = f_6(prc, cnp) \quad (B18)$$

$$\eta_c = (ETACCF)(ceff) \quad (B19)$$

$$\text{ctr} = \left(\frac{P_3}{P_{2.1}} \right)^{\frac{\gamma_c - 1}{\gamma_c}} - 1 \quad (\text{B20})$$

$$\gamma_c = f_3(\bar{T}_c, 0) \quad (\text{B21})$$

$$\bar{T}_c = \beta_c T_{2.1} + (1 - \beta_c) T_3 \quad (\text{B22})$$

$$T_3' = \left(\frac{\text{ctr}}{\eta_c} + 1 \right) T_{2.1} \quad (\text{B23})$$

$$h_3' = f_4(T_3', 0) \quad (\text{B24})$$

$$L_c = \frac{30J(h_3' - h_{2.1})\dot{w}_c}{\pi N_c} \quad (\text{B25})$$

$$h_{2.1} = f_4(T_{2.1}, 0) \quad (\text{B26})$$

$$\bar{T}_b = \beta_b T_3 + (1 - \beta_b) T_4 \quad (\text{B27})$$

$$\bar{h}_b = f_4(\bar{T}_b, 0) \quad (\text{B28})$$

$$(f/a)_4 = \frac{\dot{w}_F}{\dot{w}_b} \quad (\text{B29})$$

$$w_b = \sqrt{\frac{P_3 - P_4}{R_b}} \quad (\text{B30})$$

$$t_{1np} = \frac{(\text{CNHPCF})N_{t1}}{\sqrt{T_4}} \quad (\text{B31})$$

$$\text{prt1} = \frac{P_5}{P_4} \quad (\text{B32})$$

$$\text{fpt1} = f_7(\text{prt1}, t_{1np}) \quad (\text{B33})$$

$$\text{hpt1} = f_8(\text{prt1}, t_{1np}) \quad (\text{B34})$$

$$\dot{w}_{t1} = \frac{(\text{CNHPCF})(N_{t1})(P_4)(\text{fpt1})}{(\text{TFHPCF})(T_4)} \quad (\text{B35})$$

$$\Delta h_{t1} = \frac{(\text{DHHPCF})(\text{hpt1})(\text{CNHPCF})(N_{t1}) \sqrt{T_4}}{1000} \quad (\text{B36})$$

$$L_{t1} = \frac{30J\Delta h_{t1}\dot{w}_{t1}}{\pi N_{t1}} \quad (\text{B37})$$

$$h_5' = h_4 - \Delta h_{t1} \quad (\text{B38})$$

$$h_4 = f_4 \left[T_4, (f/a)_4 \right] \quad (\text{B39})$$

$$(f/a)_5 = \frac{(f/a)_4}{1 + \left[(f/a)_4 + 1 \right] \left(\frac{\dot{w}_{bl1}}{\dot{w}_{t1}} \right)} \quad (\text{B40})$$

$$\dot{w}_{bl1} = A_{bl1} \sqrt{\frac{g_c}{R_A} \frac{P_3 \mathcal{F}_1}{\sqrt{T_3}} \left(\frac{P_5}{P_3}, \gamma_3 \right)} \quad (\text{B41})$$

where $\mathcal{F}_1 \left(\frac{P_5}{P_3}, \gamma_3 \right)$ is fit by $(0.44208 + 0.17337 \gamma_3)$.

$$\mathcal{F}_1(\text{pr}, \gamma) \begin{cases} = \sqrt{\gamma \left(\frac{2}{\gamma+1}\right)^{\frac{\gamma+1}{\gamma-1}}} & \text{if } \text{pr} \leq 0.53685 \\ = (\text{pr})^{1/\gamma} \sqrt{\frac{2\gamma}{\gamma-1} \left[1 - \text{pr}^{(\gamma-1)/\gamma}\right]} & \text{if } \text{pr} > 0.53685 \end{cases} \quad (\text{B42})$$

$$\gamma_3 = f_3(T_3, 0) \quad (\text{B43})$$

$$t_{2np} = \frac{(\text{CNLPCF})N_{t2}}{\sqrt{T_5}} \quad (\text{B44})$$

$$\text{prt2} = \frac{P_6}{P_5} \quad (\text{B45})$$

$$\text{fpt2} = f_9(\text{prt2}, t_{2np}) \quad (\text{B46})$$

$$\text{hpt2} = f_{10}(\text{prt2}, t_{2np}) \quad (\text{B47})$$

$$\dot{w}_{t2} = \frac{(\text{CNLPCF})(N_{t2})(P_5)(\text{fpt2})}{(\text{TFLPCF})(T_5)} \quad (\text{B48})$$

$$\Delta h_{t2} = \frac{(\text{DHLPCF})(\text{hpt2})(\text{CNLPCF})(N_{t2})\sqrt{T_5}}{1000} \quad (\text{B49})$$

$$L_{t2} = \frac{30J\Delta h_{t2}\dot{w}_{t2}}{\pi N_{t2}} \quad (\text{B50})$$

$$h'_6 = h_5 - \Delta h_{t2} \quad (\text{B51})$$

$$h_5 = f_4 \left[T_5, (f/a)_E \right] \quad (\text{B52})$$

$$(f/a)_6 = \frac{(f/a)_5}{1 + \left[(f/a)_5 + 1 \right] \frac{\dot{w}_{bl2}}{\dot{w}_{t2}}} \quad (B53)$$

$$\dot{w}_{bl2} = A_{bl2} \sqrt{\frac{g_c}{R_A} \frac{P_3 \mathcal{F}_1 \left(\frac{P_6}{P_3}, \gamma_3 \right)}{\sqrt{T_3}}} \quad (B54)$$

where $\mathcal{F}_1(P_6/P_3, \gamma_3)$ is fit by $(0.44208 + 0.17337 \gamma_3)$

$$f2np = \frac{\frac{N_{f2}}{N_{f2, des}}}{\sqrt{\frac{T_2}{T_{2, des}}}} \quad (B55)$$

$$prf2 = \frac{\left(\frac{P_{3.2}}{P_2} - 1 \right)}{PRFCF} + 1 \quad (B56)$$

$$fpf2 = f_{11}(prf2, f2np) \quad (B57)$$

$$\dot{w}_{fm} = \frac{(WAFCF)(fpf2) \left(\frac{P_2}{P_{std}} \right)}{\sqrt{\frac{T_2}{T_{std}}}} \quad (B58)$$

where for SPLIT="TRUE", $\dot{w}_{f2} = \dot{w}_{fm} - \dot{w}_{f1}$; and for SPLIT="FALSE", $\dot{w}_{f2} = \dot{w}_{fm}$.

$$f2eff = f_{12}(prf2, f2np) \quad (B59)$$

$$\eta_{f2} = (\text{ETAFCF})(f2\text{eff}) \quad (\text{B60})$$

$$f2\text{tr} = \left(\frac{P_{3.2}}{P_2} \right)^{\frac{\gamma_{f2}-1}{\gamma_{f2}}} - 1 \quad (\text{B61})$$

$$\gamma_{f2} = f_3(\bar{T}_{f2}, 0) \quad (\text{B62})$$

$$\bar{T}_{f2} = \beta_{f2} T_2 + (1 - \beta_{f2}) T_{3.2} \quad (\text{B63})$$

$$T'_{3.2} = \left(\frac{f2\text{tr}}{\eta_{f2}} + 1 \right) T_2 \quad (\text{B64})$$

$$h'_{3.2} = f_4(T'_{3.2}, 0) \quad (\text{B65})$$

$$L_{f2} = \frac{30J(h'_{3.2} - h_2)\dot{w}_{f2}}{\pi N_{f2}} \quad (\text{B66})$$

$$\dot{w}_{\text{ovb}} = A_{\text{ovb}} \sqrt{\frac{g_c}{R_A}} \frac{P_3 \mathcal{F}_1}{\sqrt{T_3}} \left(\frac{P_8}{P_3}, \gamma_3 \right) \quad (\text{B67})$$

where $\mathcal{F}_1(P_8/P_3, \gamma_3)$ is fit by $(0.44208 + 0.17337 \gamma_3)$

$$\dot{w}_{\text{blc}} = A_{\text{blc}} \sqrt{\frac{g_c}{R_A}} \frac{P_{2.1} \mathcal{F}_1}{\sqrt{T_{2.1}}} \left(\frac{P_8}{P_{2.1}}, \gamma_{2.1} \right) \quad (\text{B68})$$

$$\dot{w}_{bls} = A_{bls} \sqrt{P_{2.1} - P_{3.2}} \quad (B69)$$

$$\gamma_{2.1} = f_3(T_{2.1}, 0) \quad (B70)$$

$$\dot{w}_{n1} = A_{n1} \sqrt{\frac{g_c}{R_A}} \frac{P_6 \mathcal{F}_1}{\sqrt{T_6}} \left(\frac{P_7}{P_6}, \gamma_6 \right) \quad (B71)$$

$$\dot{w}_{n2} = A_{n2} \sqrt{\frac{g_c}{R_A}} \frac{P_{3.5} \mathcal{F}_1}{\sqrt{T_{3.5}}} \left(\frac{P_7}{P_{3.5}}, \gamma_{3.5} \right) \quad (B72)$$

$$\dot{w}_{n3} = A_{n3} \sqrt{\frac{g_c}{R_A}} \frac{P_7 \mathcal{F}_1}{\sqrt{T_7}} \left(\frac{P_8}{P_7}, \gamma_7 \right) \quad (B73)$$

$$\dot{w}_{n4} = A_{n4} \sqrt{\frac{g_c}{R_A}} \frac{P_{2.2} \mathcal{F}_1}{\sqrt{T_{2.2}}} \left(\frac{P_{out}}{P_{2.2}}, \gamma_{2.2} \right) \quad (B74)$$

where P_{out} is equal to P_8 for STRM3="TRUE" and to P_7 otherwise.

$$\gamma_6 = f_3 [T_6, (f/a)_6] \quad (B75)$$

$$\gamma_{3.5} = f_3(T_{3.5}, 0) \quad (B76)$$

$$\gamma_{2.2} = f_3(T_{2.2}, 0) \quad (B77)$$

$$\gamma_7 = f_3 [T_7, (f/a)_7] \quad (B78)$$

$$(f/a)_7 = \frac{(f/a)_6}{1 + [(f/a)_6 + 1] \left(\frac{\dot{w}_{in}}{\dot{w}_{n1}} \right)} \quad (B79)$$

where \dot{w}_{in} is equal to \dot{w}_{n2} for HBPR="TRUE" and to \dot{w}_{n4} otherwise.

$$F_{n1} = C_{v,n1} \dot{w}_{n1} \sqrt{\frac{2J}{g_c} c_{p,6} T_6} \mathcal{F}_2 \left(\frac{P_{s,n1}}{P_6}, \gamma_6 \right) + A_{n1} (P_{s,n1} - P_7) \quad (B80)$$

where $P_{s,n1}$ is equal to $0.53685 P_6$ if $P_7/P_6 \leq 0.53685$ and to P_7 if $P_7/P_6 \geq 0.53685$.

$$\mathcal{F}_2(pr, \gamma) = \sqrt{1 - pr^{(\gamma-1)/\gamma}} \quad (B81)$$

$$F_{n2} = C_{v,n2} \dot{w}_{n2} \sqrt{\frac{2J}{g_c} c_{p,3.5} T_{3.5}} \mathcal{F}_2 \left(\frac{P_{s,n2}}{P_{3.5}}, \gamma_{3.5} \right) + A_{n2} (P_{s,n2} - P_7) \quad (B82)$$

where $P_{s,n2}$ is equal to $0.53685 P_{3.5}$ if $P_7/P_{3.5} \leq 0.53685$ and to P_7 if $P_7/P_{3.5} > 0.53685$.

$$F_{n3} = C_{v,n3} \dot{w}_{n3} \sqrt{\frac{2J}{g_c} c_{p,7} T_7} \mathcal{F}_2 \left(\frac{P_{s,n3}}{P_7}, \gamma_7 \right) + A_{n3} (P_{s,n3} - P_8) \quad (B83)$$

where $P_{s,n3}$ is equal to $0.53685 P_7$ if $P_8/P_7 \leq 0.53685$ and to P_8 if $P_8/P_7 > 0.53685$.

$$F_{n4} = C_{v,n4} \dot{w}_{n4} \sqrt{\frac{2J}{g_c} c_{p,2.2} T_{2.2}} \mathcal{F}_2 \left(\frac{P_{s,n4}}{P_{out}}, \gamma_{2.2} \right) + A_{n4} (P_{s,n4} - P_{out}) \quad (B84)$$

where $P_{s, n4}$ is equal to $0.53685 P_{2.2}$ if $P_{out}/P_{2.2} \leq 0.53685$ and to P_{out} if $P_{out}/P_{2.2} > 0.53685$, and P_{out} is equal to P_8 for $STRM3="TRUE"$ and to P_7 otherwise.

$$c_{p, 6} = f_{13} [T_6, (f/a)_6] \quad (B85)$$

$$c_{p, 3.5} = f_{13}(T_{3.5}, 0) \quad (B86)$$

$$c_{p, 7} = f_{13} [T_7, (f/a)_7] \quad (B87)$$

$$c_{p, 2.2} = f_{13}(T_{2.2}, 0) \quad (B88)$$

$$F_{tot} = \begin{cases} F_{n1} & \text{for TURBJ1="TRUE" or TURBJ2="TRUE"} \\ F_{n3} & \text{for MIX="TRUE", STRM3="FALSE"} \\ F_{n3} + F_{n4} & \text{for MIX="TRUE", STRM3="TRUE"} \\ F_{n1} + F_{n2} & \text{for HBPR="TRUE", MIX="FALSE", STRM3="FALSE"} \\ F_{n1} + F_{n4} & \text{for HPBR="FALSE", MIX="FALSE", STRM3="FALSE"} \\ F_{n1} + F_{n2} + F_{n4} & \text{for HBPR="TRUE", MIX="FALSE", STRM3="TRUE"} \end{cases} \quad (B89)$$

$$P_2 = \text{Constant} \quad (B90)$$

$$T_2 = \text{Constant} \quad (B91)$$

$$P_{2.1} = \frac{R_A W_{2.1} T_{2.1}}{V_{2.1}} \quad (B92)$$

$$W_{2.1} = \int_0^t (\dot{w}_{f1} - \dot{w}_c - \dot{w}_{blc} - \dot{w}_{bls} - \dot{w}_{v2}) dt + W_{2.1, i} \quad (B93)$$

$$\dot{w}_{v2} = \sqrt{\frac{P_{2.1} - P_{2.2}}{R_{v2}}} = 0 \quad \text{for HBPR='TRUE', STRM3='FALSE'} \quad (\text{B94})$$

$$T_{2.1} = \int_0^t \frac{1}{W_{2.1}} \left[\frac{\dot{w}_{f1} h'_{2.1} - h_{2.1} (\dot{w}_c + \dot{w}_{blc} + \dot{w}_{bls} + \dot{w}_{v2})}{c_{v,2.1}} \right. \\ \left. - T_{2.1} (\dot{w}_{f1} - \dot{w}_c - \dot{w}_{blc} - \dot{w}_{bls} - \dot{w}_{v2}) \right] dt + T_{2.1,i} \quad (\text{B95})$$

$$P_3 = \frac{R_A W_3 T_3}{V_3} \quad (\text{B96})$$

$$W_3 = \int_0^t (\dot{w}_c - \dot{w}_b - \dot{w}_{ovb} - \dot{w}_{bl1} - \dot{w}_{bl2}) dt + W_{3,i} \quad (\text{B97})$$

$$T_3 = \int_0^t \frac{1}{W_3} \left[\frac{\dot{w}_c h'_3 - h_3 (\dot{w}_b + \dot{w}_{ovb} + \dot{w}_{bl1} + \dot{w}_{bl2})}{c_{v,3}} \right. \\ \left. - T_3 (\dot{w}_c - \dot{w}_b - \dot{w}_{ovb} - \dot{w}_{bl1} - \dot{w}_{bl2}) \right] dt + T_{3,i} \quad (\text{B98})$$

$$h_3 = f_4(T_3, 0) \quad (\text{B99})$$

$$P_4 = \frac{R_A W_4 T_4}{V_4} \quad (\text{B100})$$

$$W_4 = \int_0^t (\dot{w}_b + \dot{w}_F - \dot{w}_{t1}) dt + W_{4,i} \quad (\text{B101})$$

$$T_4 = \int_0^t \frac{1}{W_4} \left[\frac{\dot{w}_b \bar{h}_b + \eta_b (HVF) \dot{w}_F - \dot{w}_{t1} h_4}{c_{v,4}} - T_4 (\dot{w}_b + \dot{w}_F - \dot{w}_{t1}) \right] dt + T_{4,i} \quad (B102)$$

$$P_5 = \frac{R_A W_5 T_5}{V_5} \quad (B103)$$

$$W_5 = \int_0^t (\dot{w}_{t1} + \dot{w}_{bl1} - \dot{w}_{t2}) dt + W_{5,i} \quad (B104)$$

$$T_5 = \int_0^t \frac{1}{W_5} \left[\frac{\dot{w}_{t1} h'_5 + \dot{w}_{bl1} h_3 - \dot{w}_{t2} h_5}{c_{v,5}} - T_5 (\dot{w}_{t1} + \dot{w}_{bl1} - \dot{w}_{t2}) \right] dt + T_{5,i} \quad (B105)$$

$$P_6 = \frac{R_A W_6 T_6}{V_6} \quad (B106)$$

$$W_6 = \int_0^t (\dot{w}_{t2} + \dot{w}_{bl2} - \dot{w}_{n1}) dt + W_{6,i} \quad (B107)$$

$$T_6 = \int_0^t \frac{1}{W_6} \left[\frac{\dot{w}_{t2} h'_6 + \dot{w}_{bl2} h_3 - \dot{w}_{n1} h_6}{c_{v,6}} - T_6 (\dot{w}_{t2} + \dot{w}_{bl2} - \dot{w}_{n1}) \right] dt + T_{6,i} \quad (B108)$$

$$P_{3.2} = \frac{R_A W_{3.2} T_{3.2}}{V_{3.2}} \quad (B109)$$

$$W_{3.2} = \int_0^t (\dot{w}_{f2} + \dot{w}_{bls} - \dot{w}_{v3}) dt + W_{3.2,i} \quad (B110)$$

$$T_{3.2} = \int_0^t \frac{1}{W_{3.2}} \left[\frac{\dot{w}_{f2} h_{3.2}' + \dot{w}_{bls} h_{2.1} - \dot{w}_{v3} h_{3.2}}{c_{v,3.2}} - T_{3.2} (\dot{w}_{f2} + \dot{w}_{bls} - \dot{w}_{v3}) \right] dt + T_{3.2,i} \quad (B111)$$

$$P_{3.5} = \frac{R_A W_{3.5} T_{3.5}}{V_{3.5}} \quad (B112)$$

$$W_{3.5} = \int_0^t (\dot{w}_{v3} - \dot{w}_{n2}) dt + W_{3.5,i} \quad (B113)$$

$$T_{3.5} = \int_0^t \frac{1}{W_{3.5}} \left[\frac{\dot{w}_{v3} h_{3.2} - \dot{w}_{n2} h_{3.5}}{c_{v,3.5}} - T_{3.5} (\dot{w}_{v3} - \dot{w}_{n2}) \right] dt + T_{3.5,i} \quad (B114)$$

$$P_{2.2} = \frac{R_A W_{2.2} T_{2.2}}{V_{2.2}} \quad (B115)$$

$$W_{2.2} = \int_0^t (\dot{w}_{v2} - \dot{w}_{n4}) dt + W_{2.2,i} \quad (B116)$$

$$T_{2.2} = \int_0^t \frac{1}{W_{2.2}} \left[\frac{\dot{w}_{v2} h_{2.1} - \dot{w}_{n4} h_{2.2}}{c_{v,2.2}} - T_{2.2} (\dot{w}_{v2} - \dot{w}_{n4}) \right] dt + T_{2.2,i} \quad (B117)$$

$$P_7 = \frac{R_A W_7 T_7}{V_7} \quad (B118)$$

$$W_7 = \int_0^t (\dot{w}_{in} + \dot{w}_{n1} - \dot{w}_{n3}) dt + W_{7,i} \quad (B119)$$

$$T_7 = \int_0^t \frac{1}{W_7} \left[\frac{\dot{w}_{in} h_{in} + \dot{w}_{n1} h_6 - \dot{w}_{n3} h_7}{c_{v,7}} - T_7 (\dot{w}_{in} + \dot{w}_{n1} - \dot{w}_{n3}) \right] dt + T_{7,i} \quad (B120)$$

where $\dot{w}_{in} h_{in}$ is equal to $\dot{w}_{n2} h_{3.5}$ for HBPR="TRUE", to $\dot{w}_{n4} h_{2.2}$ for HBPR="FALSE" and MIX="TRUE," and to 0 otherwise.

$$P_8 = \text{Constant} \quad (\text{B121})$$

$$\dot{w}_F = \text{Output of fuel control} \quad (\text{B122})$$

$$N_{t1} = \frac{30}{\pi I_{t1}} \int_0^t (L_{t1} - L_c) dt + N_{t1, i} \quad (\text{B123})$$

$$N_{t2} = \frac{30}{\pi I_{t2}} \int_0^t (L_{t2} - L_{f1} - L_{f2}) dt + N_{t2, i} \quad (\text{B124})$$

$$N_{f1} = K_{f1} N_{t2} \quad (\text{B125})$$

$$N_{f2} = K_{f2} N_{t2} \quad (\text{B126})$$

$$N_c = N_{t1} \quad (\text{B127})$$

$$\dot{w}_{v3} = \sqrt{\frac{P_{3.2} - P_{3.5}}{\mathcal{R}_{v3}}} \quad (\text{B128})$$

For SUPER="TRUE"

$$\text{prf1} = a + b(\text{flnp}) \quad (\text{B129})$$

$$\eta_{f1} = \text{Constant} = \eta_{sc} \quad (\text{B130})$$

$$T_{2.1} = T'_{2.1} \quad (\text{B131})$$

$$\dot{w}_{f1} = \dot{w}_c + \dot{w}_{blc} + \dot{w}_{bls} \quad (\text{B132})$$

APPENDIX C
SCALED-VARIABLE SYMBOLS

ABLC	control bleed nozzle area
ABLS	interstream bleed flow coefficient
AI(i)	DAC initial condition array, $i = 1$ to 24
ANI	nozzle area, $I = 1$ to 4
C(i)	analog coefficient array, $i = 1$ to 57
CPAB	specific heat at constant pressure of combustor air
CPI	specific heat at constant pressure at station I
CVAB	specific heat at constant volume of combustor air
CVI	specific heat at constant volume at station I
DTQT1	high-pressure-turbine differential torque
DTQT2	low-pressure-turbine differential torque
DWI	stored mass derivative at station I
FARI	fuel-air ratio at station I
FG3	compressor discharge bleed flow coefficient
FPC	high-pressure-compressor map flow parameter
FPF1	low-pressure-compressor map flow parameter
FPF2	fan map flow parameter
F1BL	control bleed flow parameter
F2BL	control bleed thrust parameter
F1NI	nozzle flow parameter, $I = 1$ to 4
F2NI	nozzle thrust parameter, $I = 1$ to 4
GMAB	specific-heat ratio of combustor air
GMI	specific-heat ratio at station I
HAB	enthalpy of combustor air
HABS	rescaled enthalpy of combustor air

HBPR	logical variable denoting separate characteristics for fan and low-pressure compressor (fan hub)
HI	enthalpy at station I
HIP	enthalpy at inlet to station I volume
HIS	rescaled enthalpy at station I
IERR	hybrid linkage routine error flag
ISF	overflow error flag (tested by LERR)
IX(k)	initial pressure-ratio search index array for MAPFUN routine, k = 1 to 12
JY(k)	initial speed search index array for MAPFUN routine, k = 1 to 12
kx	integer specifying location of component data to be scaled
LERR	logical function error detection routine
MIX	logical variable denoting mixing of streams at turbofan discharge
MN	component map index, MN = 1 to 10
MODE	integer indicating analog mode
NCV	number of curves per map, NCV=8
NMP	number of component maps, NMP ≤ 10 (MAPFUN capable of handling NMP ≤ 12)
NPT	number of points per curve, NPT=8
NSC	number of digital coefficients, NSC ≤ 125
NTBL	number of map data points stored in VALS array, NTBL=NCV*(2*NPT + 1)
NX(k)	number of points per curve array, k = 1 to NMP
NY(k)	number of curves per map array, K = 1 to NMP
N1	index on lowest component map
N2	index on highest component map
PCNC	fraction of design high-pressure-compressor speed
PCNF1	fraction of design low-pressure-compressor speed
PCNF2	fraction of design fan speed

PCNT1	fraction of design high-pressure-turbine speed
PCNT2	fraction of design low-pressure-turbine speed
PI	total pressure at station I
PRC	high-pressure-compressor map pressure ratio
PRF1	low-pressure-compressor map pressure ratio
PRF2	fan map pressure ratio
PSBL	static pressure at control bleed nozzle throat
PSNI	static pressure at nozzle throat, I = 1 to 4
SC(i)	digital coefficient array, i = 1 to NSC
SENSW	logical function routine for testing sense-switch positions
SF _t	scale factor on time t, $t' = SF_t t$
SF _X	scale factor on variable x, $X = x/SF_X$ (appropriate units)
SPLIT	logical variable denoting fan maps based on total engine flow
STRM3	logical variable denoting three-stream turbofan
SUPER	logical variable denoting linear characteristic for low-pressure compressor
TAB	combustor air temperature
TAUNI	nozzle thrust, I = 1 to 4
TAUT	total thrust
TI	total temperature at station I
TIDN	specific temperature derivative at station I
TIS	rescaled temperature at station I
TRF1	low-pressure-compressor ideal temperature rise parameter
TRQC	high-pressure-compressor torque
TRQFT	fan torque based on total inlet flow
TRQF1	low-pressure-compressor torque
TRQF2	fan torque
TRQT1	high-pressure-turbine torque
TRQT2	low-pressure-turbine torque

TURBJ1	logical variable denoting one-spool turbojet configuration
TURBJ2	logical variable denoting two-spool turbojet configuration
t'	computer time
VALS(i)	array containing unscaled component data, i = 1 to NTBL
WDB	combustor airflow
WDBLC	control bleed flow
WDBLS	interstream bleed flow
WDBL1	high-pressure-turbine cooling bleed flow
WDBL2	low-pressure-turbine cooling bleed flow
WDC	high-pressure-compressor flow
WDF	fuel flow
WDF1	low-pressure-compressor flow
WDF2	fan flow
WDFT	total engine inlet flow
W <u>I</u>	stored mass at station I
W <u>DNI</u>	nozzle flow, I = 1 to 4
W <u>DOU</u> T	flow out of control volume
W <u>DO</u> VB	overboard bleed flow
WDT1	high-pressure-turbine flow
WDT2	low-pressure-turbine flow
WDV2	second-stream duct flow
WDV3	third-stream duct flow
X	scaled variable $X = x/SF_X$
XDAC	variable transmitted through extra DAC
XSC	map pressure-ratio scale factor
XVALS (i,j,k)	scaled map pressure-ratio array, i = 1 to NPT; j = 1 to NCV; k = 1 to NMP
YSC	map speed scale factor
YVALS (j,k)	scaled map speed parameter array, j = 1 to NCV; k = 1 to NMP

ZSC map output scale factor
ZVALS (i, j, k) scaled map output array, i = 1 to NPT; j = 1 to NCV; k = 1 to NMP

APPENDIX D

DEFINITIONS OF DIGITAL AND ANALOG COEFFICIENTS

Digital Coefficients

$$SC(1) = \frac{T_2}{SF_{T2}}$$

$$SC(2) = \frac{SF_{WDN1}}{SF_{WDN4}}$$

$$SC(3) = \frac{SF_{P7}}{SF_{P22}}$$

$$SC(4) = K_{f1} \frac{N_{t2, des}}{N_{f1, des}}$$

$$SC(5) = K_{f2} \frac{N_{t2, des}}{N_{f2, des}}$$

$$SC(6) = \frac{A_{bl1} SF_{P3}}{2SF_{WDBL1}} \sqrt{\frac{\epsilon_c}{SF_{T3} R_A}}$$

$$SC(7) = \frac{A_{bl2} SF_{P3}}{2SF_{WDBL2}} \sqrt{\frac{\epsilon_c}{SF_{T3} R_A}}$$

$$SC(8) = \frac{A_{ovb} SF_{P3}}{2SF_{WDOVB}} \sqrt{\frac{\epsilon_c}{SF_{T3} R_A}}$$

$$SC(9) = \frac{SF_{P8}}{SF_{P21}} = \frac{SF_{P8}}{SF_{P22}}$$

$$SC(10) = \frac{SF_{WDBLC}}{SF_{ABLCSF_{P21}}} \sqrt{\frac{SF_{T21} R_A}{g_c}}$$

$$SC(11) = \frac{a_b^{1/2} SF_{WDB}}{\sqrt{SF_{P3}}} = \frac{a_b^{1/2} SF_{WDB}}{\sqrt{SF_{P4}}}$$

$$SC(12) = \frac{SF_{WDF}}{SF_{WDBSF_{FAR4}}}$$

$$SC(13) = \frac{SF_{WDBL1}}{SF_{WDT1}}$$

$$SC(14) = \frac{SF_{WDBL2}}{SF_{WDT2}}$$

$$SC(15) = \frac{SF_{P7}}{SF_{P6}}$$

$$SC(16) = \frac{SF_{WDN1}}{SF_{AN1SF_{P6}}} \sqrt{\frac{SF_{T6} R_A}{g_c}}$$

$$SC(17) = \frac{SF_{P7}}{SF_{P35}}$$

$$SC(18) = \frac{SF_{WDN2}}{SF_{AN2SF_{P35}}} \sqrt{\frac{SF_{T35} R_A}{g_c}}$$

$$SC(19) = \frac{SF_{TAUN2}}{SF_{WDN2} C_{v, n2}} \sqrt{\frac{g_c}{2J SF_{T35} SF_{CP35}}}$$

$$SC(20) = \frac{SF_{TAUN2}}{SF_{P35} SF_{AN2}}$$

$$SC(21) = \frac{SF_{WDN4}}{SF_{AN4} SF_{P22}} \sqrt{\frac{SF_{T22} R_A}{g_c}}$$

$$SC(22) = \frac{SF_{TAUN4}}{SF_{WDN4} C_{v, n4}} \sqrt{\frac{g_c}{2J SF_{T22} SF_{CP22}}}$$

$$SC(23) = \frac{SF_{TAUN4}}{SF_{P22} SF_{AN4}}$$

$$SC(24) = \frac{SF_{TAUN1}}{SF_{TAUT}}$$

$$SC(25) = \frac{SF_{TAUN2}}{SF_{TAUT}}$$

$$SC(26) = \frac{SF_{TAUN4}}{SF_{TAUT}}$$

$$SC(27) = \frac{SF_{WDN1}}{SF_{WDN2}}$$

$$SC(28) = \frac{SF_{P8}}{SF_{P7}}$$

$$SC(29) = \frac{SF_{WDN3}}{SF_{AN3}SF_{P7}} \sqrt{\frac{SF_{T7} R_A}{\epsilon_c}}$$

$$SC(30) = \frac{SF_{TAUN3}}{SF_{WDN3}C_{v,n3}} \sqrt{\frac{\epsilon_c}{2J SF_{T7}SF_{CP7}}}$$

$$SC(31) = \frac{SF_{TAUN3}}{SF_{P7}SF_{AN3}}$$

$$SC(32) = \frac{A_{bls}}{SF_{ABLS}}$$

$$SC(33) = \frac{SF_{WDN4}}{SF_{WDN3}}$$

$$SC(34) = \frac{SF_{WDN1}}{SF_{WDN3}}$$

$$SC(35) = \frac{SF_{WDN2}}{SF_{WDN3}}$$

$$SC(36) = \frac{SF_{TAUN3}}{SF_{TAUT}}$$

$$SC(37) = \frac{SF_{TAUN1}}{SF_{WDN1}C_{v,n1}} \sqrt{\frac{\epsilon_c}{2J SF_{T6}SF_{CP6}}}$$

$$SC(38) = \frac{SF_{TAUN1}}{SF_{P6}SF_{AN1}}$$

$$SC(39) = \frac{SF_{WDBL1}}{SF_{WDC}}$$

$$SC(40) = \frac{SF_{WDBL2}}{SF_{WDC}}$$

$$SC(41) = \frac{SF_{WDOVB}}{SF_{WDC}}$$

$$SC(42) = \beta_b$$

$$SC(43) = \frac{SF_{WDF}^{(HVF)} \eta_b}{SF_{WDB} SF_{HAB}}$$

$$SC(44) = \frac{SF_{WDF}}{SF_{WDB}}$$

$$SC(45) = \frac{SF_{WDBL1} SF_{T3}}{SF_{WDT1} SF_{T5}}$$

$$SC(46) = \frac{SF_{WDBL2} SF_{T3}}{SF_{WDT2} SF_{T6}}$$

$$SC(47) = \frac{SF_{WDC}}{SF_{WDF1}}$$

$$SC(48) = \frac{SF_{WDV2}}{SF_{WDF1}}$$

$$SC(49) = \frac{SF_{WDBLC}}{SF_{WDF1}}$$

$$SC(50) = \frac{SF_{TRQF1} (K_{f1})}{SF_{TRQT2}}$$

$$SC(51) = \frac{SF_{TRQF2} (K_{f2})}{SF_{TRQT2}}$$

$$SC(52) = \frac{SF_{TAUN2}}{SF_{TAUT}}$$

$$SC(53) = \frac{SF_{P5}}{SF_{P4}}$$

$$SC(54) = \frac{SF_{P6}}{SF_{P5}}$$

$$SC(55) = \frac{N_{t1, des} CNHPCF}{SF_{T1NP} \sqrt{SF_{T4}}}$$

$$SC(56) = \frac{N_{t2, des} CNLPCF}{SF_{T2NP} \sqrt{SF_{T5}}}$$

$$SC(57) = \frac{SF_{T4} SF_{WDI1} TFHPCF}{SF_{FPT1} SF_{P4} N_{t1, des} CNHPCF SF_{PCNT1}}$$

$$SC(58) = \frac{SF_{T5} SF_{WDT2} TFLPCF}{SF_{FPT2} SF_{P5} N_{t2, des} CNLPCF SF_{PCNT2}}$$

$$\left. \begin{aligned} \text{SC}(59) &= \frac{\text{SF}_{\text{WDF1}}}{\text{SF}_{\text{WDFT}}} \\ \text{SC}(60) &= \frac{\text{SF}_{\text{WDF2}}}{\text{SF}_{\text{WDFT}}} \end{aligned} \right\} \text{ SPLIT} = \text{"TRUE"}$$

$$\text{SC}(61) = \frac{1000 \text{SF}_{\text{DHT1}}}{\text{SF}_{\text{HPT1}} N_{t1, \text{des}} \sqrt{\text{SF}_{\text{T4}}} \text{DHHPCF} \text{CNHPCF} \text{SF}_{\text{PCNT1}}}$$

$$\text{SC}(62) = \frac{1000 \text{SF}_{\text{DHT2}}}{\text{SF}_{\text{HPT2}} N_{t2, \text{des}} \sqrt{\text{SF}_{\text{T5}}} \text{DHLPCF} \text{CNLPCF} \text{SF}_{\text{PCNT2}}}$$

$$\text{SC}(63) = \frac{2 \text{SF}_{\text{DHT1}}}{\text{SF}_{\text{T4}}}$$

$$\text{SC}(64) = \frac{2 \text{SF}_{\text{DHT2}}}{\text{SF}_{\text{T5}}}$$

$$\text{SC}(65) = \frac{15 \text{J} \text{SF}_{\text{DHT1}} \text{SF}_{\text{WDT1}}}{\pi \text{SF}_{\text{TRQT1}} N_{t1, \text{des}} \text{SF}_{\text{PCNT1}}}$$

$$\text{SC}(66) = \frac{15 \text{J} \text{SF}_{\text{DHT2}} \text{SF}_{\text{WDT2}}}{\pi \text{SF}_{\text{TRQT2}} N_{t2, \text{des}} \text{SF}_{\text{PCNT2}}}$$

$$\text{SC}(67) = \frac{\text{SF}_{\text{P21}}}{\text{SF}_{\text{PRF1}} \text{SF}_{\text{P2}} \text{PRICF}} ; \frac{\text{SF}_{\text{P21}}}{15 \text{SF}_{\text{P2}}} \text{ for SUPER} = \text{"TRUE"}$$

$$SC(68) = \frac{SF_{P3}}{SF_{PRC} SF_{P21} PRCCF}$$

$$SC(69) = \frac{SF_{P32}}{SF_{PRF2} SF_{P2} PRFCF}$$

$$SC(70) = \frac{SF_{T2}}{2T_{2, des}}$$

$$SC(71) = \frac{SF_{T21}}{2T_{2.1, des}}$$

$$SC(72) = \frac{SF_{T2}}{2T_{2, des}}$$

$$SC(73) = \frac{SF_{FPF1} SF_{P2}}{2P_{sl} SF_{WDF1}} \sqrt{\frac{T_{std}}{T_{2, des}}} \quad WAICF$$

$$SC(74) = \frac{SF_{FPC} SF_{P21}}{2P_{sl} SF_{WDC}} \sqrt{\frac{T_{std}}{T_{2.1, des}}} \quad WACCF$$

$$SC(75) = \frac{SF_{FPF2} SF_{P2}}{2P_{sl} SF_{WDF2}^*} \sqrt{\frac{T_{std}}{T_{2, des}}} \quad WAFCF$$

$$SC(76) = \beta_{f1}$$

$$SC(77) = \beta_c$$

*Use SF_{WDFT} for `SPLIT="TRUE."`

$$SC(78) = \beta_{f2}$$

$$SC(79) = \frac{SF_{P21}}{15SF_{P2}}$$

$$SC(80) = \frac{SF_{P3}}{15SF_{P21}}$$

$$SC(81) = \frac{SF_{P32}}{15SF_{P2}}$$

$$SC(82) = \frac{SF_{TRQF1} N_{f1, des} SF_{PCNF1} \pi}{SF_{WDF1} SF_{H21S}^{30J}}$$

$$SC(83) = \frac{SF_{TRQC} N_c, des SF_{PCNC} \pi}{SF_{WDC} SF_{H3S}^{30J}}$$

$$SC(84) = \frac{SF_{TRQF2} * N_{f2, des} SF_{PCNF2} \pi}{SF_{WDF2} * SF_{H32S}^{30J}}$$

$$SC(85) = \frac{A_{n4}}{SF_{AN4}}$$

$$SC(86) = \frac{A_{blc}}{SF_{ABLC}}$$

$$SC(87) = \frac{SF_{TRQF2}}{SF_{TRQFT}} \quad \text{for SPLIT="TRUE"}$$

*Use SF_{WDF1} and SF_{TRQFT} for SPLIT="TRUE."

$$SC(88) = \frac{\alpha^{1/2} SF_{WDV3}}{\sqrt{SF_{P32}}} = \frac{\alpha^{1/2} SF_{WDV3}}{\sqrt{SF_{P35}}}$$

$$SC(89) = \frac{\alpha^{1/2} SF_{WDV2}}{\sqrt{SF_{P21}}} = \frac{\alpha^{1/2} SF_{WDV2}}{\sqrt{SF_{P22}}}$$

$$SC(90) = \eta_{sc}$$

$$SC(91) = \frac{\pi SF_{TRQF1} N_{f1, des} SF_{PCNF1}}{30J SF_{H21} SF_{WDF1}} \quad \text{for SUPER="TRUE"}$$

$$SC(92) = \frac{1 - \frac{1}{PRICF}}{SF_{PRF1}}$$

$$SC(93) = \frac{1 - \frac{1}{PRCCF}}{SF_{PRC}}$$

$$SC(94) = \frac{1 - \frac{1}{PRFCF}}{SF_{PRF2}}$$

$$SC(95) = \frac{0.25}{ETAICF}$$

$$SC(96) = \frac{0.25}{ETACCF}$$

$$SC(97) = \frac{0.25}{ETAFCF}$$

$$SC(98) = \frac{SF_{P32}}{SF_{P21}}$$

$$SC(99) = \frac{SF_{WDBLS}}{\sqrt{SF_{P21}SF_{ABLS}}}$$

$$SC(100) = \frac{SF_{WDBLS}}{SF_{WDF2}} = \frac{SF_{WDBLS}}{SF_{WDV3}}$$

$$SC(101) = \frac{SF_{WDBLS}}{SF_{WDF1}} = \frac{SF_{WDBLS}}{SF_{WDC}}$$

$$SC(102) = \frac{A_{n3}}{SF_{AN3}}$$

$$SC(103) = \frac{P_8}{SF_{P8}}$$

Analog Coefficients

$$C(1) = \frac{SF_{WDF1}}{SF_{W21}SF_{t'}}$$

$$C(2) = \frac{W_{2.1, i}}{SF_{W21}}$$

$$C(3) = \frac{SF_{WDF1}}{SF_{W21} SF_{t'}}$$

$$C(4) = \frac{T_{2.1, i}}{SF_{T21}}$$

$$C(5) = \frac{SF_{WDV2}}{SF_{W22} SF_{t'}}$$

$$C(6) = \frac{W_{2.2, i}}{SF_{W22}}$$

$$C(7) = \frac{SF_{WDV2}}{SF_{W22} SF_{t'}}$$

$$C(8) = \frac{T_{2.2, i}}{SF_{T22}}$$

$$C(9) = \frac{W_{3, i}}{SF_{W3}}$$

$$C(10) = \frac{T_{3, i}}{SF_{T3}}$$

$$C(11) = \frac{SF_{WDC}}{SF_{W3}SF_{t'} (10)}$$

$$C(12) = \frac{SF_{WDC}}{SF_{W3}SF_{t'} (10)}$$

$$C(13) = \frac{W_{4, i}}{SF_{W4}}$$

$$C(14) = \frac{T_{4, i}}{SF_{T4}}$$

$$C(15) = \frac{SF_{WDB}}{SF_{W4}SF_{t'} (10)}$$

$$C(16) = \frac{SF_{WDB}}{SF_{W4}SF_{t'} (10)}$$

$$C(17) = \frac{W_{5, i}}{SF_{W5}}$$

$$C(18) = \frac{T_{5, i}}{SF_{T5}}$$

$$C(19) = \frac{SF_{WDT1}}{SF_{W5}SF_t, (10)}$$

$$C(20) = \frac{SF_{WDT1}}{SF_{W5}SF_t, (10)}$$

$$C(21) = \frac{W_{6, i}}{SF_{W6}}$$

$$C(22) = \frac{T_{6, i}}{SF_{T6}}$$

$$C(23) = \frac{SF_{WDN1}}{SF_{W6}SF_t, (10)}$$

$$C(24) = \frac{SF_{WDN1}}{SF_{W6}SF_t, (10)}$$

$$C(25) = \frac{SF_{WDV3}}{SF_{W35}SF_t,}$$

$$C(26) = \frac{R_A SF_{W21} SF_{T21}}{SF_{P21} V_{2.1}} \quad (10)$$

$$C(27) = \frac{W_{3.5, i}}{SF_{W35}}$$

$$C(28) = \frac{R_A SF_{W35} SF_{T35}}{SF_{P35} V_{3.5}} \quad (10)$$

$$C(29) = \frac{SF_{WDF2}}{SF_{W32} SF_{t'}}$$

$$C(30) = \frac{R_A SF_{W22} SF_{T22}}{SF_{P22} V_{2.2}} \quad (10)$$

$$C(31) = \frac{W_{3.2, i}}{SF_{W32}}$$

$$C(32) = \frac{R_A SF_{W32} SF_{T32}}{SF_{P32} V_{3.2}} \quad (10)$$

$$C(33) = \frac{SF_{WDN3}}{SF_{W7} SF_{t'}}$$

$$C(34) = \frac{R_A SF_{W3} SF_{T3}}{SF_{P3} V_3} \quad (10)$$

$$C(35) = \frac{W_{7, i}}{SF_{W7}}$$

$$C(36) = \frac{R_A SF_{W7} SF_{T7}}{SF_{P7} V_7 (10)}$$

$$C(37) = \frac{30 SF_{TRQT1}}{\pi I_{t1} N_{t1, des} SF_t SF_{PCNT1}}$$

$$C(38) = \frac{R_A SF_{W4} SF_{T4}}{SF_{P4} V_4 (10)}$$

$$C(39) = \frac{N_{t1, i}}{N_{t1, des} SF_{PCNT1}}$$

$$C(40) = \frac{30 SF_{TRQT2}}{\pi I_{t2} N_{t2, des} SF_t SF_{PCNT2}}$$

$$C(41) = \frac{R_A SF_{W5} SF_{T5}}{SF_{P5} V_5 (10)}$$

$$C(42) = \frac{N_{t2, i}}{N_{t2, des} SF_{PCNT2}}$$

$$C(43) = \frac{R_A SF_{W6} SF_{T6}}{SF_{P6} V_6} \quad (10)$$

$$C(44) = \frac{SF_{WDV3}}{SF_{W35} SF_t}$$

$$C(45) = \frac{T_{3.5, i}}{SF_{T35}}$$

$$C(46) = \frac{SF_{WDF2}}{SF_{W32} SF_t}$$

$$C(47) = \frac{T_{3.2, i}}{SF_{T32}}$$

$$C(48) = \frac{SF_{WDN3}}{SF_{W7} SF_t}$$

$$C(49) = \frac{T_{7, i}}{SF_{T7}}$$

$$C(50) = \frac{bSF_{F1NP}}{SF_{PRF1}}$$

$$C(51) = \frac{a}{SF_{PRF1}}$$

$$C(52) = \frac{P_2 SF_{PRF1}}{(10) SF_{P21}}$$

$$C(53) = \frac{K_{f1} N_{t2, des}}{N_{f1, des}} \sqrt{\frac{T_{2, des}}{T_2}} \frac{1}{10}$$

SUPER="TRUE"

a + b(f1np) = prf1

$$C(54) = \frac{A_{n2}}{SF_{AN2}}$$

$$C(55) = \frac{P_2}{SF_{P2}}$$

$$C(56) = \frac{A_{n1}}{SF_{AN1}}$$

$$C(57) = \frac{\dot{w}_{F, i}}{SF_{WDF}}$$

APPENDIX E

COMPUTER LISTINGS OF DATA INPUT PROGRAM,

MAIN PROGRAM, AND SUBROUTINES

GENERALIZED TURBOFAN ENGINE DATA INPUT PROGRAM

```

DIMENSION VALS(168)
SCALED FRACTION SC(125),AI(24),XVALS(10,8,12),YVALS(8,12),
1 ZVALS(10,8,12)
COMMON/MAPS/XVALS,YVALS,ZVALS,IX(12),JY(12),NX(12),NY(12)
COMMON/AZ/SC/BZ/MN/CZ/AI
DEFINE ISF('635)
LOGICAL SENSW,LERR
C*****DETERMINE MAP NUMBERS AS USED IN MAIN PROGRAM
1 TYPE 2
2 FORMAT(/3X,60HDEPRESS SENSE SWITCHES TO SELECT CONFIGURATION. THE
1 N R-S-R./)
PAUSE
5 IF(SENSW(5)) GO TO 7
IF(SENSW(2)) GO TO 8
N1=1
N2=8
GO TO 10
7 N1=3
N2=6
GO TO 10
8 N2=10
IF(SENSW(7)) GO TO 9
N1=1
GO TO 10
9 N1=3
10 NMP=N2-N1+1
ISF=0
TYPE 13
13 FORMAT(/3X,63HPLACE DATA TAPE FOR DIGITAL COEFFICIENTS IN HSPTR.
1 THEN R-S-R./)
PAUSE 1
READ (4,14)NSC
14 FORMAT(I4)
READ (4,15)(SC(I),I=1,NSC)
15 FORMAT(5S8)
TYPE 16
16 FORMAT(/3X,65HPLACE DATA TAPE FOR DAC INITIAL CONDITIONS IN HSPTR.
1 THEN R-S-R./)
PAUSE 2
READ (4,15)(AI(I),I=1,24)
C*****INITIALIZE FOR READING MAP DATA
NCV=8
NPT=8
NTBL=NCV*(2*NPT+1)
TYPE 17,N1,N2
17 FORMAT(/3X,30HPLACE DATA TAPES FOR MAPS NO. ,I2,IH-,I2,I0H IN HSPT

```



```

1R./)
TYPE 18
18 FORMAT(/3X,42HDEPRESS SSW(A) FOR DATA LIST. THEN R-S-R./)
DO 26 N=N1,N2
PAUSE 3
READ (4,19)XSC,YSC,ZSC
19 FORMAT(3F9.2)
C*****READ Y VALUES
READ (4,20)(VALS(I),I=1,NCV)
20 FORMAT(8F9.3)
J=NCV+1
C*****READ X,Z PAIRS
READ (4,21)(VALS(I),I=J,NTBL)
21 FORMAT(8F9.4)
C*****SCALE MAP VALUES
DO 22 J=1,NCV
DO 22 I=1,NPT
IF(VALS(J).EQ.YSC) GO TO 30
YVALS(J,N)=VALS(J)/YSC
GO TO 31
30 YVALS(J,N)=.99999S
31 KX=NCV+2*((J-1)*NPT+I)-1
IF(VALS(KX).EQ.XSC) GO TO 32
XVALS(I,J,N)=VALS(KX)/XSC
GO TO 33
32 XVALS(I,J,N)=.99999S
33 IF(VALS(KX+1).EQ.ZSC) GO TO 34
ZVALS(I,J,N)=VALS(KX+1)/ZSC
GO TO 22
34 ZVALS(I,J,N)=.99999S
22 CONTINUE
C*****TEST FOR SCALED FRACTION OVERFLOW
IF(.NOT.LERR(13)) GO TO 24
TYPE 23
23 FORMAT(24HSCALED FRACTION OVERFLOW)
PAUSE 4
ISF=0
24 IX(N)=1
JY(N)=1
NX(N)=NPT
NY(N)=NCV
IF(.NOT.SENSW(1)) GO TO 26
TYPE 25,(YVALS(J,N),J=1,NCV)
25 FORMAT(8S7)
DO 26 J=1,NCV
TYPE 25,(XVALS(I,J,N),ZVALS(I,J,N),I=1,NPT)
26 CONTINUE
TYPE 27
27 FORMAT(/3X,15HDATA IS LOADED./)
PAUSE 5
END

```

GENERALIZED TURBOJET OR TURBOFAN ENGINE SIMULATION

C*****ADC VARIABLES

SCALED FRACTION P21,T21,P22,T22,P3,T3,P4,T4,P5,T5,P6,T6,
1 P35,T35,P32,T32,P7,T7,PCNT1,PCNT2,AN2,P2,AN1,WDF

C*****DAC VARIABLES

SCALED FRACTION T21DN,DW21,T22DN,DW22,T35DN,DW35,T32DN,DW32,
1 T3DN,DW3,T4DN,DW4,T5DN,DW5,T6DN,DW6,T7DN,DW7,DTQT1,DTQT2,
2 PRC,FPC,TAUT,XDAC

SCALED FRACTION ABL5,T2,P8,SC(125),PCNF1,PCNF2,PCNC,T21S,
1 T3S,T5S,T6S,T35S,T7S,CP21,GM21,CV21,CP35,CV35,GM35,CP3,CV3,
2 GM3,FG3,WDBL1,WDBL2,WDOVB,PSN4,F2N4,F1N4,WDBLC,WDB,
3 FAR4,CP4,CV4,GM4,WDF1,TRQF1,WDC,TRQC,WDT1,TRQT1,FAR5,
4 CP5,CV5,GM5,WDT2,TRQT2,FAR6,CP6,CV6,GM6,PSN1,F2N1,F1N1,
5 WDN1,WDF2,H3,H3S,H21,H21S,H4,H4S,H21P,H3P,H5P,H6P,H5,
6 TRQF2,PSN2,F2N2,F1N2,WDN2,WDN4,FAR7,CP7,CV7,GM7,WDF1,TRQFT,
7 PSN3,F2N3,F1N3,WDN3,TAB,CPAB,GMAB,CVAB,PRF1,FPF1,PRF2,FPF2,
8 PRF1S,AI(24),XVALS(10,8,12),YVALS(8,12),ZVALS(10,8,12),SSQRT

SCALED FRACTION PSBL,F2BL,F1BL,AN4,ABLC,TAUN1,TAUN4,
1 TAUN2,TAUN3,T32S,T22S,CP22,CV22,GM22,CP32,CV32,GM32,WDV2,
2 WDV3,WDOUB,TRF1,H5S,H6,H6S,H32,H32S,H35,H35S,H7,H7S,
3 H22,H22S,HAB,HABS,T2S,CP2,CV2,GM2,H2S,H2,H32P,AN3,WDBLS
COMMON/MAFS/XVALS,YVALS,ZVALS,IX(12),JY(12),NX(12),NY(12)
COMMON/AZ/SC/BZ/MN/CZ/AI

DEFINE ISF('635)

LOGICAL SENSW,LERR,HBPR,MIX,STRM3,TURBJ1,TURBJ2,SUPER,SPLIT

C*****INITIALIZE ANALOG

CALL QSHYIN(IERR,680)
CALL QSRUN(IERR)
CALL QSSECN(IERR)

C*****ESTABLISH CONFIGURATION

TYPE 17

17 FORMAT(/3X,60HDEPRESS SENSE SWITCHES TO SELECT CONFIGURATION. THE
IN R-S-R./)

PAUSE

IF(SENSW(2)) GO TO 1

HBPR=.FALSE.

CALL QWCLL(2,.FALSE.,IERR)

GO TO 2

1 HBPR=.TRUE.

CALL QWCLL(2,.TRUE.,IERR)

2 IF(SENSW(3)) GO TO 3

MIX=.FALSE.

CALL QWCLL(3,.FALSE.,IERR)

GO TO 4

3 MIX=.TRUE.

CALL QWCLL(3,.TRUE.,IERR)

4 IF(SENSW(4)) GO TO 5

STRM3=.FALSE.

CALL QWCLL(4,.FALSE.,IERR)

GO TO 6

5 STRM3=.TRUE.

CALL QWCLL(4,.TRUE.,IERR)

6 IF(SENSW(5)) GO TO 7

TURBJ1=.FALSE.

CALL QWCLL(5,.FALSE.,IERR)

```

GO TO 8
7 TURBJ1=.TRUE.
CALL QWCLL(5,.TRUE.,IERR)
8 IF(SENSW(6)) GO TO 9
TURBJ2=.FALSE.
CALL QWCLL(6,.FALSE.,IERR)
GO TO 10
9 TURBJ2=.TRUE.
CALL QWCLL(6,.TRUE.,IERR)
10 IF(SENSW(7)) GO TO 11
SUPER=.FALSE.
CALL QWCLL(7,.FALSE.,IERR)
GO TO 12
11 SUPER=.TRUE.
CALL QWCLL(7,.TRUE.,IERR)
12 IF(SENSW(8)) GO TO 13
SPLIT=.FALSE.
GO TO 14
13 SPLIT=.TRUE.
C*****STOP PROGRAM IF CONFIGURATION SPECIFIED IS NOT ALLOWED
14 IF(TURBJ1.AND.TURBJ2) STOP1
IF((TURBJ1.OR.TURBJ2).AND.(HBPR.OR.MIX.OR.STRM3.OR.SUPER.OR.
1 SPLIT)) STOP2
IF(.NOT.HBPR.AND.(STRM3.OR.SUPER.OR.SPLIT)) STOP3
IF(STRM3.AND.SUPER) STOP4
C*****INITIALIZE REQUIRED INPUT/OUTPUT
PB=SC(103)
T2=SC(1)
TAUN1=.00000S
TAUN2=.00000S
TAUN3=.00000S
TAUN4=.00000S
WDF1=.00000S
WDF2=.00000S
WDN1=.00000S
WDN2=.00000S
WDN3=.00000S
WDN4=.00000S
AN4=SC(85)
AN3=SC(102)
ABLC=SC(86)
ABLS=SC(32)
WDV2=.00000S
WDV3=.00000S
TRQF2=.00000S
TRQF1=.00000S
TRQT2=.00000S
WDBLC=.00000S
WDBLS=.00000S
15 CALL QWBDAS(AI,0,24,IERR)
20 CALL QSTDA
30 CALL QSIC(IERR)
ISF=0
TYPE 35
35 FORMAT(/3X,44HPROCEED TO DYNAMIC PART OF PROGRAM BY R-S-R./)
PAUSE
40 CALL QRBADS(P21,0,24,IERR)
42 PCNF1=SC(4)*PCNT2

```

```

PCNF2=SC(5)*PCNT2
PCNC=PCNT1
T2S=.20000S*T2
T22S=.20000S*T22
T32S=.20000S*T32
T35S=.20000S*T35
T3S=.40000S*T3
T5S=.80000S*T5
T6S=.50000S*T6
T7S=.50000S*T7
CALL PROCOM(T2S,.00000S,CP2,CV2,GM2,H2S)
H2=H2S/.33333S
CALL PROCOM(T3S,.00000S,CP3,CV3,GM3,H3S)
H3=H3S/.66667S
FG3=.44208S+.34674S*GM3
WDBL1=((SC(6)*FG3*P3)/SSQRT(T3))/.50000S
WDBL2=((SC(7)*FG3*P3)/SSQRT(T3))/.50000S
WDOVB=((SC(8)*FG3*P3)/SSQRT(T3))/.50000S
45 IF(.NOT.SUPER) GO TO 55
PRF1S=(SC(67)*P21)/P2
CALL TRAT(PRF1S,.70000S,TRF1)
T21=((.25000S*TRF1/SC(90)+.20000S)*T2)/.20000S
55 T21S=.20000S*T21
CALL PROCOM(T21S,.00000S,CP21,CV21,GM21,H21S)
H21=H21S/.33333S
IF(TURBJ1) GO TO 90
CALL WOZZL(P21,P8,SC(9),F1BL,F2BL,PSBL)
WDBLC=((P21*F1BL*ABLC)/SSQRT(T21))/SC(10)
90 WDB=(SSQRT(P3-P4))/SC(11)
FAR4=(SC(12)*WDF)/WDB
CALL PROCOM(T4,FAR4,CP4,CV4,GM4,H4S)
H4=H4S*.60000S
MN=1
IF(TURBJ1.OR.SUPER) MN=3
IF(MN.EQ.3) GO TO 95
CALL FNCMP(1,P2,T2,H2,P21,T21,PCNF1,WDF1,H21P,TRQF1,PRF1,FPF1)
MN=MN+1
95 CALL FNCMP(2,P21,T21,H21,P3,T3,PCNC,WDC,H3P,TRQC,PRC,FPC)
IF(.NOT.HBPR) GO TO 96
IF(ABLS.LE..00001S) GO TO 96
WDBLS=(ABLS*SSQRT(P21-SC(98)*P32))/SC(99)
96 IF(.NOT.SUPER) GO TO 97
WDF1=WDC*SC(47)+WDBLC*SC(49)+WDBLS*SC(101)
TRQF1=((H21-H2)/SC(91))*WDF1/PCNF1
97 MN=MN+1
XDAC=WDF1
CALL TURB(1,P4,T4,H4,P5,PCNT1,WDT1,H5P,TRQT1)
MN=MN+1
FAR5=(FAR4*.50000S)/(.50000S+(.50000S+.02500S*FAR4)*SC(13))*
1 WDBL1/WDT1)
CALL PROCOM(T5S,FAR5,CP5,CV5,GM5,H5S)
H5=H5S*.75000S
IF(.NOT.TURBJ1) GO TO 100
T6=T5/.62500S
T6S=.50000S*T6
FAR6=FAR5
P6=P5
GO TO 110

```

```

100 CALL TURB(2,P5,T5,H5,P6,PCNT2,WDT2,H6P,TRQT2)
    MN=MN+1
    FAR6=(FAR5*.50000S)/(.50000S+(.50000S+.02500S*FAR5)*SC(14)*
1 WDBL2/WDT2)
110 CALL PROCOM(T6S,FAR6,CP6,CV6,GM6,H6S)
    H6=H6S/.53333S
    CALL NOZZL(P6,P7,SC(15),FIN1,F2N1,PSN1)
    WDN1=((P6*FIN1*AN1)/SSQRT(T6))/SC(16)
140 IF(.NOT.HBPR) GO TO 215
    CALL PROCOM(T32S,.00000S,CP32,CV32,GM32,H32S)
    H32=H32S/.33333S
    CALL PROCOM(T35S,.00000S,CP35,CV35,GM35,H35S)
    H35=H35S/.33333S
    CALL FNCMP(3,P2,T2,H2,P32,T32,PCNF2,WDF2,H32P,TRQF2,PRF2,FPF2)
    IF(.NOT.SPLIT) GO TO 150
    WDF2=WDF2
    TRQF2=TRQF2
    WDF2=(WDF2-SC(59)*WDF1)/SC(60)
    TRQF2=(SC(60)*TRQF2*WDF2/WDF1)/SC(87)
150 XDAC=WDF2
    CALL NOZZL(P35,P7,SC(17),FIN2,F2N2,PSN2)
    WDN2=((P35*FIN2*AN2)/SSQRT(T35))/SC(18)
190 WDV3=(SSQRT(P32-P35))/SC(88)
193 DW32=WDF2-WDV3+WDBLS*SC(100)
    T32DN=(H32P*WDF2-H32*WDV3+H21*WDBLS*SC(100))/CV32-T32*DW32
    DW35=WDV3-WDN2
    T35DN=(H32*WDV3-H35*WDN2)/CV35-T35*DW35
    IF(MIX) GO TO 200
    TAUN1=(WDN1*F2N1*SSQRT(CP6*T6))/SC(37)+(AN1*(PSN1-SC(15)*
1 P7))/SC(38)
    TAUN2=(WDN2*F2N2*SSQRT(CP35*T35))/SC(19)+(AN2*(PSN2-SC(17)*
1 P7))/SC(20)
    IF(STRM3) GO TO 210
    TAUT=SC(24)*TAUN1+SC(52)*TAUN2
    GO TO 228
200 FAR7=(FAR6*.50000S)/(.50000S+(.50000S+.02500S*FAR6)/(SC(27)*
1 WDN1/WDN2))
    CALL PROCOM(T7S,FAR7,CP7,CV7,GM7,H7S)
    H7=H7S/.53333S
    CALL NOZZL(P7,P8,SC(28),FIN3,F2N3,PSN3)
    WDN3=((P7*FIN3*AN3)/SSQRT(T7))/SC(29)
    TAUN3=(WDN3*F2N3*SSQRT(CP7*T7))/SC(30)+(AN3*(PSN3-SC(28)*
1 P8))/SC(31)
206 DW7=-WDN3+SC(34)*WDN1+SC(35)*WDN2
    T7DN=(.40000S*SC(35)*H35*WDN2+SC(34)*H6*WDN1-H7*WDN3)
1 /CV7-T7*DW7
    IF(STRM3) GO TO 210
    TAUT=TAUN3
    GO TO 228
210 CALL NOZZL(P22,P8,SC(9),FIN4,F2N4,PSN4)
211 CALL PROCOM(T22S,.00000S,CP22,CV22,GM22,H22S)
    H22=H22S/.33333S
    WDN4=((P22*FIN4*AN4)/SSQRT(T22))/SC(21)
    WDV2=(SSQRT(P21-P22))/SC(89)
    DW22=WDV2-WDN4
    T22DN=(H21*WDV2-H22*WDN4)/CV22-T22*DW22
    IF(.NOT.HBPR) GO TO 219
    TAUN4=(WDN4*F2N4*SSQRT(CP22*T22))/SC(22)+(AN4*(PSN4-SC(9)*

```

```

1 P8))/SC(23)
IF(MIX) GO TO 212
TAUT=SC(24)*TAUN1+SC(25)*TAUN2+SC(26)*TAUN4
GO TO 227
212 TAUT=SC(36)*TAUN3+SC(26)*TAUN4
GO TO 227
215 IF(TURBJ1.OR.TURBJ2) GO TO 220
CALL NOZZL(P22,P7,SC(3),FIN4,F2N4,PSN4)
GO TO 211
219 IF(MIX) GO TO 222
TAUN4=(WDN4*F2N4*SSQRT(CP22*T22))/SC(22)+(AN4*(PSN4-SC(3)*
1 P7))/SC(23)
220 TAUN1=(WDN1*F2N1*SSQRT(CP6*T6))/SC(37)+(AN1*(PSN1-SC(15)*
1 P7))/SC(38)
TAUT=SC(24)*TAUN1+SC(26)*TAUN4
GO TO 227
222 FAR7=(FAR6*.50000S)/(.50000S+(.50000S+.025000S*FAR6)/(SC(2)*
1 WDN1/WDN4))
CALL PROCOM(T7S,FAR7,CP7,CV7,GM7,H7S)
H7=H7S/.83333S
CALL NOZZL(P7,P8,SC(28),FIN3,F2N3,PSN3)
WDN3=((P7*FIN3*AN3)/SSQRT(T7))/SC(29)
TAUN3=(WDN3*F2N3*SSQRT(CP7*T7))/SC(30)+(AN3*(PSN3-SC(28)*
1 P8))/SC(31)
DW7=-WDN3+SC(34)*WDN1+SC(33)*WDN4
T7DN=(.40000S*SC(33)*H22*WDN4+SC(34)*H6*WDN1-H7*WDN3)/CV7-T7*DW7
TAUT=TAUN3
227 IF(TURBJ1) GO TO 230
IF(TURBJ2) GO TO 228
WDOUT=SC(48)*WDV2
GO TO 229
228 WDOUT=.00000S
229 IF(SUPER) GO TO 230
DW21=WDF1-SC(47)*WDC-WDOUT-SC(49)*WDBLC-SC(101)*WDBLS
T21DN=(H21P*WDF1-H21*(SC(47)*WDC+WDOUT+SC(49)*WDBLC+SC(101)*
1 WDBLS))/CV21-T21*DW21
230 DW3=WDC-WDB-SC(39)*WDBL1-SC(40)*WDBL2-SC(41)*WDOVB
T3DN=(H3P*WDC-H3*(WDB+SC(39)*WDBL1+SC(40)*WDBL2+SC(41)
1 *WDOVB))/CV3-T3*DW3
TAB=(.40000S*T3-T4)*SC(42)+T4
CALL PROCOM(TAB,.00000S,CPAB,CVAB,GMAB,HABS)
HAB=HABS*.60000S
DW4=WDB-WDT1+SC(44)*WDF
T4DN=(HAB*WDB+SC(43)*WDF-H4*WDT1)/CV4-T4*DW4
IF(TURBJ1) WDT2=WDN1
DW5=WDT1-WDT2+SC(39)*WDBL1
T5DN=(H5P*WDT1+SC(45)*H3*WDBL1-H5*WDT2)/CV5-T5*DW5
IF(TURBJ1) GO TO 235
DW6=WDT2-WDN1+SC(40)*WDBL2
T6DN=(H6P*WDT2+SC(46)*H3*WDBL2-H6*WDN1)/CV6-T6*DW6
235 DTQT1=TRQT1-TRQC
DTQT2=TRQT2-SC(50)*TRQF1-SC(51)*TRQF2
C*****TEST FOR SCALED FRACTION OVERFLOW
IF(.NOT.LERR(13)) GO TO 250
C*****TEST FOR OPERATE MODE
CALL GRAMI(MODE)
IF(MODE.EQ.4) CALL QSH(IERR)
TYPE 240

```

```

240 FORMAT(24HSCALED FRACTION OVERFLOW)
    PAUSE
    ISF=0
    IF(MODE.EQ.4) CALL QSOP(IERR)
250 IF(.NOT.SENSW(1)) GO TO 370
C*****TYPE CURRENT VALUES
C*****TEST FOR OPERATE MODE
    CALL QRAMI(MODE)
    IF(MODE.EQ.4) CALL QSH(IERR)
260 TYPE 270
270 FORMAT(5X,43H WDF1      WDC      WDB      WDT1      WDT2 )
    TYPE 280,WDF1,WDC,WDB,WDT1,WDT2
280 FORMAT(3X,5(S7,2X)/)
    TYPE 290
290 FORMAT(5X,43H WDN1      WDN2      WDN3      WDN4      WDF2 )
    TYPE 280,WDN1,WDN2,WDN3,WDN4,WDF2
    TYPE 300
300 FORMAT(5X,43H P2      P21      P35      P3      P4 )
    TYPE 280,P2,P21,P35,P3,P4
    TYPE 310
310 FORMAT(5X,43H P5      P6      P7      P22      P32 )
    TYPE 280,P5,P6,P7,P22,P32
    TYPE 320
320 FORMAT(5X,43H T35      T3      T4      T5      T6 )
    TYPE 280,T35,T3,T4,T5,T6
    TYPE 330
330 FORMAT(5X,43H T7      T2      T21      TAUN1      TAUN2)
    TYPE 280,T7,T2,T21,TAUN1,TAUN2
    TYPE 340
340 FORMAT(5X,43H TAUN3      WDF      PCNT1      PCNT2      PCNF1)
    TYPE 280,TAUN3,WDF,PCNT1,PCNT2,PCNF1
    TYPE 350
350 FORMAT(5X,43H PCNF2      PCNC      AN1      AN2      AN3 )
    TYPE 280,PCNF2,PCNC,AN1,AN2,AN3
    TYPE 360
360 FORMAT(5X,43H AN4      ABLC      ABLS      TAUNA      TAUT )
    TYPE 280,AN4,ABLC,ABLS,TAUNA,TAUT
    IF(MODE.EQ.4) CALL QSOP(IERR)
C*****OUTPUT TO ANALOG AND RETURN
370 CALL QWBDA(T21DN,0,24,IERR)
    CALL QSTDA
    GO TO 40
    END

```

GENERALIZED FAN AND COMPRESSOR SUBROUTINE VERSION II

```

SUBROUTINE FNCMP(N,PIN,TIN,HIN,POUT,TOUT,SPD,FLO,HOUTP,TORQ,PR,FP)
    SCALED FRACTION PIN,TIN,POUT,TOUT,SPD,FLO,TOUTP,CPOUT,
1  CVOUT,GMOUT,TORQ,PR,FP,K,ITERM,SSQRT,NP,MAPFUN,TAV,CP,
2  CV,GM,TR,FOOTS,TINS,SC(125),XVALS(10,8,12),YVALS(8,12),
3  ZVALS(10,8,12),EFF,HIN,HOUTP,HS,HOUTS,KH,PRS
    COMMON/MAFS/XVALS,YVALS,ZVALS,IX(12),JY(12),NX(12),NY(12)
    COMMON/AZ/SC/BZ/MN
    PR=(SC(N+66)*POUT)/PIN+SC(N+91)
    ITERM=.70711S*SSQRT(SC(N+69)*TIN)

```

```

NP=(.50000S*SPD)/TTERM
FP=MAPFUN(MN,PR,NP)
MN=MN+1
EFF=MAPFUN(MN,PR,NP)
FLO=(SC(N+72)*FP*PIN)/TTERM
IF(N.EQ.2) GO TO 100
K=.20000S
KH=.33333S
TINS=TIN
GO TO 200
100 K=.40000S
KH=.66667S
TINS=.50000S*TIN
200 TAV=K*(TOUT+SC(N+75)*(TINS-TOUT))
CALL PROCOM(TAV,.00000S,CP,CV,GM,HS)
PRS=(SC(N+78)*POUT)/PIN
CALL TRAT(PRS,GM,TR)
TOUTP=((SC(N+94)*TR/EFF+.20000S)*TINS)/.20000S
TOUTS=K*TOUTP
CALL PROCOM(TOUTS,.00000S,CPOUT,CVOUT,GMOUT,HOUTS)
TORQ=((FLO*(HOUTS-.33333S*HIN))/SPD)/SC(N+81)
HOUTP=HOUTS/KH
RETURN
END

```

GENERALIZED TURBINE SUBROUTINE VERSION II

```

SUBROUTINE TURB(N,PIN,TIN,HIN,POUT,SPD,FLO,HOUTP,TORQ)
SCALED FRACTION PIN,TIN,HIN,POUT,SPD,FLO,HOUTP,TORQ,PR,FP,HP,KI,
1 TTERM,SSQRT,NP,MAPFUN,DHT,SC(125),XVALS(10,8,12),YVALS(8,12),
2 ZVALS(10,8,12)
COMMON/MAPS/XVALS,YVALS,ZVALS,IX(12),JY(12),NX(12),NY(12)
COMMON/AZ/SC/BZ/MN
TTERM=SSQRT(TIN)
PR=(SC(N+52)*POUT)/PIN
NP=(SC(N+54)*SPD)/TTERM/.50000S
FP=MAPFUN(MN,PR,NP)
MN=MN+1
HP=MAPFUN(MN,PR,NP)
FLO=((FP*PIN*SPD)/TIN)/SC(N+56)
IF(N.NE.1) GO TO 100
KI=.80000S
GO TO 200
100 KI=.62500S
200 DHT=(HP*SPD*TTERM)/SC(N+60)
HOUTP=(HIN-SC(N+62)*DHT)/KI
TORQ=((SC(N+64)*DHT*FLO)/SPD)/.50000S
RETURN
END

```


GENERALIZED CONVERGENT NOZZLE SUBROUTINE VERSION II

```

SUBROUTINE NOZZL(PIN,POUT,A,F1,F2,PS)
SCALED FRACTION PIN,POUT,A,F1,F2,PS,PR
INTEGER ERRFLG
PR=(A*POUT)/PIN
IF(PR.LE..53685S) GO TO 1#
PS=A*POUT
GO TO 2#
1# PR=.53685S
PS=PR*PIN
2# CALL NRMPN(PR,PRN,ERRFLG)
IF(ERRFLG.NE.1) GO TO 3#
CALL CLCFN(PRN,F2)
CALL CLCWN(F1)
GO TO 5#
3# TYPE 4#
4# FORMAT(26HNOZZLE INPUTS OUT OF RANGE)
5# RETURN
END

```

PROCOM - CP, CV, GAMMA, & H CALCULATIONS

```

SUBROUTINE PROCOM(T,FA,CP,CV,GAM,H)
SCALED FRACTION T,FA,CP,CV,GAM,H,CPA,HA,AMW,R,TD,CPF,HF
IF(T.GE..46000S) GO TO 5#
IF(T.GE..24000S) GO TO 4#
CPA=.48068S-(.12464S-T/.98246S)*T
HA=.00176S+(.56558S+.14075S*T)*T
GO TO 6#
4# CPA=.40528S+(.52545S-.38182S*T)*T
HA=.00119S+(.56298S+.16150S*T)*T
GO TO 6#
5# CPA=.46063S+(.30024S-.15378S*T)*T
HA=-.01870S+(.64968S+.06700S*T)*T
6# AMW=.57940S-.00090S*FA
R=.07945S/AMW
TD=.70000S-T
CPF=.93330S-(.29350S+.81750S*TD)*TD
HF=-.03305S+(.63624S+.38625S*T)*T
H=(.66667S*HA+.06667S*HF*FA)/(.50000S+.02500S*FA)
CP=(.80000S*CPA+.08000S*CPF*FA)/(.80000S+.04000S*FA)
CV=CP-R
GAM=.50000S*CP/CV
RETURN
END

```

C*****TWO-SPOOL ENGINE ISENTROPIC TEMP RATIO CALCULATIONS

```

SUBROUTINE TRAT(PRC,GAM,TR)
SCALED FRACTION GAM,TR,PRC,S,C,TRC
INTEGER ERRFLG
REAL XN
150 IF(GAM.GE..67500S) GO TO 300
   IF(PRC.GE..33333S) GO TO 200
   S=.50526S+.77229S*PRC-.95164S*PRC*PRC
   GO TO 700
200 S=.58745S+.23850S*PRC-.09000S*PRC*PRC
   GO TO 700
300 IF(PRC.GE..33333S) GO TO 400
   S=.45911S+.89475S*PRC-(PRC*PRC)/.92895S
   GO TO 700
400 S=.55215S+.29319S*PRC-.10919S*PRC*PRC
700 C=((.67500S-GAM)*S)/.02500S
   CALL NMXTR(PRC,XN,ERRFLG)
   IF(ERRFLG.NE.1) GO TO 800
   CALL CLCTR(XN,TRC)
   GO TO 900
800 TYPE 850
850 FORMAT(24HTRAT INPUTS OUT OF RANGE)
   GO TO 1000
900 TR=(TRC*(.80000S-.16000S*C))/.80000S
1000 RETURN
END

```

NOZZLE PRESSURE RATIO NORMALIZATION

```

SUBROUTINE NRMPN
SCALED FRACTION BRKPT(14)
DATA BRKPT(1),BRKPT(2),BRKPT(3),BRKPT(4),BRKPT(5),
1 BRKPT(6),BRKPT(7),BRKPT(8),BRKPT(9),BRKPT(10),
2 BRKPT(11),BRKPT(12),BRKPT(13),BRKPT(14)/.00000S,
3 .10000S,.20000S,.30000S,.40000S,.50000S,.53685S,
4 .60000S,.70000S,.80000S,.85000S,.90000S,.95000S,
5 .99999S/
CALL VBNS(BRKPT(1),BRKPT(14),BRKPT(6))
RETURN
END

```

NOZZLE THRUST-VELOCITY CALCULATION,GAMMA=1.35

```

SUBROUTINE CLCFN
SCALED FRACTION T(14)
DATA T(1),T(2),T(3),T(4),T(5),T(6),T(7),T(8),T(9),
1 T(10),T(11),T(12),T(13),T(14)/.99999S,.67046S,.58408S,
2 .51780S,.45983S,.40557S,.38592S,.35219S,.29719S,
3 .23709S,.20312S,.16415S,.11494S,.00000S/
CALL FNGN1(T(1))

```

RETURN
END

NOZZLE FLOW CALCULATION AT GAMMA=1.35

```
SUBROUTINE CLCWN
SCALED FRACTION G(14)
DATA G(1),G(2),G(3),G(4),G(5),G(6),G(7),G(8),G(9),
1 G(10),G(11),G(12),G(13),G(14)/.67614S,.67614S,
2 .67614S,.67614S,.67614S,.67614S,.67614S,.67614S,
3 .63379S,.55818S,.50018S,.42169S,.30732S,.00000S/
CALL FNLK1(G(1))
RETURN
END
```

ISENTROPIC PRESSURE RATIO NORMALIZATION

```
SUBROUTINE NMXTR
SCALED FRACTION XLOLIM,XHILIM,XINTVL
DATA XLOLIM,XHILIM,XINTVL/.06667S,.99380S,.06667S/
CALL CBNS(XLOLIM,XHILIM,XINTVL)
RETURN
END
```

ISENTROPIC TEMPERATURE RATIO CALCULATION

```
SUBROUTINE CLCTR
SCALED FRACTION T(140)
DATA T(1),T(2),T(3)/.00000S,.02001S,.03872S/
DATA T(4),T(5),T(6)/.05631S,.07292S,.08868S/
DATA T(7),T(8),T(9)/.10367S,.11799S,.13169S/
DATA T(10),T(11),T(12)/.14484S,.15749S,.16967S/
DATA T(13),T(14),T(15)/.18144S,.19282S,.20384S/
DATA T(16),T(17),T(18)/.21452S,.22489S,.23496S/
DATA T(19),T(20),T(21)/.24477S,.25432S,.26362S/
DATA T(22),T(23),T(24)/.27270S,.28157S,.29023S/
DATA T(25),T(26),T(27)/.29870S,.30699S,.31511S/
DATA T(28),T(29),T(30)/.32306S,.33085S,.33849S/
DATA T(31),T(32),T(33)/.34599S,.35335S,.36057S/
DATA T(34),T(35),T(36)/.36768S,.37466S,.38152S/
DATA T(37),T(38),T(39)/.38827S,.39492S,.40146S/
DATA T(40),T(41),T(42)/.40790S,.41424S,.42049S/
DATA T(43),T(44),T(45)/.42665S,.43272S,.43871S/
DATA T(46),T(47),T(48)/.44462S,.45045S,.45620S/
DATA T(49),T(50),T(51)/.46187S,.46748S,.47301S/
DATA T(52),T(53),T(54)/.47848S,.48388S,.48922S/
DATA T(55),T(56),T(57)/.49449S,.49971S,.50486S/
DATA T(58),T(59),T(60)/.50996S,.51500S,.51999S/
```

```

DATA T(61),T(62),T(63)/.52492S,.52980S,.53463S/
DATA T(64),T(65),T(66)/.53941S,.54414S,.54883S/
DATA T(67),T(68),T(69)/.55347S,.55807S,.56262S/
DATA T(70),T(71),T(72)/.56712S,.57159S,.57601S/
DATA T(73),T(74),T(75)/.58040S,.58474S,.58905S/
DATA T(76),T(77),T(78)/.59332S,.59775S,.60174S/
DATA T(79),T(80),T(81)/.60590S,.61003S,.61412S/
DATA T(82),T(83),T(84)/.61818S,.62220S,.62619S/
DATA T(85),T(86),T(87)/.63015S,.63408S,.63798S/
DATA T(88),T(89),T(90)/.64185S,.64569S,.64950S/
DATA T(91),T(92),T(93)/.65328S,.65703S,.66076S/
DATA T(94),T(95),T(96)/.66446S,.66813S,.67178S/
DATA T(97),T(98),T(99)/.67540S,.67900S,.68257S/
DATA T(100),T(101),T(102)/.68612S,.68964S,.69314S/
DATA T(103),T(104),T(105)/.69661S,.70007S,.70350S/
DATA T(106),T(107),T(108)/.70690S,.71029S,.71366S/
DATA T(109),T(110),T(111)/.71700S,.72032S,.72362S/
DATA T(112),T(113),T(114)/.72691S,.73017S,.73341S/
DATA T(115),T(116),T(117)/.73663S,.73983S,.74302S/
DATA T(118),T(119),T(120)/.74618S,.74933S,.75246S/
DATA T(121),T(122),T(123)/.75557S,.75866S,.76174S/
DATA T(124),T(125),T(126)/.76480S,.76784S,.77087S/
DATA T(127),T(128),T(129)/.77388S,.77687S,.77984S/
DATA T(130),T(131),T(132)/.78280S,.78575S,.78868S/
DATA T(133),T(134),T(135)/.79159S,.79449S,.79737S/
DATA T(136),T(137),T(138)/.80024S,.80309S,.80593S/
DATA T(139),T(140)/.80876S,.81157S/
CALL FNGN1(T(1))
RETURN
END

```

SCALED FRACTION MAPFUN (10,8,12)

```

SCALED FRACTION FUNCTION MAPFUN(N,XIN,YIN)
SCALED FRACTION XIN,YIN,YINCR,XHI,XLO,XFRAC,ZL,ZR,Y1,Y2,
I MAPFUN,XVALS(10,8,12),YVALS(8,12),ZVALS(10,8,12)
COMMON/MAPS/XVALS,YVALS,ZVALS,IX(12),JY(12),NX(12),NY(12)
NYC=NY(N)
NXP=NX(N)
I=IX(N)
J=JY(N)
100 Y1=YIN-YVALS(J,N)
IF(Y1.GT..00000S) GO TO 110
IF(Y1.EQ..00000S) GO TO 120
IF(J.LE.1) GO TO 500
J=J-1
GO TO 100
110 Y2=YIN-YVALS(J+1,N)
IF(Y2.LT..00000S) GO TO 140
IF(Y2.EQ..00000S) GO TO 130
J=J+1
IF(J.GE.NYC) GO TO 500
Y1=Y2
GO TO 110
120 YINCR=.00000S

```

```

      GO TO 200
130 YINCR=.99999S
      GO TO 200
140 YINCR=YI/(Y1-Y2)
200 XLO=XVALS(I,J,N)+YINCR*(XVALS(I,J+1,N)-XVALS(I,J,N))
      IF(XIN.GT.XLO) GO TO 220
      IF(XIN.EQ.XLO) GO TO 230
      IF(I.LE.1) GO TO 500
      I=I-1
      GO TO 200
220 XHI=XVALS(I+1,J,N)+YINCR*(XVALS(I+1,J+1,N)-XVALS(I+1,J,N))
      IF(XIN.LT.XHI) GO TO 300
      I=I+1
      IF(XIN.EQ.XHI) GO TO 230
      IF(I.GE.NXP) GO TO 500
      XLO=XHI
      GO TO 220
230 MAPFUN=ZVALS(I,J,N)+YINCR*(ZVALS(I,J+1,N)-ZVALS(I,J,N))
      GO TO 400
300 ZR=ZVALS(I+1,J,N)+YINCR*(ZVALS(I+1,J+1,N)-ZVALS(I+1,J,N))
      ZL=ZVALS(I,J,N)+YINCR*(ZVALS(I,J+1,N)-ZVALS(I,J,N))
      XFRAC=(XIN-XLO)/(XHI-XLO)
      MAPFUN=ZL+XFRAC*(ZR-ZL)
400 IX(N)=I
      JY(N)=J
      RETURN
500 CALL MOOR(N,XIN,YIN)
      RETURN
      END

```

MAP OUT OF RANGE ROUTINE (MOOR)

```

      SUBROUTINE MOOR(N,XIN,YIN)
      SCALED FRACTION XIN,YIN
C.....TEST FOR OPERATE MODE
      CALL QRAMI(ILOC)
      IF(ILOC.EQ.4) CALL QSH(IIERR)
      TYPE 600,N,XIN,YIN
600 FORMAT(/7HMAP NO.,I3,20H INPUTS OUT OF RANGE/6HXIN = ,S7,
! 8H YIN = ,S7/)
      PAUSE
      IF(ILOC.EQ.4) CALL QSOP(IIERR)
      RETURN
      END

```

APPENDIX F

SUMMARY OF SCALED EQUATIONS SOLVED ON ANALOG COMPUTER

$$W_{21} = \int_0^{t'} C(1) * DW_{21} dt' + C(2) \quad (F1)$$

$$T_{21} = \int_0^{t'} C(3) * \frac{T_{21DN}}{W_{21}} dt' + C(4) \quad (F2)$$

$$P_{21} = 10 * C(26) * W_{21} * T_{21} \quad (F3)$$

$$W_3 = \int_0^{t'} 10 * C(11) * DW_3 dt' + C(9) \quad (F4)$$

$$T_3 = \int_0^{t'} 10 * C(12) * \frac{T_{3DN}}{W_3} dt' + C(10) \quad (F5)$$

$$P_3 = 10 * C(34) * W_3 * T_3 \quad (F6)$$

$$W_4 = \int_0^{t'} 10 * C(15) * DW_4 dt' + C(13) \quad (F7)$$

$$T_4 = \int_0^{t'} 10 * C(16) * \frac{T_{4DN}}{W_4} dt' + C(14) \quad (F8)$$

$$P4 = 10 * C(38) * W4 * T4 \quad (F9)$$

$$W5 = \int_0^{t'} 10 * C(19) * DW5 \, dt' + C(17) \quad (F10)$$

$$T5 = \int_0^{t'} 10 * C(20) * \frac{T5DN}{W5} \, dt' + C(18) \quad (F11)$$

$$P5 = 10 * C(41) * W5 * T5 \quad (F12)$$

$$W6 = \int_0^{t'} 10 * C(23) * DW6 \, dt' + C(21) \quad (F13)$$

$$T6 = \int_0^{t'} 10 * C(24) * \frac{T6DN}{W6} \, dt' + C(22) \quad (F14)$$

$$P6 = 10 * C(43) * W6 * T6 \quad (F15)$$

$$W7 = \int_0^{t'} C(33) * DW7 \, dt' + C(35) \quad (F16)$$

$$T7 = \int_0^{t'} C(48) * \frac{T7DN}{W7} \, dt' + C(49) \quad (F17)$$

$$P7 = 10 * C(36) * W7 * T7 \quad (F18)$$

$$W32 = \int_0^{t'} C(29)*DW32 dt' + C(31) \quad (F19)$$

$$T32 = \int_0^{t'} C(46)* \frac{T32DN}{W32} dt' + C(47) \quad (F20)$$

$$P32 = 10 *C(32)*W32*T32 \quad (F21)$$

$$W35 = \int_0^{t'} C(25)*DW35 dt' + C(27) \quad (F22)$$

$$T35 = \int_0^{t'} C(44)* \frac{T35DN}{W35} dt' + C(45) \quad (F23)$$

$$P35 = 10 *C(28)*W35*T35 \quad (F24)$$

$$W22 = \int_0^{t'} C(5)*DW22 dt' + C(6) \quad (F25)$$

$$T22 = \int_0^{t'} C(7)* \frac{T22DN}{W22} dt' + C(8) \quad (F26)$$

$$P22 = 10 *C(30)*W22*T22 \quad (F27)$$

$$PCNT1 = \int_0^{t'} C(37)*DTQT1 dt' + C(39) \quad (F28)$$

$$PCNT2 = \int_0^{t'} C(40) * DTQT2 dt' + C(42) \quad (F29)$$

$$AN1 = C(56) \quad (F30)$$

$$AN2 = C(54) \quad (F31)$$

$$P2 = C(55) \quad (F32)$$

$$WDF = C(57) + \text{Output of controller} \quad (F33)$$

If SUPER="TRUE",

$$P21 = 10 * C(52) * [C(51) + 10 * C(50) * C(53) * PCNT2] \quad (F34)$$

APPENDIX G

COMPUTER LISTING OF TURBINE DATA CONVERSION PROGRAM

```

DIMENSION DHT(10),NRT(5),WRTP(10,9),ETA(10,9),PR(10,9)
DIMENSION PP1(12),WRTP2(12),F1(12),F2(12)
DIMENSION RATIO(10,9),DHT1(10,9),WRTP1(10,9),LWRT(10,9),
1 WTPN(10,9),NRTF1(10,9),NRTF2(10,9),LWRTF2(10,9)
REAL NRT,LWRT,NRTF1,NRTF2,LWRTF2
NAMELIST/HEAT/DHT/SPEED/NRT/FLCW/WRTP/EFF/ETA
NAMELIST/PARAM1/PR1/PARAM2/WRTP2
CP=.28555
GAM=1.3312
READ(5,HEAT)
READ(5,SPEED)
READ(5,FLCW)
READ(5,EFF)
READ(5,PARAM1)
READ(5,PARAM2)
C
C-----PRINT TURBINE DATA TABLE HEADING
C
WRITE(6,100)
100 FORMAT(1H1,50X,18HTURBINE DATA TABLE)
WRITE(6,101)
101 FORMAT(1HK,14X,3HDHT//7X,3HNRT,5X,3HETA/15X,4HWRTP/15X,2HPR)
WRITE(6,102) (DHT(I),I=1,10)
102 FORMAT(1HK,14X,10(F6.4,3X))
C
C-----CALCLATE TURBINE PRESSURE RATIO
C
DO 2 J=1,9
DO 1 I=1,10
DHCF=1./1.61906
ETTCF=.97264
PP(I,J)=(1.-DHT(I)/(CP*ETA(I,J)*DHCF*ETTCF))**(GAM/(GAM-1.))
1 CONTINUE
C
C-----PRINT TURBINE DATA TABLE
C
WRITE(6,103) NRT(J),(ETA(I,J),I=1,10)
103 FORMAT(1HK,6X,F5.1,3X,10(F6.4,3X))
WRITE(6,104) (WRTP(I,J),I=1,10), (PR(I,J),I=1,10)
104 FORMAT(1HJ,14X,10(F6.3,3X)/15X,10(F6.4,3X))
2 CONTINUE
C
C-----PRINT TURBINE PRESSURE RATIO MAP HEADING
C
WRITE(6,105)
105 FORMAT(1H1,45X,26HTURBINE PRESSURE RATIO MAP)
WRITE(6,106)
106 FORMAT(1HK,14X,2HPR//7X,3HNRT,5X,3HDHT/15X,4HWRTP/15X,4HLWRT/15X,
1 4HWTPN/14X,5HNRTF1/13X,6HLWRTF2/14X,5HNRTF2)
WRITE(6,111) (PR1(K),K=1,12)
C
C-----INTERPOLATE TABLE FOR CONSTANT PRESSURE RATIOS

```

```

C
CC 6 J=1,9
CC 5 K=1,12
PF2= PR1(K)
F1(K)= SQRT(1.C-PR2*PF2)
F2(K)= SQRT(1.C- PR1(K) ** ((GAM -1.0) / GAM))
IF((PR1(K).GT. PR(1,J)).OR.(PR1(K).LT.PR(10,J))) GC TC 5
CC 2 I=1,10
IF(PR1(K)-PR(I,J)) 3,4,4
2 CCNTINUE
4 RATIO(K,J)= (PF(I-1,J)-PR1(K))/(PR(I-1,J)-PR(I,J))
DHT1(K,J)= DHT(I-1)+RATIO(K,J)*(DHT(I)-DHT(I-1))
WRTP1(K,J)= WRTP(I-1,J) + RATIO(K,J) * (WRTP(I,J) - WRTP(I-1,J))
LWRT(K,J)= DHT1(K,J) / NRT(J)
WTPN(K,J)= WRTP1(K,J) / NRT(J)
NRTE1(K,J)= NRT(J) / F1(K)
NRTE2(K,J)= NRT(J) / F2(K)
LWRTF2(K,J)= LWRT(K,J) / F2(K)
5 CCNTINUE
WRITE(6,107) NRT(J), (DHT1(K,J),K=1,12)
107 FORMAT(1H K,6X,F5.1,3X,12(F6.4,3X))
WRITE(6,111) (WRTP1(K,J), K=1,12), (LWRT(K,J), K=1,12),
1 (WTPN(K,J), K=1,12), (NRTE1(K,J), K=1,12), (LWRTF2(K,J),
2 K=1,12), (NRTE2(K,J), K=1,12)
111 FORMAT (1H J, 14X, 12(F6.2 ,3X) / 15X, 12(E9.3) / 15X, 12(F6.4,
1 3X) / 15X, 12(F6.1, 3X) / 15X, 12(F7.6, 2X) / 15X, 12(F6.1, 3X))
6 CCNTINUE

```

```

C
C-----PRINT TURBINE FLOW MAP HEADING
C
WRITE(6,108)
108 FORMAT(1H1,45X,16HTURBINE FLOW MAP)
WRITE(6,109)
109 FORMAT(1H K,14X,4HWRTP//7X,3HNRT,5X,3HDHT)
WRITE(6,110) (WRTP2(K), K=1,12)
110 FORMAT(1H K,14X,12(F6.3,3X))

```

```

C
C-----INTERPOLATE TABLE FOR CONSTANT FLOW
C
CC 12 J=1,9
CC 12 K=1,12
DHT1(K,J)= 0.C
12 CCNTINUE
CC 11 J=1,9
CC 10 K=1,12
IF((WRTP2(K).LT.WRTP(1,J)).OR.(WRTP2(K).GT.WRTP(12,J))) GC TC 10
CC 7 I=1,10
IF(WRTP(I,J)-WRTP2(K)) 7,8,8
7 CCNTINUE
8 IF(WRTP(I-1,J)-WRTP(I,J)) 9,10,9
9 RATIO(K,J)= (WRTP(I-1,J)-WRTP2(K))/(WRTP(I-1,J)-WRTP(I,J))
DHT1(K,J)= DHT(I-1)+RATIO(K,J)*(DHT(I)-DHT(I-1))
10 CCNTINUE
WRITE(6,107) NRT(J), (DHT1(K,J),K=1,12)
11 CCNTINUE
STOP
END

```

\$DATA

```

$HEAT [HT(1)= .01,.02,.03,.035,.04,.0483,.055,.06,.07,.08$
$SPEED NRT(1)=41.36,49.63,57.90,66.17,74.44,
79.98,82.71,90.99,99.26$
$FLOW WRTP(1,1)=65.,88.,103.,107.,110.2,
112.,114.8,115.5,116.,116.3,
WRTP(1,2) =64.0,84.,98.,103.,107.,
110.5,112.,113.,114.,115.,
WRTP(1,3) =65.,82.,95.,100.,103.5,
108.,110.1,111.5,112.8,113.3,
WRTP(1,4) =66.,82.,92.,98.,101.,
105.6,108.,109.2,111.7,112.5,
WRTP(1,5) =65.,82.,91.,95.,98.5,
102.,106.5,107.5,110.,111.5,
WRTP(1,6) =71.,82.,90.5,94.,97.,
102.23,105.,107.,108.,111.,
WRTP(1,7) =71.5,82.,90.5,93.5,96.5,
102.,104.,106.,109.,110.5,
WRTP(1,8) =75.,82.5,90.,93.,96.,
100.,102.5,104.,107.,109.,
WRTP(1,9) =76.,83.,90.,92.5,95.,
99.,102.,103.,106.,107.5$
$EFF ETA(1,1)= .88,.86,.78,.71,.64,
.55,.55,.55,.55,.55,
ETA(1,2) = .82,.89,.87,.84,.81,
.75,.71,.67,.61,.55,
ETA(1,3) = .75,.882,.903,.9,.887,
.855,.83,.815,.78,.75,
ETA(1,4) = .64,.84,.90,.91,.913,
.903,.892,.882,.855,.835,
ETA(1,5) = .55,.80,.877,.895,.907,
.922,.916,.911,.901,.89,
ETA(1,6) = .52,.75,.845,.88,.897,
.918,.925,.922,.913,.905,
ETA(1,7) = .50,.72,.84,.865,.89,
.91,.925,.925,.918,.91,
ETA(1,8) = .45,.7,.8,.835,.86,
.892,.907,.922,.93,.92,
ETA(1,9) = .45,.65,.76,.8,.825,
.865,.892,.902,.925,.925$
$PARAM1 PF1(1)=.1,.2,.3,.4,.5,.6,.7,.75,.8,.85,.9,.95$
$PARAM2 WRTP2(1)=50.,60.,70.,80.,90.,95.,
100.,102.2,105.,107.5,110.,115.$

```

APPENDIX H

TURBOFAN FUEL CONTROL SIMULATION

In order to investigate the dynamics of turbojet and turbofan engines, it is often necessary to simulate the engine fuel control system, as well as the engine. The use of the HYDES program dictates that the fuel control be simulated on the analog computer.

A portion of a proposed fuel control was simulated on the analog computer to allow transient variations in the operating point of the selected turbofan engine. The primary function of the control is to maintain the low-pressure-turbine rotor speed N_{t2} at a demanded value $N_{t2, dem}$. Figure 16 illustrates, in block diagram form, the operation of the speed control loop.

The measured speed $N_{t2, m}$ is subtracted from the demanded value, which is scheduled as a function of power lever angle α and inlet temperature $T_{2, m}$. The error is amplified and then reduced by the output of a derivative-plus-lag circuit whose input

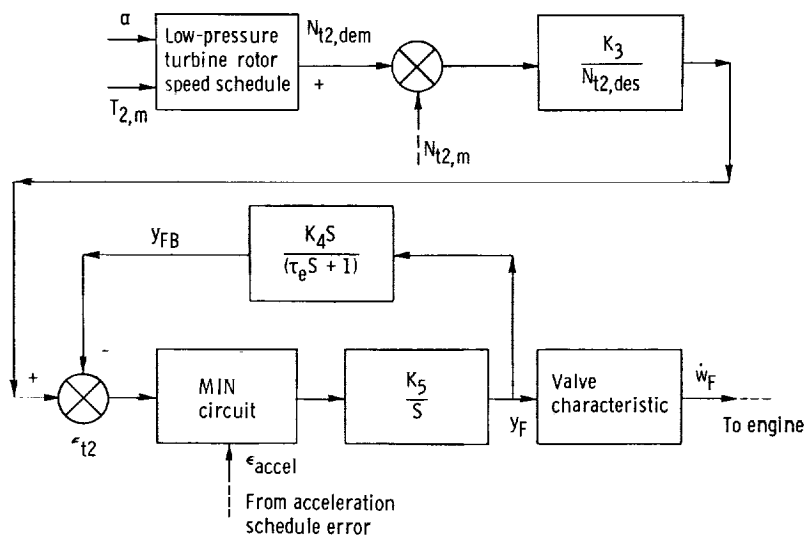


Figure 16. - Turbofan low-pressure-turbine rotor-speed control.

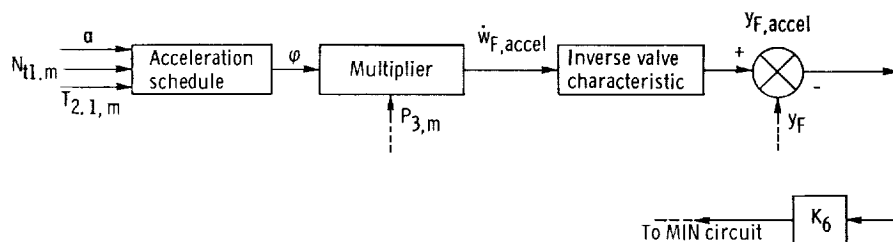


Figure 17. - Turbofan acceleration control.

is fuel valve position y_F . The feedback provides proportional-plus-integral dynamics between the valve position and the speed error. For near-steady-state conditions, the MIN circuit (output equals smallest of its inputs) transmits the speed error signal to the fuel valve servomechanism.

In order to combine fast thrust increases with overtemperature and compressor stall protection, an acceleration schedule feature is included in the control and is illustrated in figure 17.

A sudden increase in the power lever angle α causes a corresponding increase in the speed error signal. The MIN circuit then transmits the acceleration error signal to the fuel valve servomechanism. An acceleration schedule parameter φ is scheduled as a function of α , high-pressure-turbine rotor speed $N_{t1, m}$, and compressor inlet temperature $T_{2.1, m}$. The output of the acceleration schedule is multiplied by compressor discharge pressure to determine the acceleration fuel flow and corresponding valve position. The amplified position error is then transmitted to the fuel valve servomechanism, giving a first-order lag response of valve position to the command acceleration position. The engine then accelerates along the acceleration schedule until the speed error signal becomes smaller than the acceleration position error signal.

Physical limits are built into the valve position. That is $y_{F, \min} \leq y_F \leq y_{F, \max}$. The speed control feedback signal (fig. 16) is also limited to $y_{FB, \min} \leq y_{FB} \leq y_{FB, \max}$.

For the turbofan transient demonstration, the low-pressure-turbine rotor speed demand $N_{t2, \text{dem}}$ was ramped from its initial value to the final value in 50 milliseconds (5 sec computer time). The acceleration schedule was fit by a function of compressor inlet temperature and speed. The following equations were implemented on the analog computer:

$$N_{t1, m} = 100 \int_0^t (N_{t1} - N_{t1, m}) dt + N_{t1, i} \quad (\text{H1})$$

$$N_{t2, m} = 100 \int_0^t (N_{t2} - N_{t2, m}) dt + N_{t2, i} \quad (\text{H2})$$

$$T_{2.1, m} = 2 \int_0^t (T_{2.1} - T_{2.1, m}) dt + T_{2.1, i} \quad (\text{H3})$$

$$P_{3,m} = 50 \int_0^t (P_3 - P_{3,m}) dt + \frac{R_A W_{3,i} T_{3,i}}{V_3} \quad (\text{H4})$$

$$\dot{w}_F = 4.653 (y_F + 0.0846)^2 \quad (\text{H5})$$

$$y_F = 1.664 \int_0^t \text{MIN} \left\{ \begin{array}{l} \epsilon_{t2} \\ \epsilon_{\text{accel}} \end{array} \right\} dt + y_{F,i} \quad (\text{H6})$$

$$\epsilon_{t2} = \frac{25.91}{N_{t2,des}} (N_{t2,dem} - N_{t2,m}) - y_{FB} \quad (\text{H7})$$

$$y_{FB} = 18.014 \int_0^t \left(\dot{y}_F - \frac{y_{FB}}{9.007} \right) dt \quad (\text{H8})$$

$$\epsilon_{\text{accel}} = 33.00 (y_{F, \text{accel}} - y_F) \quad (\text{H9})$$

$$y_{F, \text{accel}} = \left[\frac{\dot{w}_{F, \text{accel}}}{4.653} \right]^{1/2} \quad (\text{H10})$$

$$\dot{w}_{F, \text{accel}} = \frac{\varphi P_{3,m}}{3600} \quad (\text{H11})$$

$$\varphi = \left(K_{\varphi} + 33 \frac{N_{t1, m}}{N_{t1, des}} \sqrt{\frac{T_{std}}{T_{2.1, m}}} \right) \left(0.3124 + 0.6895 \frac{T_{2.1, m}}{T_{std}} \right) \quad (\text{H12})$$

$$K_{\varphi, \text{nom}} = -5.4$$

REFERENCES

1. McKinney, John S.: Simulation of Turbofan Engine. Part I. Description of Method and Balancing Technique. Rep. AFAPL-TR-67-125, Air Force Aero Propulsion Lab. (AD-825197), Nov. 1967.
2. McKinney, John S.: Simulation of Turbofan Engine. Part II. User's Manual and Computer Program Listing. Rep. AFAPL-TR-67-125, Air Force Aero Propulsion Lab. (AD-825198), Nov. 1967.
3. Koenig, Robert W.; and Fishbach, Laurence H.: GENENG - A Program for Calculating Design and Off-Design Performance for Turbojet and Turbofan Engines. NASA TN D-6552, 1972.
4. Fishbach, Laurence H.; and Koenig, Robert W.: GENENG - A Program for Calculating Design and Off-Design Performance of Two- and Three-Spool Turbofans with as Many as Three Nozzles. NASA TN D-6553, 1972.
5. Szuch, John R.: Analysis of Integral Lift-Fan Engine Dynamics. NASA TM X-2691, 1973.
6. Shapiro, Ascher H.: The Dynamics and Thermodynamics of Compressible Fluid Flow. Vol. I. Ronald Press Co., 1953.
7. Keenan, Joseph H.; and Kaye, Joseph: Gas Tables. John Wiley & Sons, Inc., 1955.
8. Seldner, Kurt; Mihalow, James R.; and Blaha, Ronald J.: Generalized Simulation Technique for Turbojet Engine System Analysis. NASA TN D-6610, 1972.
9. Anon.: 690 Hybrid Computing System Reference Handbook. Publ. No. 00800. 3040-0, Electronic Associates Inc., Mar. 1969.
10. Anon.: Scaled Fraction (FORTRAN Run-Time Library). Publ. No. 00827-8624-1, Electronic Associates Inc., Oct. 1969.
11. Anon.: 640 Function Generation Subroutines. Publ. No. 00827-8610-2, Electronic Associates Inc., Feb. 1970.

